

Water Resources Research Center Annual Technical Report FY 2005

Introduction

Introduction to Annual Report Maryland Water Resources Research Center

Two important goals were achieved in our 2005 program. For some time the Center has encouraged the participation of early career scientists to submit proposals for funding. All three funded proposals were submitted by assistant professors at their respective universities. In addition to funding early career scientists, a proposal submitted by a university student was also funded for the summer fellowship. Our second goal was to encourage projects that would improve the quality of waters reaching the Chesapeake Bay. All projects had a Bay focus. The Bay is one of Maryland's major economic assets. Problems associated with the Bay are wide spread and complex. One of our most serious problems has been the tremendous population growth within the State. The Center cooperates with other State and Federal agencies engaged in Bay Research. For example, the Center co-sponsored a conference on Urbanization: Stresses on Maryland's Water Resources with the MD Sea Grant College. Over 100 people from across the state attended the conference. Dr. Robert Hirsch, Associate Director of the USGS at Reston, was the keynote speaker. Six additional speakers representing University and State scientists also addressed this important topic.

We are always pleased when results from one of our funded projects are published in a distinguished journal. A project that was funded by the MDWRRC in 2003 concerning the genetics of the Eastern Oyster was published in 2006 (Rose et al., *Journal of Heredity* 97:158-170). This research, conducted by a Ph.D. student in the Biology Department, measured the geographic pattern of gene flow among 'wild' oyster reefs throughout Chesapeake Bay. Genetic patterns indicated that oyster larvae typically do not disperse far from their parents, even among Chesapeake tributaries not previously recognized as retaining larvae in a "trap-like" manner. This has important implications for the spatial scale of restoration impacts

Research Program

Three traditional projects and one student summer fellowship were supported in 2005. Also 2 supplemental projects were supported through the Center.

Theoretical and experimental evaluation of acetate thresholds as a monitoring tool for in situ bioremediation

Basic Information

Title:	Theoretical and experimental evaluation of acetate thresholds as a monitoring tool for in situ bioremediation
Project Number:	2005MD78B
Start Date:	3/1/2005
End Date:	2/28/2006
Funding Source:	104B
Congressional District:	5th District of Maryland
Research Category:	Water Quality
Focus Category:	Toxic Substances, Groundwater, Methods
Descriptors:	
Principal Investigators:	Jennifer G. Becker, Hubert J Montas, Eric A. Seagren

Publication

Final Report

Theoretical and experimental evaluation of acetate thresholds as a monitoring tool for in situ bioremediation

Jennifer G. Becker (PI), Eric A. Seagren (Co-PI), and Hubert Montas (Co-PI)

The primary objectives of this project were to demonstrate: (1) that characteristic acetate thresholds exist for different terminal electron accepting processes (TEAPs) and increase as the amount of energy released by the electron acceptor reduction decreases; and (2) the usefulness of acetate thresholds as an indicator of dominant TEAPs in contaminated sediments. The thesis research projects of two M.S. students in the Dept. of Civil and Environmental Engineering, Gayle Davis and Supida Piwkhaw, were supported through the Maryland Water Resources Research Center grant. To date, their work has focused primarily on refining methods for conducting the threshold determination experiments and quantifying acetate at micromolar concentrations, characterizing the dominant TEAPs in contaminated sediments, and characterizing acetate thresholds in contaminated sediments and in pure cultures of acetate-oxidizing bacteria.

Example data that were collected using the protocol that was adopted for the pure culture threshold experiments are shown in Fig. 1. The data in Fig. 1 were obtained by growing *Geobacter metallireducens* strain GS-15 under Fe^{3+} (electron acceptor)-limited conditions. Samples were collected at 4-8 h intervals for the analysis of acetate, iron, and biomass concentrations. Acetate was analyzed using an enzymatic/high performance liquid chromatography (HPLC) method. Fe^{3+} and Fe^{2+} were measured using bipyridine colorimetric method. Biomass levels in terms of volatile suspended solids (VSS) were estimated from protein concentrations measured using a bicinchoninic acid assay. The results indicate that within 25 h, strain GS-15 reduced Fe^{3+} from 28 mM down to a steady-state level of 7.8 mM. During this period, biomass and Fe^{2+} concentrations increased, as expected. Biomass and Fe^{2+} are needed to fit a respiration model to the experimental data. Repeated efforts were made to quantify acetate concentrations in the Fe^{3+} -citrate media used to grow strain GS-15. However, constituents in this and other media used to grow pure acetate-oxidizing cultures appeared to be incompatible with the reactants used in the enzymatic method. Therefore, we are in the process of developing a new ^{14}C -based method for quantifying acetate in the pure cultures. In order to implement this method, our HPLC system had to be reconfigured with several new components, including column switching valves, an ion exchange column, and a fraction collector. Briefly, $[\text{U-}^{14}\text{C}]$ acetate will be added along with unlabeled acetate to pure cultures. Aqueous samples obtained from the cultures will be injected onto the HPLC. During the period that acetate elutes from the system, the effluent will be collected in scintillation cocktail, which will be subsequently counted to determine the acetate concentration. There are several advantages to the $[\text{U-}^{14}\text{C}]$ -method compared with the enzymatic method for quantifying acetate concentrations. First, the acetate detection limit will be much lower when $[\text{U-}^{14}\text{C}]$ acetate is used.

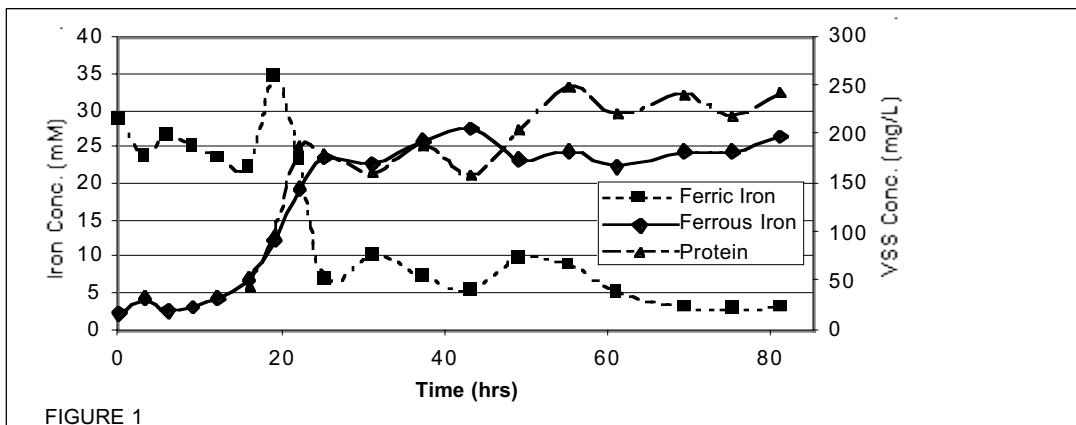


FIGURE 1

Second, $^{14}\text{CO}_2$ and [^{14}C]biomass fractions can also be readily quantified, which will improve our ability to fit model parameters to the experimental data.

The enzymatic method could be used to reliably measure acetate concentrations in natural sediment, provided the pH of the samples and standards was controlled with an organic buffer. It was used to measure acetate thresholds in sediment dominated by different TEAPs. Before threshold experiments involving the sediment could be conducted, the dominant TEAPs in sediments had to be determined. Sediment and groundwater were collected from an Aberdeen Proving Ground (MD) wetland site contaminated with chlorinated volatile organic compounds, including tetrachloroethene (PCE), which can be used as a TEA by some bacteria. After confirming that nitrate, O_2 , and PCE were not present in the groundwater in measurable amounts, the importance of Fe^{3+} -reduction and methanogenesis were evaluated by monitoring $\text{Fe}^{3+}/\text{Fe}^{2+}$ levels and CH_4 production in acetate-amended sediment/groundwater microcosms, respectively. The importance of sulfate reduction was determined by evaluating the effect of molybdate, an inhibitor of sulfate-reducing bacteria, on CH_4 production. CH_4 was produced in the acetate-amended bottles, but greater CH_4 levels were detected in the molybdate-treated bottles. This suggests that sulfate-reduction and methanogenesis were the dominant TEAPs in the sediment. Acetate levels reached threshold concentrations of $10\ \mu\text{M}$ in the molybdate-treated microcosms, but decreased to $4\ \mu\text{M}$ in the microcosms that did not receive molybdate. The amount of free energy released by the reduction of sulfate is greater than that released by the reduction of CO_2 . Thus, the finding that the acetate threshold in the microcosms in which sulfate-reduction was presumably active was lower than in the microcosms dominated by methanogenesis is consistent with theoretical considerations.

Fingerprinting Sediment to Determine Sources in an Urban Watershed

Basic Information

Title:	Fingerprinting Sediment to Determine Sources in an Urban Watershed
Project Number:	2005MD85B
Start Date:	3/1/2005
End Date:	12/31/2006
Funding Source:	104B
Congressional District:	5
Research Category:	Water Quality
Focus Category:	Sediments, Geochemical Processes, Methods
Descriptors:	None
Principal Investigators:	Brian Needelman, Jerry C Ritchie, Allen C Gellis

Publication

1. Devereux, O.H., B.A. Needelman, A.C. Gellis, K.L. Prestegaard, and J.C. Ritchie. 2005. Determining sediment source in the Anacostia River through fingerprinting and GIS data analysis. In Annual Meetings Abstracts [CD-ROM]. SSSA, Madison, WI.
2. Devereux, O.H., B.A. Needelman, K.L. Prestegaard, A.C. Gellis, and J.C. Ritchie. 2005. Determining sediment sources in the Anacostia River watershed. American Geophysical Union Fall Meeting. December 5-9, San Francisco, CA.

Fingerprinting Sediment to Determine Sources in an Urban Watershed
MWRRC Project #2005MD85B
Interim Project Report

Due to the nature of this study, we will not be completed until approximately December, 2006. Therefore please consider this an update report. We will submit a final report by Dec. 31, 2006.

The goal of the project is to test a methodology for determining the source of sediment in urban watersheds using the North East Branch, which drains to the Anacostia and the Chesapeake Bay. To recap, the objectives included:

1. Identify and quantify the source types and locations of suspended sediments,
2. Apply a composite sediment fingerprinting model for an urban watershed, and
3. Perform a soil survey of the subwatershed.

In year one (3/1/05 to 2/28/06), we had committed to obtaining soil samples of streambanks and upland areas. All source area samples have been collected and analyzed.

An additional objective for the first year was to perform morphological descriptions of soils and a topographical analysis. This objective has been fully completed. By providing a pedological context, we have actual data about the soil-landscape to guide our analysis, rather than expectations guiding data collection and analysis. This methodology is innovative and has already identified fingerprint components that have not commonly been used in other sediment fingerprinting studies. The soil survey indicated that banks are the primary source of erosive material in this urban watershed.

The third objective for the first year of the grant was to determine a composite fingerprint for each source type and area. Source areas have been determined based on those tracers that provide differentiation between sites, and similarities within source areas. The significant tracers were determined using the Kruskal Wallis test. The source areas were determined using multivariate discriminate function analysis.

While it had been anticipated that the physiographic boundary would provide definition between source areas, the subwatershed boundary showed a more significant difference between source sediments. The well-timed 10-year storm that occurred in January 2005 provided a good representative of suspended sediment and allowed us to test the mixing model to differentiate the source areas. In addition, sediment from five storm events has been collected since July 2006. Suspended sediment from will continue to be collected through June 2006. Laboratory analyses are underway with those samples already collected. Street residue was also collected to determine how much sediment washes off impermeable surfaces and from where.

Headwater erosion and sedimentation of waterways continues to be an important topic. Indeed, the "Urbanization: Stresses on Maryland's Water Resources" conference repeatedly referenced the importance of determining sources of sediment for establishing

sediment TMDLs. It is our hope that this research will validate a method that is effective in urban watersheds.

Should you have any questions or concerns, please feel free to contact me at 301-405-8227 (Needelman) or 301-405-1309 (Devereux). Once again, thank you for supporting this project.

Brian Needelman, PI
Olivia Devereux, Graduate Research Assistant

Chemical and Biological Availability of Zinc in Road Runoff Entering Stormwater Retention Ponds

Basic Information

Title:	Chemical and Biological Availability of Zinc in Road Runoff Entering Stormwater Retention Ponds
Project Number:	2005MD89B
Start Date:	3/1/2005
End Date:	2/28/2006
Funding Source:	104B
Congressional District:	2
Research Category:	Water Quality
Focus Category:	Non Point Pollution, Sediments, Toxic Substances
Descriptors:	
Principal Investigators:	Ryan E. Casey, Edward R Landa, Steven M Lev, Joel Wade Snodgrass

Publication

Problem and Research Objective

Growth in urban areas leads to the development of new roads, highways, and other types of impervious surfaces. With this increase in impervious surfaces there is a growing concern about the contaminant contributions of roadway runoff during storm events. Runoff carries with it any pollutants and particulates that have built up on the road. Of these pollutants, heavy metals are of growing concern due to their presence at increased levels in urban stormwater. There can be a number of sources of heavy metals in stormwater runoff including building siding, building roofing, wet and dry deposition, automobile parts, and gas and oil (Davis et al. 2001, Breault and Granato 2000, Councell et al. 2004). The metals that were found from these sources were Zn, Pb, Cu and Cd in order from highest estimated annual loads to lowest. Brake wear was found to be the biggest contributor of Cu while brick buildings and tire wear were the biggest contributors of Zn. The importance of automobile parts as sources of these metals has been previously studied. Councell et al (2004) estimated that tires are composed of 1% Zn by weight and they estimated that in 1999 alone, a total of about 11,000 tons of Zn was released from tire wear nationwide. Davis et al (2001) estimated from the literature a discharge estimate of 75 ug Cu/km-vehicle from brake pads.

Stormwater retention ponds are becoming a common tool in managing stormwater runoff and in the state of Maryland they are an acceptable best management practice (BMP). Retention ponds allow suspended sediments to settle and pollutants to contact and adsorb to the surface of pond sediments (Lawrence et al 1996). Since runoff often contains high concentrations of heavy metals it is expected that these ponds will also contain high levels of metals. Liebens et al (2001) studied 24 ponds that were located in residential and commercial areas. In all 24 ponds metal concentrations were higher than in control ponds. The work also suggested that older

ponds had higher concentrations than younger ponds. Pond sediment concentrations ranged from 0.27-622 mg/kg of Zn and bdl-55 mg/kg of Cu. Casey et al (2004) also quantified trace metals in retention pond sediments. They found Zn concentrations ranging from 53-1155 mg/kg and Cu concentrations ranging from 18-341 mg/kg. In both these studies it appears that the ponds are removing and storing at least some of the heavy metals that are coming off of the roadway.

The presence of heavy metals in these ponds is a concern due to their effects on the organisms that inhabit the area. Toxicity due to heavy metals has been studied in a variety of organisms including fish, amphipods, mussels and amphibians (Bailey et al 1998, Karouna-Renier et al 1997, Anderson et al 2004, Lefcort et al 1998). Throughout all of these studies, the specific effects that are seen in the organisms vary a great deal. Differences in type of organism, type and concentration of the metal(s), the pH of the environment, bioavailability, and the sediment characteristics that are present are all factors that have been found to influence toxicological effects (Karouna-Renier and Sparling 2001, Anderson et al 2004). There is a growing push to look at metal toxicity and accumulation in amphibians, especially anuran juveniles as well as adults. Because of their presence in many urban streams and ponds, studying these amphibians is important in determining if they will be negatively affected by the metals in their environment. Metals have been found to decrease hatching success (Haywood et al 2004), reduce the growth of tadpoles (Haywood et al 2004) and reduce tadpole survival (Haywood et al 2004, Lefcort et al 1998). Lefcort et al (1998) also found that in a laboratory study, metals reduced the fright response of *Rana luteiventris*, which could decrease the rate of survival of the tadpoles in natural environments. Even when metal exposures did not cause substantial lethal or sub-lethal affects, tadpoles accumulated heavy metals in their tissues and guts when exposed to

metal contaminated water and/or sediment (Sparling et al 1996, Lefcort et al 1998, James et al, Loumboudis et al 1998). The high concentration of metals accumulating in the bodies of the tadpoles could result in trophic transfer to organisms that prey on them (Sparling et al 1996, Haywood et al 2004).

Study Objective

The purpose of the present study was to determine if Cu and Zn were major constituents of stormwater runoff, roadway dust, and retention pond sediments and then to determine if they were in a form that was easily available for uptake by biota.

Materials and Methods

Background Soils:

Background soil samples were taken throughout the study site along 4 transects (Figure 1). In each transect, samples were taken approximately 15 m apart. At each sampling point a surface sample was taken down to a depth of about 3 cm. Periodically a bulk sample was also taken down to a depth of about 8 cm.

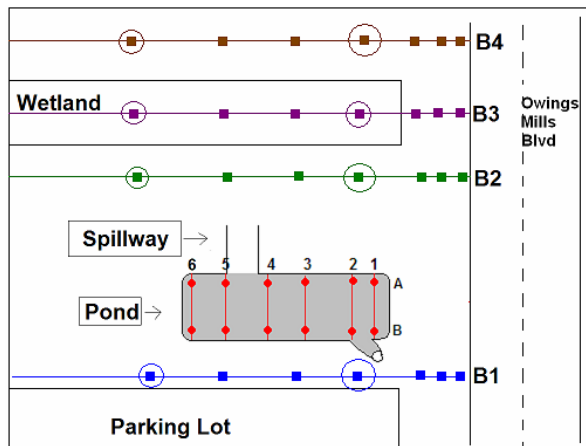
All samples were dried in an oven at 70° C. A portion of each dried soil sample was ground using a SPECS Mixer/Mill 2500. The mixer/mill was cleaned between each sample using DI water and methanol. The ground samples were used for the determination of trace elements by XRF (X-Ray Fluorescence). For XRF preparation, ground samples were pressed into pellets using the SPEC X-Press. Approximately 7 g of sample and 0.7 g of a cellulose binder were mixed together and placed into the pressing die. Each pellet was then kept in a desiccator until analyzed by the XRF. NIST SRM 2709 (San Joaquin Soil) was used during

XRF analysis for QA/QC. The samples were analyzed for copper, chromium, nickel, lead, vanadium, and zinc.

Pond Sediments:

Sediment cores were collected from within the pond along six transects. Each transect was sampled twice, once on the left side of the pond and once on the right side of the pond (Figure 1). Final core depths varied between 50 and 90 cm. Sediment cores were collected using a McCauley peat sampler. There was an unconsolidated, organic top layer that was difficult to collect using the peat sampler. For this top layer, a PVC pipe was used. Sediment cores were separated according to depth and placed into plastic bags for transport and storage.

Figure 1: Sampling Map



The wet mass of each core was determined to allow for subsequent estimates of metal storage in each area of the pond and a sub-sample was then used for dry weight determination.

For ICP-MS analysis, approximately 60 mg dry sample was placed into a clean Teflon vial. Samples were acidified using 1 ml of HF and 3 ml of HNO₃ and placed on a hot plate overnight. Both acids were of trace metal grade. The samples were dried and 3 mL of hydrogen peroxide was added to the vessels and placed onto the hot plate. The samples were again dried and HF and HNO₃ was added in the same proportions as before and placed onto the hot plate.

This extra digestion step was to ensure that the samples were completely digested. Finally samples were dried and an internal standard solution of 2% HNO₃ containing 10 ppb of germanium and 1 ppb of indium was added to each vial and samples were put back onto the hotplate for re-digestion. Samples were then analyzed by ICP-MS for total metal concentrations. The NIST standard reference material 2709 (San Joaquin Soil) was also analyzed with the sediment samples to monitor external reproducibility.

Using the mass of the sediment cores, the surface area of the sampler, and the area of the sampling grid, total pond storage was estimated for Cu and Zn.

Selected pond sediments also underwent sequential extraction process to determine the possible bioavailability of the metals within the pond. The method used was based on the work published by Tessier et al. (1979).

Road Dust

Road dust was sampled from the roadway surface around the storm drains leading into the retention pond. Dust was obtained using a forensic vacuum with a 0.2 µm filter. Samples were collected starting in the spring of 2005, and were collected at least once every season over the next year. Total metal concentrations were determined in the same manner as the pond sediments. The road dust was also separated by wet sieving using a <63 µm nylon sieve and a <5 µm nylon sieve. Each of these fractions underwent total digestion as well as sequential extractions.

Storm Events:

An ISCO sampler was installed at the outflow of the storm pipe that leads directly into the drainage pond. The sampler activated when a specified flow was reached and continued to collect samples on a time basis. For storms 1-7, samples were collected every 20 minutes

throughout the duration of the storm. Beginning with storm 8, bottles 1-12 collected samples every 4 minutes, the remainder of the bottles collected samples every 30 minutes. Samples were recovered and returned to the lab. Five mL of sample was filtered through a 0.45 um nylon filter and then acidified to 0.2N using 6N HNO₃. This represents the truly dissolved metals in the sample. Another 5 mL of the same water sample was acidified to 0.2N using 6N HNO₃ and then filtered through a 0.45um nylon filter. This represents the truly dissolved plus particulate bound metals. These water samples were then analyzed by ICP-MS along with the NIST standard reference 2096 (Mussel Tissue) to validate calibration and reproducibility. The runoff concentrations along with the discharge during the storm were used to determine the total runoff load for both the dissolved and particulate bound Cu and Zn.

For storms 1-3, the remainder of the storm sample was vacuum filtered through Whatman ashless 25 um filter paper to determine total suspended solids. Starting with storm 4, samples were filtered through a preweighed 0.45 um cellulose nitrate filter. A small number of these filters underwent total digestion. Filters were placed into clean Teflon vials and digested as described above. Samples were analyzed by ICP-MS for Cr, Ni, Cu, Zn, As, Se, Cd, and Pb.

Sediment Bioassay:

To assess the toxicity of stormwater pond sediments to early developmental stages of amphibians potentially utilizing stormwater ponds as breeding sites we exposed eggs and larvae to pond sediments and clean sand controls in laboratory microcosms. Developing wood frog eggs (*Rana sylvatica*) and subsequent larvae were exposed to either pond sediments or clean sand in the first experiment. In the second experiment American toad eggs (*Bufo americanus*) were exposed to pond sediments or clean sand and evaluated for hatching success and subsequent time to metamorphosis.

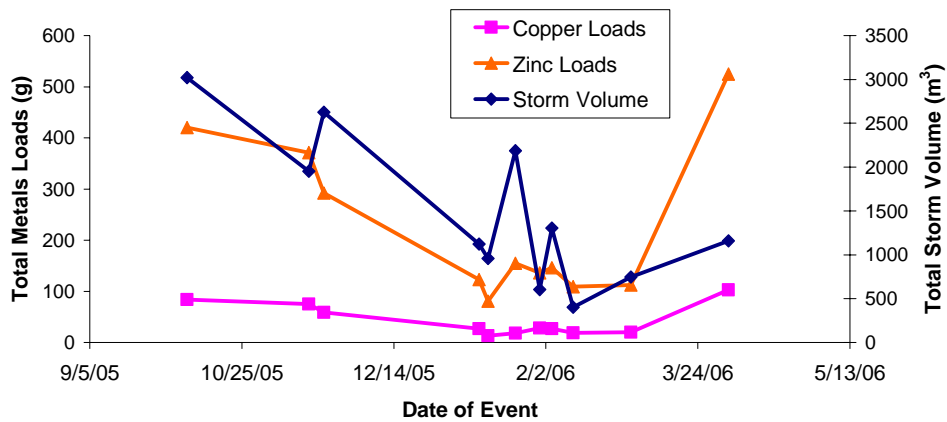
Principal Findings and Significance

Storm Events

A total of 12 storm events were collected and analyzed. Average total metal concentrations for each storm were between 6-36 ug/L for Cu and 23-169 ug/L for Zn. Within each storm however, concentrations were as high as 366 ug/L for Zn and 80 ug/L for Cu. Along with metal concentrations, storm loads were also determined for both Cu and Zn (Figure 2).

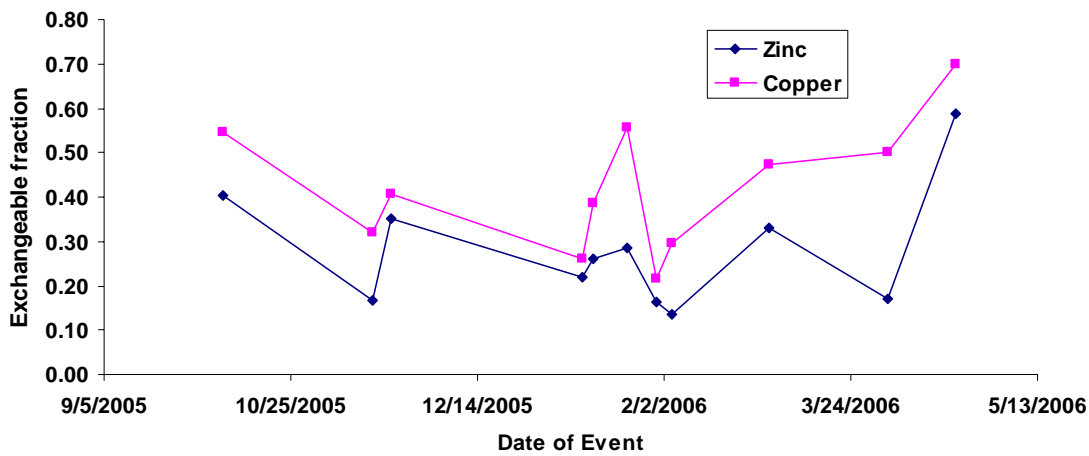
Zinc loads were generally 2-4 times higher than copper loads.

Figure 2: Total zinc and copper loads from stormwater entering the retention pond in storm runoff



Exchangeable and total metal concentrations were also determined for each storm. Both copper and zinc were mainly particulate bound, however the fraction of dissolved copper was higher in all storms compared to zinc (Figure 3). It is important to determine the speciation of the metals entering the pond because dissolved metals are more available to biota. Since the culvert drains only the roadway, it is likely that Cu and Zn largely originate from automobile wear such as brake pad particulates and tire particulates. Therefore these data are consistent with metals being mainly particulate bound.

Figure 3: Fraction of exchangeable metal loads out of the total metal loads entering the retention pond in storm runoff.



Pond Sediments

The next step of the project was to determine metal concentrations within the retention pond sediments. Cores were taken down to a depth of at least 50 cm, however the majority of the metal concentrations were found to be in the top 10 cm of the sediments cores (Figure 4 and 5). The top 10 cm consisted mainly of unconsolidated organic matter. Concentrations of Zn in this top layer ranged from 136-1031 mg/kg and for Cu ranged from 99-215 mg/kg. Pond sediment concentrations were substantially higher than background concentrations indicating that there was an input of both Cu and Zn into the pond from the roadway. Comparison with background levels indicates that some vertical transport of Zn and Cu may be occurring at these sites given the elevated concentrations below the immediate depositional zone.

Road Dust

Trace metal concentrations in road dust were determined for three separate size fractions. These fractions were bulk road dust, the less than 63 micron fraction and a less than 5 micron fraction. The highest concentration of both copper and zinc was in the less than 5 micron

fraction. A comparison of the road dust fractions with the pond sediments and background soils are shown in Figures 6 and 7. Pond sediments represent mixing between background soils and the influx of particulates from the roadway. In this case, it appears that the pond sediments are a mixture of the background soils and the <5micron and <63 micron fractions.

Figure 4: Zinc depth profile for pond sediments. Solid vertical line represents mean background concentration and dotted vertical lines represent +/- one standard deviation.

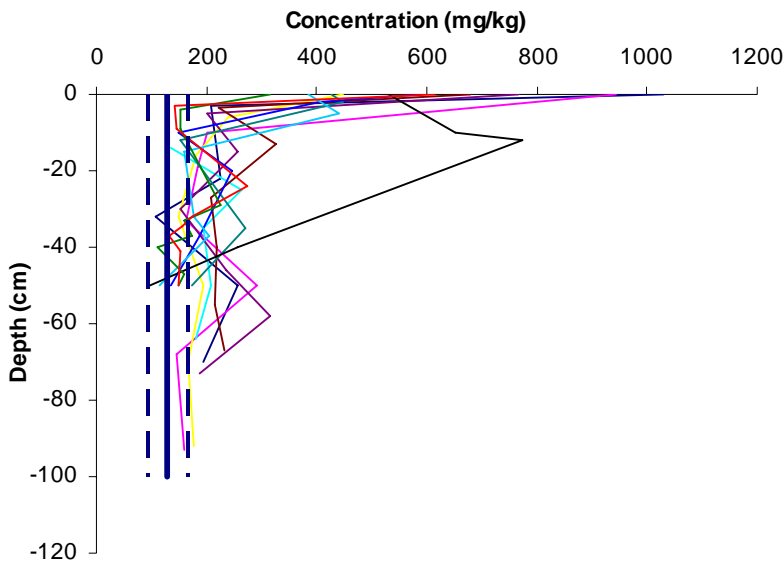


Figure 5: Copper depth profile for pond sediments. Solid vertical line represents mean background concentration and dotted vertical lines represent +/- one standard deviation.

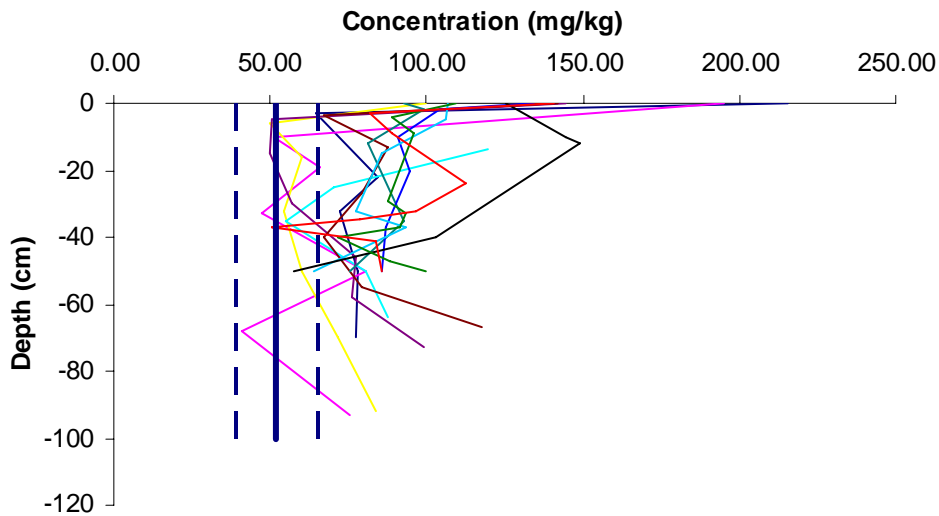


Figure 6: Total zinc levels in road dust in comparison with background and pond surface sediments.

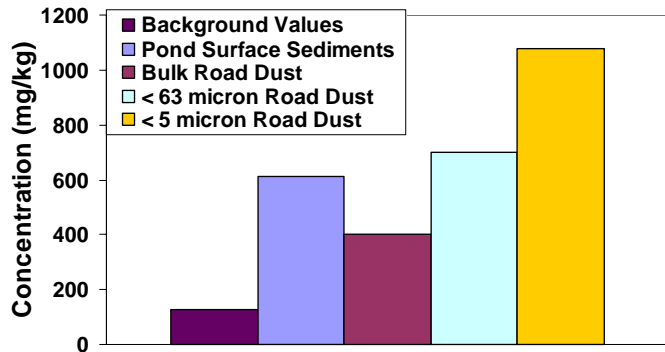
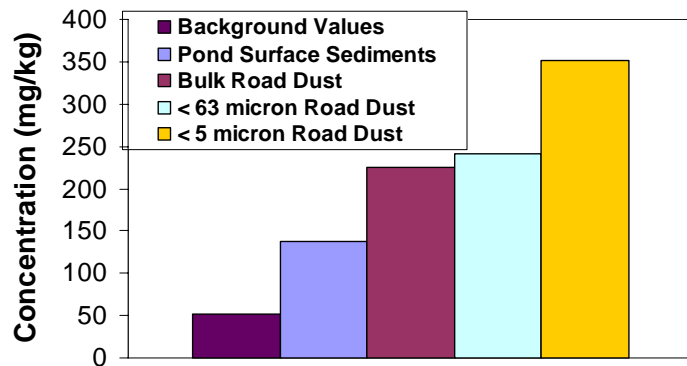


Figure 7: Total copper levels in road dust in comparison with background and pond surface sediments.



Sequential extractions were performed on pond sediments and the bulk and <5 micron road dust fractions (Figures 8 and 9). The extractions performed on the pond sediments revealed that there was little to no available copper in the sediments. In all surface sediments, copper was in the most recalcitrant fraction. For zinc, there was a small amount bound to carbonates and Fe and Mn oxides. Depending on the conditions that these sediments undergo, these fractions could release zinc into the water column. For the most part however, Zn is in the most recalcitrant fraction.

Figure 8. Sequential extraction of zinc and copper from surface stormwater pond sediments.

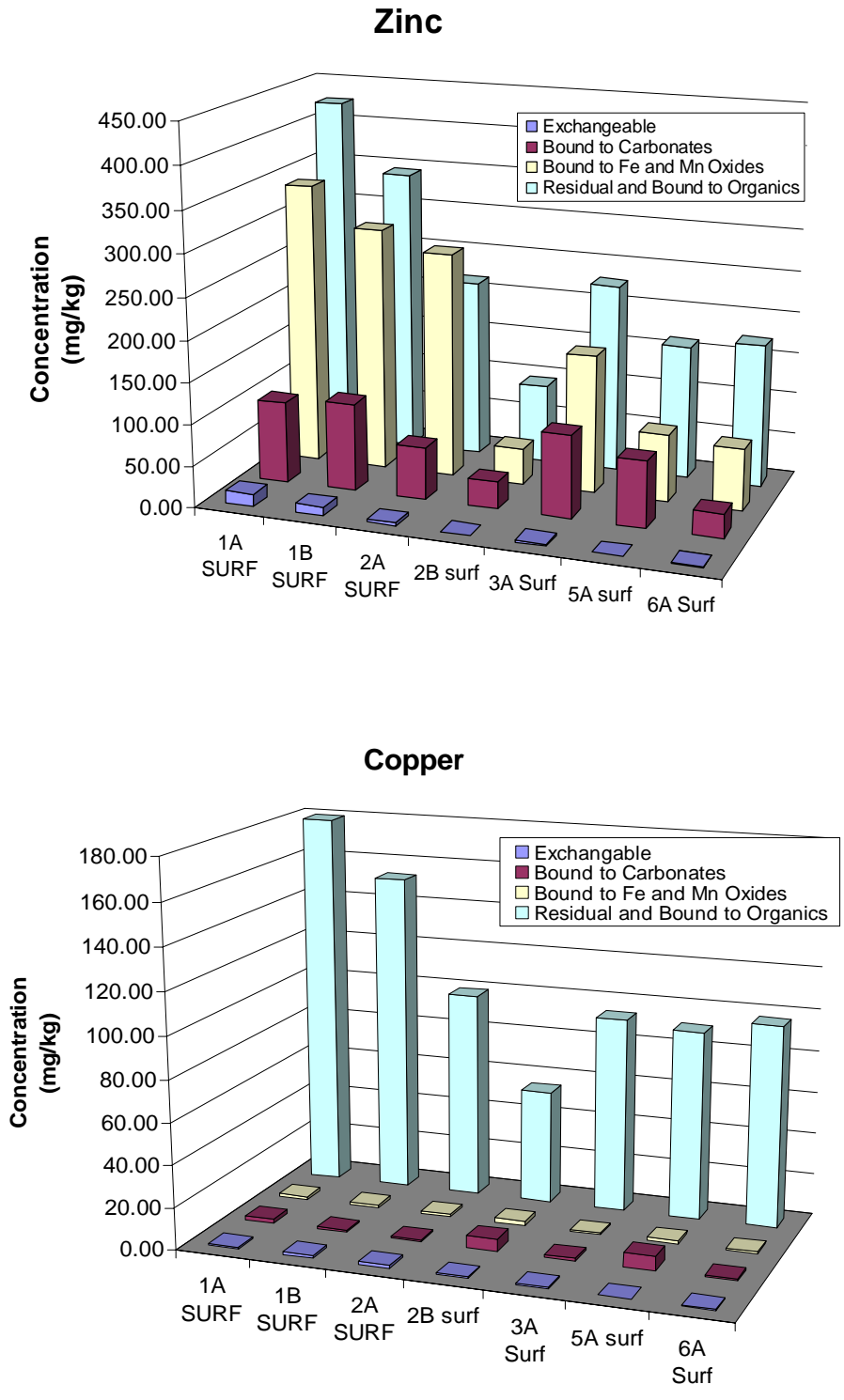
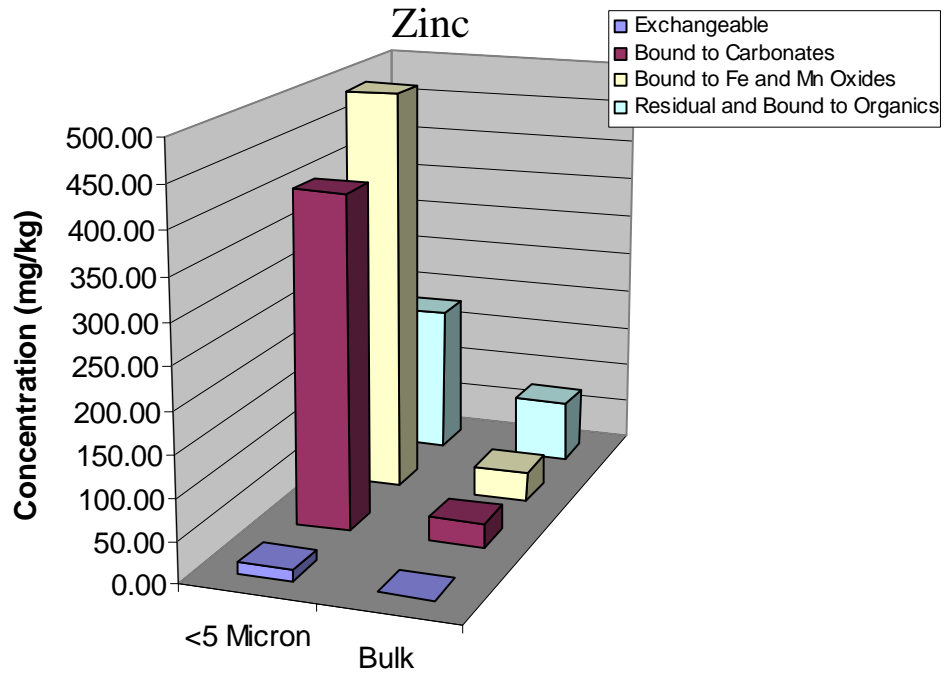
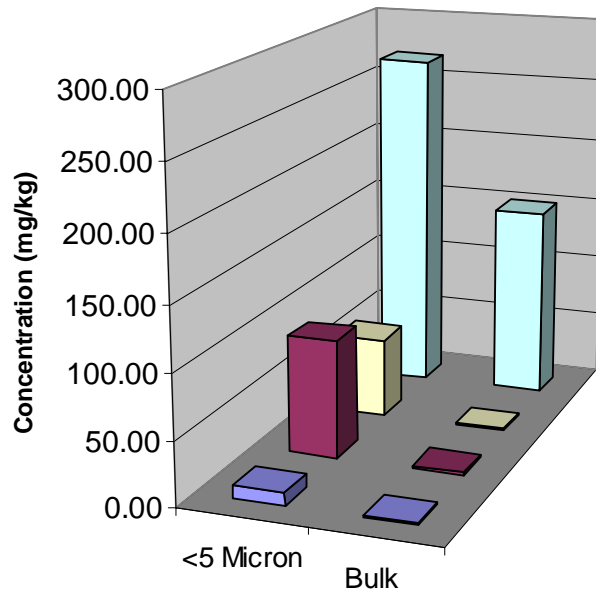


Figure 9. Sequential extraction of zinc and copper from road dust.



Copper



With the road dust extractions the <5 micron fractions for both Cu and Zn had metals that were bound to carbonates and bound to Mn and Fe oxides (Figure 9). The highest concentrations of zinc were found in these two fractions. While there was some Cu in both of these forms, most of it was in the residual and organic bound forms. For the bulk road dust, the majority of both Cu and Zn were not readily available.

Finally, pond sediment cores were used to determine total pond storage and compared to storm loads to determine how well the pond is retaining these pollutants. Zn storage within the pond is approximately 16.5 kg while Cu storage is approximately 6.0 kg. For Zn, this represents about 73 storm events while for Cu this represents close to 140 storm events using the average loads in storm inflow determined in this study.

Sediment Bioassay

Developing wood frog eggs (*Rana sylvatica*) exposed to pond sediments experienced reduced hatching success in comparison to controls and no larvae exposed to pond sediments survived to metamorphosis (Figure 10). In contrast, hatching success of American toad eggs (*Bufo americanus*) exposed to pond sediments was high and similar to eggs exposed to clean sand. Furthermore, while metamorphs showed sublethal effects of exposure to pond sediments (Figure 11), metamorphic success was similar between larvae exposed to pond sediments and those exposed to clean sand. Analyses of trace metal levels and water chemistry in the microcosms suggested contamination of sediments from road salting was responsible for the lethal effects observed among developing wood frogs embryos and larvae (Figure 12). Overall, our results suggest contamination of stormwater ponds with road salt is a factor in reducing the

wildlife habitat quality of ponds and the role of ponds as ecological traps for pond-breeding amphibians warrants further investigation.

Figure 10. Mean percentage of embryo and larval wood frogs surviving as a function of days of exposure to clean sand (control) and sediment from a stormwater management pond in Owings Mills, Maryland.

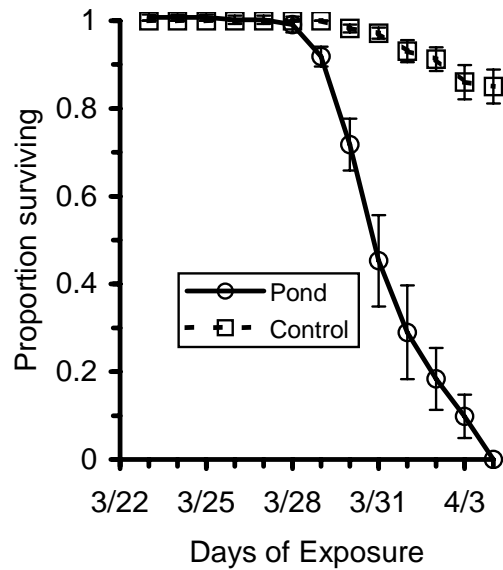


Figure 11. Mean size at front limb emergence and metamorphosis of American toad larvae exposed to sediments from two stormwater management ponds and clean sand (controls).

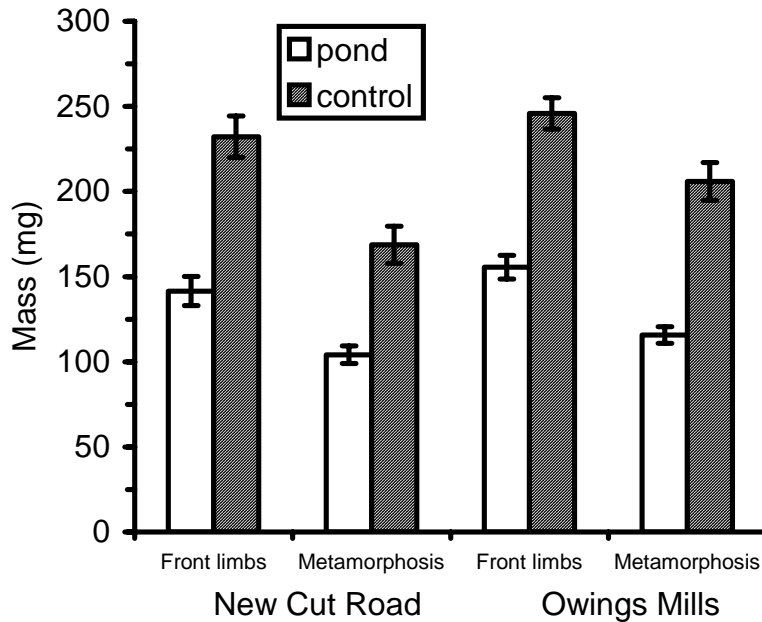
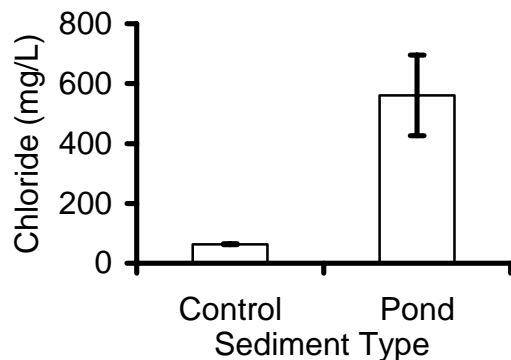


Figure 12. Mean concentration of chloride in water from bins used in wood frog exposures.



Discussion

The high concentrations of both Cu and Zn metals in stormwater runoff are likely the result of automobile wear debris. Zinc concentrations in stormwater runoff were also higher than copper concentrations for all storm events. This is consistent with numerous other studies that have looked at these metals in stormwater runoff (Drapper et al 2000, Sansalone and Buchberger 1997, Kayanian et al 2003). Metal concentrations and metal loadings varied a great deal between storm events. Storm intensity, storm duration and antecedent dry periods can all influence these differences in metal concentrations.

The fraction of Cu and Zn that is dissolved in runoff also varied a great deal within storms and between storms. On average 30% of the zinc was dissolved and about 40% of the copper. Other studies have shown that 53-95% of zinc present in runoff is dissolved and 31-56% of copper present is dissolved (Legret et al 1999, Sansalone et al 1997). The fraction of dissolved zinc is lower in this study than previous studies, however a major factor that influences these fractions is the source of the metal. Galvanized railings, roofing material, and building

siding are all contributors of zinc to stormwater runoff. Areas where these are major contributors of zinc could have higher dissolved fractions of the metals. Runoff from buildings and galvanized railings were not major contributors at this site which may explain the low dissolved fraction of zinc.

Retention pond sediment metal levels were substantially higher than background soils. Dissolved metals that enter the pond from the roadway may be adsorbing onto the sediment surfaces contributing to these elevated concentrations. The mean concentration of copper in the pond surface sediments was 131 mg kg^{-1} and for zinc the mean sediment concentration was 611 mg kg^{-1} . Other studies that have looked at retention pond sediments have shown similar concentrations of both zinc and copper. In comparison with general consensus-derived sediment quality guidelines (MacDonald et al. 2000), levels of Cu and Zn in the pond sediments exceed threshold effects concentrations (TEC; Cu = 31.6 mg kg^{-1} ; Zn = 121 mg kg^{-1}) as well as probable effects concentrations (PEC; Cu = 149 mg kg^{-1} ; Zn = 459 mg kg^{-1}) above which adverse effects are likely to occur. However sequential extraction data indicate that while metal concentrations are high, there is a relatively small amount that would be readily available for uptake by organisms inhabiting the pond.

One of the most important observations of biotic impact at this site has been the presence of elevated levels of salt from deicing operations persisting into the summer months. Levels up to $45,000 \text{ } \mu\text{S}$ (approximately 0.5 M chloride) were found in the water column through the last sampling event in June. No amphibian larvae were observed in the pond during the spring and toxicity tests conducted with sediment from the site demonstrated that wood frog (*Rana sylvatica*) eggs and larvae were severely impacted by the elevated salt levels. In contrast, American toad (*Bufo americanus*) eggs and larvae showed no impact on hatching success or

survival when exposed to the salt-contaminated sediments in a subsequent experiment. This suggests that the habitat value of this pond is controlled more by road salt application than the metal content of roadway runoff. The elevated salt level in this pond may also affect transport of metal ions due to increased formation of metal complexes and may have contributed to the vertical transport of metals through the pond sediment profile.

References

Anderson B.C., Bell T., Hodson P. Marsalek J. and Watt W.E. (2004). "Accumulation of trace metals in freshwater invertebrates in stormwater management facilities." *Water Qual. Res. J. Canada*, 39, 362- 373

Bailey H.C., Elphick J.R., Potter A. and Zak B. (1999). "Zinc Toxicity in stormwater runoff from sawmills in British Columbia." *Wat. Res.* 33(11), 2721-2725

Breault, RF and Granato, GE 2000. A synopsis of technical issues of concern for monitoring trace elements in highway and urban runoff. USGS Open File Report 00-422 [available at <http://ma.water.usgs.gov/fhwa/products/ofr00-422.pdf>]

Casey R. E., Shaw A.N., Massal L.R. and Snodgrass J.W. (2005). "Multimedia evaluation of trace metal distribution within stormwater retention ponds in suburban Maryland, USA." *Bull. Environ. Contam. Toxicol.*, 74, 273-280

Councell, T.B., Duckenfield, K.U., Landa, E.R., and Callender, E. (2004). "Tire-wear particles as a source of zinc to the environment." *Environ. Sci. Technol.* 38, 4206-4214

Davis, A.P., Shokouhian, M., Shubei, N. (2000). "Loading estimates of lead, copper, cadmium, and zinc in urban runoff from specific sources." *Chemosphere*, 44, 997-1009

Drapper D., Tomlinson R. and Williams P. (2000). "Pollutant concentrations in road runoff: southeast Queensland case study." *Journal of Environmental Engineering*, 126, 313-320

Haywood L.K., Alexander G.J., Byrne M.I. and Cukrowska E. (2004). "*Xenopus laevis* embryos and tadpoles as models for testing for pollution by zinc, copper, lead and cadmium." *African Zoology*, 39(2), 163-174

James S.M., Little E.E. and Semlitsch, R.D. (2004). "The effect of soil composition and hydration on the bioavailability and toxicity of cadmium to hibernating juvenile American toads (*Bufo americanus*)." *Environmental Pollution*, 132, 523-532

- Karouna-Renier N.K. and Sparling D.W. (2001). "Relationships between ambient geochemistry, watershed land-use and trace metal concentrations in aquatic invertebrates living in stormwater treatment ponds." *Environmental Pollution*, 112, 183-192
- Karouna-Renier N.K. and Sparling D.W. (1997). "Toxicity of stormwater treatment pond sediments to *Hyalella azteca* (amphipoda)." *Bull. Environ. Contam. Toxicol.*, 58, 550-557
- Kayhanian M., Singh A., Suverkropp C. and Borroum S. (2003). "Impact of annual average daily traffic on highway runoff pollutant concentrations." *Journal of Environmental Engineering*, 129, 975-990
- Lawrence A.I., Marselek J., Ellis J.B. and Urbonas B. (1996). Stormwater detention & BMPs. *Journal of Hydraulic Research*, 34, 799-813
- Lee H., Lau S., Kayhanian M. and Stenstrom M.K. (2004). "Season first flush phenomenon of urban stormwater discharges." *Water Research*, 38, 4153-4163
- Lefcort H, Meguire R.A., Wilson L.H., and Ettinger W.F. (1998). "Heavy metals alter the survival, growth, metamorphosis, and antipredatory behavior of Columbian spotted frog (*Rana luteiventris*) tadpoles." *Arch. Environ. Contam. Toxicol*, 35, 447-456
- Legret M. and Pagotto C. (1999). "Evaluation of pollutant loadings in runoff waters from a major rural highway." *The Science of the Total Environment*, 235, 143-150
- Lieben, J. (2001). "Heavy metal contamination of sediments in stormwater management systems: the effect of land use, particle size, and age." *Environmental Geology*, 41, 341-351
- Loumbourdis N.S. and Wray D. (1998). "Heavy-metal concentration in the frog *Rana ridibunda* from a small river of Macedonia, Northern Greece." *Environment International*, 24(4), 427-431
- MacDonald D.D., Ingersoll C.G. and Berger T.A. (2000) "Development and evaluation of consensus-based sediment quality guidelines for freshwater ecosystems." *Arch. Environ. Contam. Toxicol*, 39, 20-31
- Sansalone J.J. and Buchberger S.G. (1997). "Partitioning and first flush of metals in urban roadway storm water." *Journal of Environmental Engineering*, 134-143
- Sparling D.W. and Lowe T.P. (1996). "Metal concentrations of tadpoles in experimental ponds." *Environmental Pollution*, 91, 149-159
- Tessier, A. Campbell, P.G.C., and Bisson, M. (1979) "Sequential extraction procedure for the speciation of particulate trace metals." *Analytical Chemistry*, 51(7), 844-851

Utilization of High Carbon Fly Ash to Remediate Groundwater-Summer Student Research

Basic Information

Title:	Utilization of High Carbon Fly Ash to Remediate Groundwater-Summer Student Research
Project Number:	2005MD99B
Start Date:	6/1/2005
End Date:	9/15/2005
Funding Source:	104B
Congressional District:	Maryland 5
Research Category:	Engineering
Focus Category:	Toxic Substances, Groundwater, Hydrogeochemistry
Descriptors:	None
Principal Investigators:	Allen Davis, Allen Davis

Publication

Utilization of High Carbon Content Fly Ash as a Reactive Medium during the Remediation of NAPLs from Subsurface Waters

Summary Report

Submitted to:

**Maryland Water Resources Center
for the Summer Graduate Fellowship**

Date: August 30, 2005

Mehmet M. Demirkan

**Department of Civil and Environmental Engineering
Geotechnical Engineering Program
University of Maryland-College Park**

The primary goal of the proposed research was to investigate the fundamental factors affecting the reuse of fly ash as sorptive medium during groundwater

clean up. This re-use of fly ash has a potential for minimizing the movement of organic chemicals found in the soil and the groundwater. To achieve the objective, two tasks were conducted as part of this assessment: (1) evaluation of the sorption capacity of two different Maryland fly ashes in remediating the contaminated soils and contaminated groundwater, and (2) investigation of the leaching of chemicals from fly ash-soil mixed medium.

The batch adsorption technique was employed for determining adsorption isotherms and estimating partitioning coefficients of geologic materials. In the current study, batch adsorption tests were conducted on the borrow material and fly ash by following the standard procedures outlined in ASTM D5285. It was critical to determine the solid-to-solution ratio for the materials tested, i.e., the ratio of the weight of the solid to the volume of the naphthalene solution. ASTM D 5285 recommends a solid-to-solution ratio that would result in 20 to 80% sorption of the contaminant. After a series of preliminary tests conducted at different solid-to-solution ratios, a mass ratio of 1/120 was selected for fly ash which resulted in 50% sorption of naphthalene onto the ash. The fly ash and naphthalene solutions were equilibrated with end-over-end rotator shaker for 6, 12, 24 and 48 hrs and a series of batch kinetic tests were performed. The results suggested an equilibrium time of 24 hrs for future tests. These observations of a faster time for equilibrium for fly ash compared to borrow material (clayey sand) were consistent with current literature and indicated that the initial rapid sorption generally occurs by hydrogen bonding and van der Waals forces and is expected to occur instantaneously upon contact of naphthalene with fly ash. Batch adsorption tests were conducted on the Chalk Point and Brandon Shores fly ash, which has total carbon content of 2.9% and 18% respectively, to identify their naphthalene sorption characteristics.

Based on the literature and the experimental data, the Freundlich isotherm was selected to model adsorption behavior of the fly ash. The equation used to describe the isotherm is:

$$q_i = K_f [C_{aq}]_{NAPTH}^{(1/n)} \quad (1)$$

where q_i is the concentration sorbed onto the solid phase (mg/kg), $[C_{aq}]_{NAPTH}$ is the concentration of naphthalene in aqueous solution after sorption (mg/L), K_f is Freundlich equilibrium isotherm constant (L/kg), and n is a dimensionless empirical constant that indicates a nonlinear relationship between the organic contaminant and the sorbent (fly ash). This phenomenon is directly related to the properties of the surfaces that are available for adsorption. The results shown in Figure 1 indicate that the Freundlich isotherm constant for Brandon Shores fly ash for naphthalene is 567.3 L/kg with a n value of 0.3. The same parameters are 85.92 L/kg and 0.14, respectively, for the Chalk Point fly ash. The high sorption capacity of the Brandon Shores fly ash is evident from Figure 1. The test results also indicate that the Chalk Point has sorptive capacity that is less

than Brandon Shores fly ash, accordingly related to the unburned carbon content.

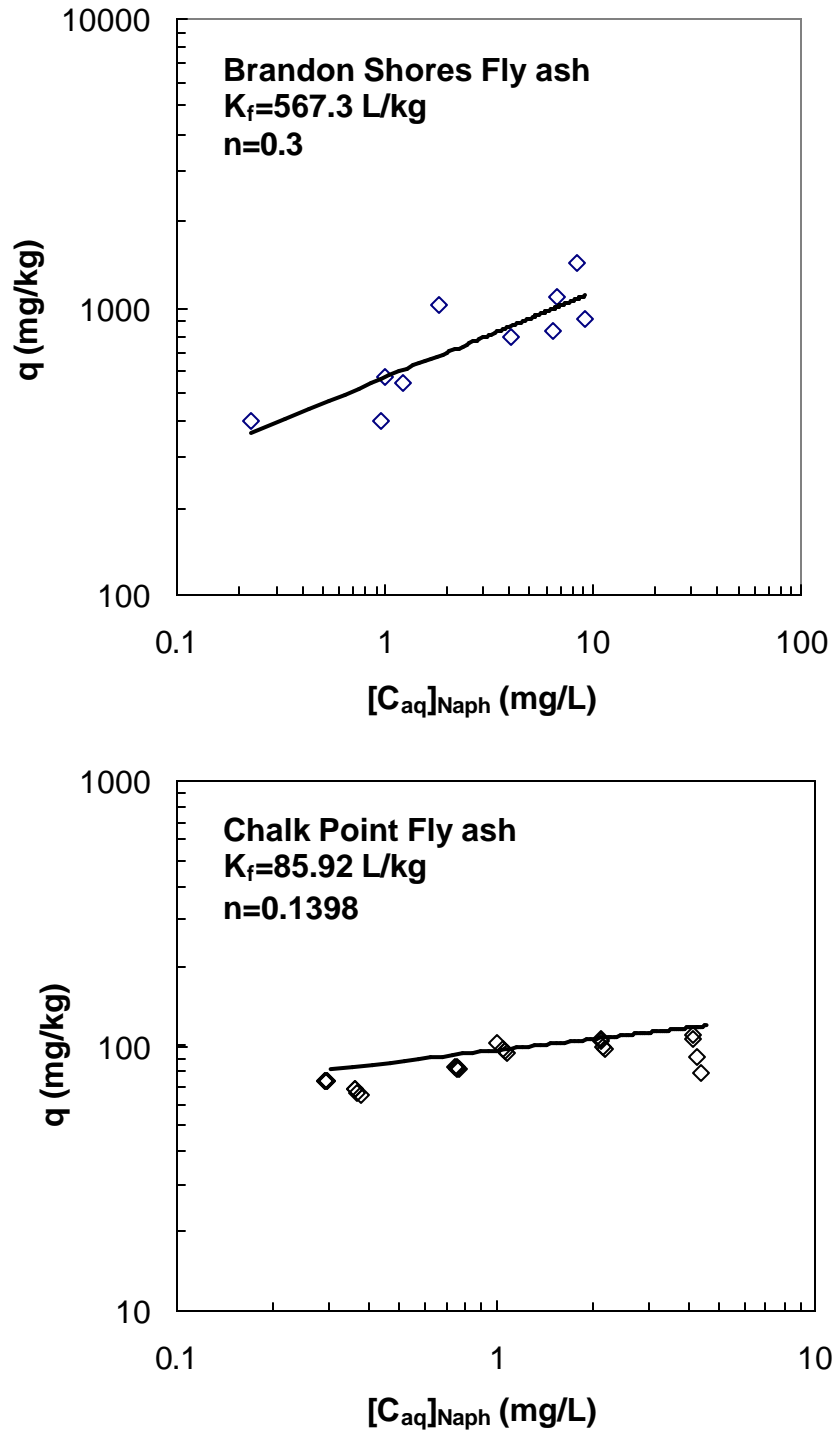


FIGURE 1 Freundlich sorption isotherms for the Chalk Point and Brandon Shores Fly ash

Column leaching tests performed during Summer 2005 consisted of the continuous flow of liquid through a solid matrix (petroleum contaminated soil herein). Naphthalene and o-xylene concentrations were measured in the samples collected from the effluent sampling ports of the columns. The diameter and height of the test specimen were 101.6 mm and 114.3 mm, respectively. A clayey sand which is labeled as borrow material by the highway engineers, was used as main soil medium. The borrow material and borrow material/fly ash mixture specimens were spiked with model NAPL before compacting them using standard Proctor energy. One of the two columns included contaminated borrow material only and was noted as the control column. The other column included 10% fly ash. The height of the stainless steel column was 177.8 mm, and the upper 63.5 mm-section of the column was devoted to influent collection, i.e. used as an influent reservoir. A supply (influent) tank was placed above the columns, and used to apply the hydraulic gradient of 4 to 5, which was selected based on the flow rate. An effluent reservoir was located between the bottom of the specimen and lower base of the column. The effluent leaving the specimen was collected in Teflon effluent bags. From the sampling port attached to the base of column, the effluent was monitored daily for the first two months of the tests. Due to relatively stabilized flow rates, weekly monitoring was adopted after two months. Tests were terminated after ensuring the stabilization of the flow and steady-state concentration of the contaminants. The liquid-to-liquid extraction and GC analysis procedures used in the batch-sorption tests were followed for analysis of the effluent samples collected from the columns. The temporal variations in o-xylene and naphthalene concentrations that were measured in the collected effluent samples are shown in Figure 2. For both organic compounds, the concentrations released from the control column are generally higher than the concentrations released from the columns with fly ash-amended borrow material. The fluctuations in the concentrations after sampling are attributed to the changes in water head due to refilling of the influent tank. Under the applied hydraulic gradients (4 to 5), mobilization of o-xylene and naphthalene from the borrow material (clayey sand) was extremely slow. Hence, the fluctuations in the applied hydraulic gradient are believed to have a very limited effect on NAPL mobilization.

Figure 2 shows that there is an initial release of o-xylene and naphthalene in the control columns. The initial concentrations were measured as 66.04 mg/L and 102.02 mg/L for o-xylene and naphthalene, respectively, and dropped to about 5 mg/L within 8 days. The low sorptive capacity of the borrow material is believed to have caused this effect. The fly ash, on the other hand, limited this release and immobilized the contaminants due to its high sorptive capacity. The initial effluent concentrations from the fly ash-amended specimens are quite low as compared to those measured in the effluent collected from the borrow material. The o-xylene and naphthalene concentrations are 4.17 mg/L and 1.58 mg/L, respectively, for the column with 10% fly ash. The profound difference between control and fly ash-amended columns and high control concentrations indicate there was an initial release of NAPL in the control column. The results

suggest that the high carbon content in the fly ash is suitable for immobilization of organic constituents in soils contaminated with petroleum residues.

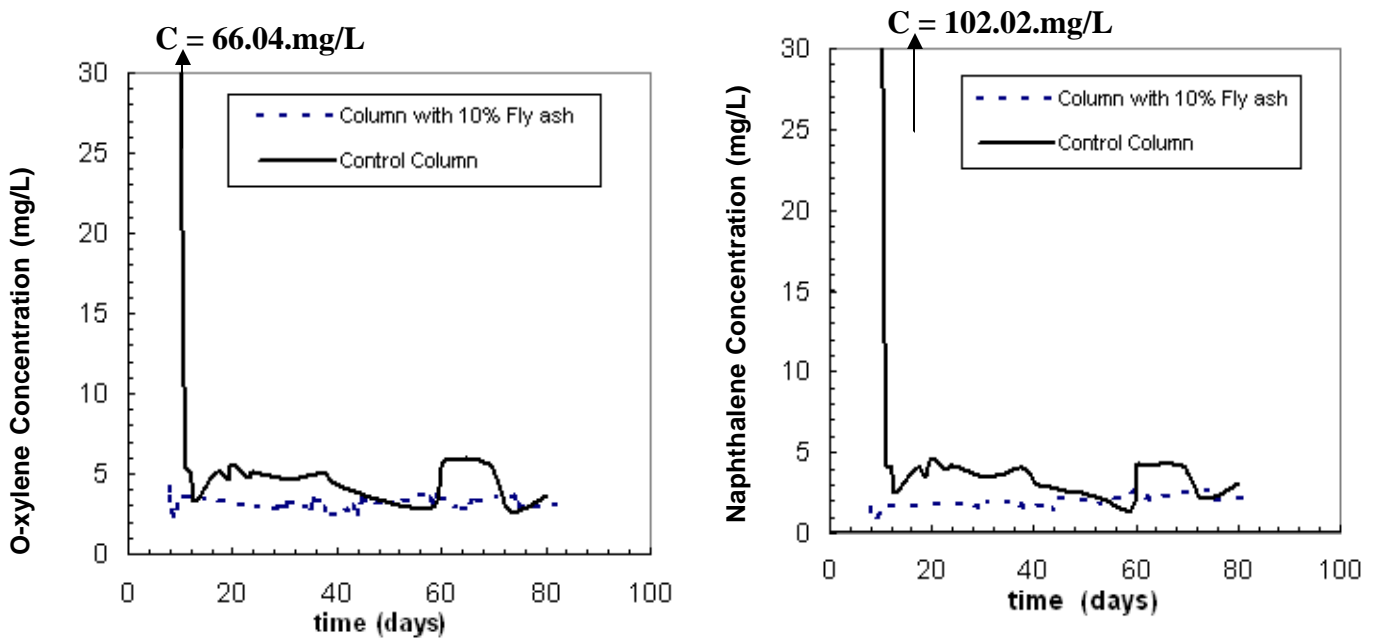


FIGURE 2 O-xylene and naphthalene concentrations measured in the effluents collected from the two columns.

To conclude, we observed that the results of the batch-scale adsorption tests conducted on the fly ashes revealed that the unburned carbon content of the fly ash controlled the sorption capacity and Brandon Shores fly ash had very good naphthalene sorption properties due to the presence of high carbon content in its structure.

Column leaching tests were performed on the fly ash stabilized specimens and borrow material originally contaminated with a synthetic NAPL. The results indicated that the naphthalene and o-xylene concentrations in the effluents collected from the fly ash stabilized specimens were lower than those collected from the control specimen (i.e., borrow material). Moreover, addition of fly ash limited the initial release of the contaminants from the specimen, compared to a longer release observed for the control column.

Grant No. 05HQGR0124 State of the Art Models and Practices Review and Design Document Development for a Navigation System Simulation Model

Basic Information

Title:	Grant No. 05HQGR0124 State of the Art Models and Practices Review and Design Document Development for a Navigation System Simulation Model
Project Number:	2005MD141S
Start Date:	5/1/2005
End Date:	9/30/2006
Funding Source:	Supplemental
Congressional District:	05 MD
Research Category:	Engineering
Focus Category:	Models, None, None
Descriptors:	
Principal Investigators:	Paul Schonfeld

Publication

1. Tao, X., and Schonfeld, P., Selection and Scheduling of Interdependent Transportation Projects with Island Models, Annual TRB Meeting, Jan. 2006, (06-1105), forthcoming in Transp. Res. Record.
2. Wang, S., Tao, X., and Schonfeld, P., Modeling Shippers Response to Scheduled Waterway Lock Closures, Annual TRB Meeting, Jan. 2006, (06-1833), forthcoming in Transp. Res. Record.

ANALYSIS OF TOWBOAT OPERATING AREAS

Draft Report Prepared for the Institute for Water Resources (IWR)

By

Min Wook Kang and Paul Schonfeld

March 16, 2006

Department of Civil and Environmental Engineering
University of Maryland, College Park

TABLE OF CONTENTS

EXECUTIVE SUMMARY.....	5
1. INTRODUCTION.....	6
2. ANALYTIC APPROACH.....	7
2.1. Study Area.....	7
2.2. Data	10
2.3. Definition of Towboat Lockages.....	13
2.4. Seasonal Variation of Towboat Lockages.....	13
3. TOWBOAT MOVEMENTS.....	16
3.1. Identification of Unique Towboats Using the UMR Locks during the Peak	16
3.2. Tracking of Towboats during the UMR Off-peak.....	17
3.3. Lock Use by Towboats in the Study Area	23
4. CONCLUSIONS	32
ACKNOWLEDGEMENTS.....	32
REFERENCES	33
APPENDIX	36

LIST OF FIGURES

Figure 1. Study Area	8
Figure 2. Lock Names in the Study Area	11
Figure 3. Lock Numbers in the Study Area.....	12
Figure 4. Average Monthly Towboat Lockages by Districts (2000-2004).....	14
Figure 5. Average Monthly Towboat Lockages for the UMR, Illinois, and Ohio (2000-2004)....	15
Figure 6. Average Monthly Towboat-Loackges by the Unique Towboats Using the UMR Locks during the Peak (2000-2004).....	16
Figure 7. Districts Visited by the 90% Unique Towboats during the UMR Off-peak.....	22
Figure 8. UMR Towboat Lockages during the Peak and Off-peak (2000-2004).....	25
Figure 9. Illinois Towboat Lockages during the UMR Peak and Off-peak (2000-2004).....	25
Figure 10. Ohio Towboat Lockages during the UMR Peak and Off-peak (2000-2004).....	28
Figure 11. Tennessee Towboat Lockages during the UMR Peak and Off-peak (2000-2004).....	28
Figure 12. Towboat Lockages on Gulf Intra-coastal Waterway during the UMR Peak and Off-peak (2000-2004).....	29
Figure 13. Average Monthly Towboat Traffic of the 90% Unique Towboats at the UMR and IL Locks during the UMR Peak and Off-peak (2000-2004).....	34
Figure 14 (a). Average Monthly Towboat Traffic of the 90% Unique Towboats at the Ohio Locks during the UMR Peak (2000-2004).....	35
Figure 14 (b). Average Monthly Towboat Traffic of the 90% Unique Towboats at the Ohio Locks during the UMR Off-Peak (2000-2004).....	36
Figure 15 (a). Average Monthly Towboat Traffic of the 90% Unique Towboats in the Lower MVD, SWD, and SAD during the UMR Peak (2000-2004).....	37
Figure 15 (b). Average Monthly Towboat Traffic of the 90% Unique Towboats in the Lower MVD, SWD, and SAD during the UMR Off-Peak (2000-2004).....	37

LIST OF TABLES

Table 1. Analytic Tasks for Identifying the Impact of the UMR Seasonality	6
Table 2. Districts in the Study Area	7
Table 3. Locks in the Study Area.....	9
Table 4. Three Notable States of UMR Towboat Traffic over 12 Months	15
Table 5. Tracking Results for the 90% Towboats during the UMR Off-Peak (2000-2004)	17
Table 6. Off-peak States of the 90% Unique Towboats.....	21
Table 7. Lock Use by Towboats in the UMR and Illinois Systems (2000-2004).....	24
Table 8. Lock Use by Towboats in the Ohio and Its Tributaries (2000-2004)	26
Table 9. Lock Use by Towboats in the Lower MVD and SWD (2000-2004).....	30
Table 10. Lock Use by Towboats in the SAD, NAD, and NWD (2000-2004)	30

EXECUTIVE SUMMARY

Towboats migrate to the Upper Mississippi River (UMR) during the early spring and out of it in late fall; thus, seasonal variation in the system use would be significant and also affect other river basins. Therefore, it should be noted that serious distortions could result in analyzing this waterway system unless we take such seasonal fluctuations into account.

According to several studies on UMR lock operation (1-3), the seasonality is driven not only by the UMR's physical operating conditions (freezing during winter) but also by the seasonal variation in demand (e.g., grains and coal shipments). Among these, Sweeney (2004) and Center for Transportation Studies (CTS) at the University of Missouri–St. Louis (2005), which largely motivated the present analysis, indicate that towboats which choose to operate on the UMR system during the peak period move outside that system and operate during the winter because they can thus earn greater profit. Those studies suggest that the towboats are always busy. However, it should be noted that some towboats may not operate during the winter due either to lack of demand or the freezing the UMR. In order to identify the fraction of the towboats that continue to operate during the winter and their winter operation areas, (i) three distinct UMR time frames are specified based on its monthly towboat traffic; peak (April through November), off-peak (January and February), and transition periods (December and March). In addition, (ii) we determine the unique towboats that contribute most UMR towboat lockages during the peak and (iii) try to track them during the off-peak.

The tracking results during the winter for every unique towboat in the 90% group as well as lock use by towboats throughout the study area are the main outputs of the analysis. However, it should be noted that the tracking results may miss some vessels that operate without passing through locks since they depend on lock data (OMNI for 2000-2004) from the U.S. Army Corps of Engineers. The study area of this analysis includes all divisions of the U.S. waterway system to which the towboats serving the UMR can realistically shift in winters.

It is found that during the UMR off-peak towboats hardly operate upstream of UMR Lock #25 and decrease their operation significantly in the segment bounded by UMR Locks #26 and #27. In addition, towboat lockages at the lower Illinois (IL) locks (#07 and #08) increase during the UMR off-peak due to towboats shifting from the UMR. Ohio (OH) towboat lockages decrease slightly during the UMR off-peak; however, towboats shifting from the UMR to Ohio during the off-peak have more Ohio lockages than those generated by towboats shifting during the peak. Finally, it seems that the UMR seasonality affects mostly the Illinois, Ohio and the UMR itself. Detailed results are summarized in the conclusions of this report. These results are intended to support the development of the NASS navigation simulation model and help improve the effectiveness of the U.S. inland waterways.

1. INTRODUCTION

The Upper Mississippi River (UMR), which has 29 lock and dam facilities along it, carries a large fraction of the cargo moving on the U.S. inland waterways. It periodically experiences severe congestion (particularly at the lower UMR locks) due to seasonal variations in system use as well as to the relatively short (600 ft) lock chambers provided at most locks. Many towboats now exceed the 600 ft length and require relatively slow double cut lockages. According to Sweeney (2004) and the UMSL Center for Transportation Studies (CTS) (2005), the UMR seasonality is evident because the operating conditions become extremely difficult or impossible in winter due to the freezing of the river and demand (e.g., grains and coal shipments) is seasonal as well. Many towboats migrate to the UMR during the early spring and out of it in late fall; cyclic influx and efflux of towboats to the UMR has been observed in the previous studies (1-3). The objective of this analysis is to understand characteristics of the UMR towboat operation and provide practical information about towboat use in the study area for the UMR navigation system simulation (NaSS) model, which is being developed by the U.S. Army Corps of Engineers. Some obvious questions that provide the major impetus for this analysis are listed below.

- *When are the peak and off-peak seasons for the UMR towboat operation?*
- *What fractions of the towboats that normally operate on the UMR in summers continue to operate during in winters?*
- *Where else (if anywhere) do they go?*
- *What is the impact of the UMR seasonality on the other river systems?*

We hope the answer to the questions will help support the development of the NaSS model by identifying seasonal operating patterns and interactions among various rivers; furthermore, the analysis procedures presented in this study should help in developing demand and equipment assignment inputs for simulating waterways. Table 1 presents the analytic tasks conducted in this study to resolve the questions. The study area, data, and definition of towboat lockages required for the analytic tasks are illustrated in the next sections.

Table 1. Analytic Tasks for Identifying the Impact of the UMR Seasonality

Task 1	Identify seasonal variation of towboat lockages at the UMR system over 12 months
Task 2	Determine the departing and entering periods of the towboats to the UMR system
Task 3	Identify the number and IDs of unique towboats required to account for most (90%) UMR towboat lockages during non-freezing condition
Task 4	Determine the state of the unique towboats during the winter (whether they continue to use locks or not and where they operate)
Task 5	Compare total towboat lockages and the lockages attributable to the unique towboats

2. ANALYTIC APPROACH

2.1. Study Area

The study area of this analysis includes all divisions of the U.S. waterway system in which the towboats serving the UMR locks can realistically operate. The Pacific Ocean Division (POD) is excluded in the study area since towboats are assumed to stay on inland waterways. Figure 1 shows districts in the study area by divisions. The official symbol and Engineer Reporting Organization Code (EROC) of each district in the study area are shown in Table 2.

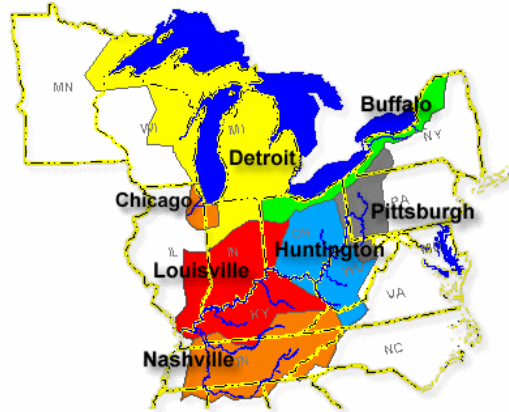
Table 2. Districts in the Study Area

Name	Official Symbol	EROC
Mississippi Valley Division	MVD	B0
St. Paul District	MVP	B6
Rock Island District	MVR	B5
St. Louis District	MVS	B3
Memphis District	MVM	B1
Vicksburg District	MVK	B4
New Orleans District	MVN	B2
Great Lakes & Ohio River Division	LRD	H0
Huntington District	LRH	H1
Louisville District	LRL	H2
Nashville District	LRN	H3
Pittsburgh District	LRP	H4
Buffalo District	LRB	H5
Chicago District	LRC	H6
Detroit District	LRE	H7
North Atlantic Division	NAD	E0
Baltimore District	NAB	E1
New York District	NAN	E3
Norfolk District	NAO	E4
Philadelphia District	NAP	E5
New England District	NAE	E6
Southwestern Division	SWD	M0
Fort Worth District	SWF	M2
Galveston District	SWG	M3
Little Rock District	SWL	M4
Tulsa District	SWT	M5
South Atlantic Division	SAD	K0
Charleston District	SAC	K2
Jacksonville District	SAJ	K3
Mobile District	SAM	K5
Savannah District	SAS	K6
Wilmington District	SAW	K7
Northwestern Division	NWD	G0
Portland District	NWP	G2
Seattle District	NWS	G3
Walla Walla District	NWW	G4
Kansas City District	NWK	G5
Omaha District	NWO	G6
South Pacific Division	SPD	L0
Los Angeles District	SPL	L1
Sacramento District	SPK	L2
San Francisco District	SPN	L3
Albuquerque District	SPA	L4

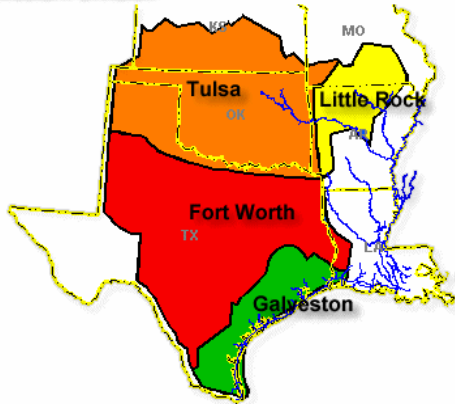
Mississippi Valley Division



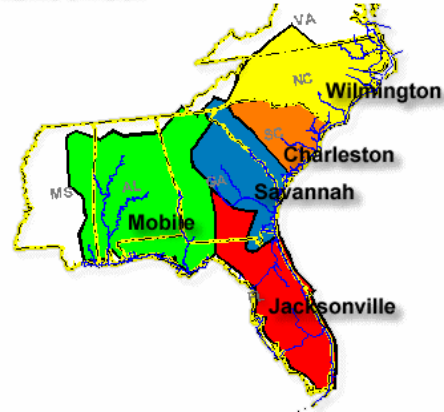
Great Lakes and Ohio River Division



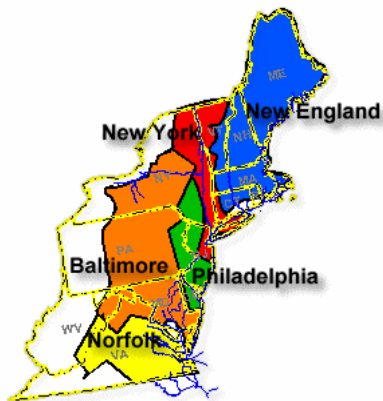
Southwestern Division



South Atlantic Division



North Atlantic Division



Northwestern Division

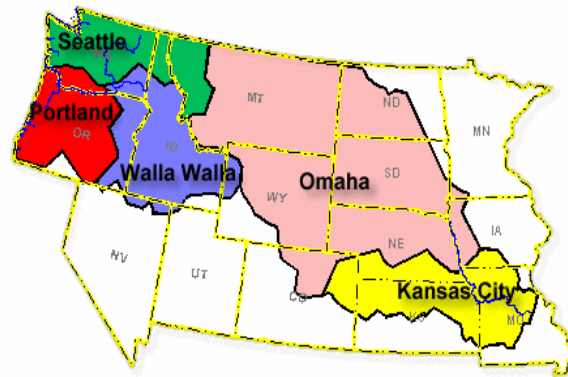


Figure 1. Study Area¹

¹ Figures are quoted from the Navigation Data Center of the U.S. Army Corps of Engineers

In the current inland waterway system, locks are critical data-collection points at which various kinds of information about vessel movements are recorded, including unique ID, start and end of lockage time and travel direction of the vessel. Our analysis track vessels movements based on the information recorded at locks. Table 3 shows the locks on various rivers in the districts of the study area. Many districts in the study area (e.g., all districts in the South Pacific Division (SPD) and Memphis (MVM), Baltimore (NAB), Philadelphia (NAP), New England (NAE), Fort Worth (SWF), Charleston (SAC), Kansas City (NWK), and Omaha (NWO) districts) have no locks on their rivers. Most locks in Table 3 are shown in Figures 2 and 3; however, some locks shaded in the table are not presented in the figures since towboat lockages are never observed in such areas. It is noted that the unique lock numbers presented in Figure 3 (rather than the lock names) are used throughout this report.

Table 3. Locks in the Study Area

Division	District (EROC)	River (Code)	# of Locks	Names of Lock
MVD	MVP (B6)	Mississippi River (MI)	13	1, 2, 3, 4, 5, 5A, 6, 7, 8, 9, 10, Upper St. Anthony Falls, Lower St. Anthony Falls
	MVR (B5)	Illinois River (IL)	8	Lagrange, Peoria, Starved Rock, Marseilles, Dresden Island, Brandon Road, Lockport, Thomas J. O'Brien
		Mississippi River (MI)	12	11, 12, 13, 14, 15, 16, 17, 18, 19, 20, 21, 22
	MVS (B3)	Kaskaskia River (KS)	1	Kaskaskia
		Mississippi River (MI)	4	24, 25, 26 (Melvin Price), 27
	MVK (B4)	Ouachita and Black Rivers (OB)	6	Jonesville, Columbia, Felsenthal, H.K. Thatcher, 6, 8
		Red River (RR)	5	L.C. Boggs, John H. Overton, 3, Russell B. Long, Joe D. Waggonner
		Pearl River (PR)	3	1, 2, 3
	MVN (B2)	Old River (OD)	1	Old River
		Atchafalaya River (AT)	1	Berwick
		Gulf Intra-coastal Waterway (GI)	10	Port Allen, Bayou Sorrel, Inner Harbor Navigation Canal, Algiers, Harvey, Bayou Boeuf, Leland Bowman, Calcasieu, Schooner Bayou Control Structure, Catfish Point Control Structure
		Bayou Tech (BT)	1	Keystone
		Freshwater Bayou (FB)	1	Freshwater Bayou
	Calcasieu River (CA)	1	Calcasieu Salt Water Barrier	
LRD	LRH (H1)	Kanawha River (KA)	3	Winfield, Marmet, London
		Ohio River (OH)	6	Willow Island, Belleville, Racine, Greenup, Robert C. Byrd, Capt. A. Meldahl,
	LRL (H2)	Green & Barren R. (GB)	4	1, 2
		Ohio R. (OH)	9	Olmsted, 53, 52, Smithland, J.T. Myers, Newburgh, Cannelton, McAlpine, Markland
	LRN (H3)	Clinch River (CI)	1	Melton Hill
		Cumberland River (CU)	4	Barkley, Cheatham, Old Hickory
		Tennessee River (TN)	9	Kentucky, Pickwick, Wilson, Wheeler, Guntersville, Nickajack, Chickamauga, Watts Bar, Ft. Loudon
	LRP (H4)	Allegheny River (AG)	8	2, 3, 4, 5, 6, 7, 8, 9
		Monongahela River (MN)	10	2, 3, 4, Maxwell, Grays Landing, 7, Point Marion, Morgantown, Hidebrand, Opekiska
		Ohio River (OH)	6	Hannibal, Pike Island, New Cumberland, Montgomery, Dashields, Emsworth

Division	District (EROC)	River (Code)	# of Locks	Names of Lock
LRD	LRB (H5)	Black Rock Channel & Tonawanda Harbor (BR)	1	Black Rock
	LRE (H7)	Fox River (FX).	19	De Pere, Little Kaukauna, Rapide Croche, Kaukauna Guard, Kaukauna 1~5, Little Chute Guard, Little Chute 2, Upper Little Chute Combined, Lower Little Chute Combined, Cedars, Appleton 1~4, Menasha
		St. Marys River (SM)	4	Sabin, Davis, New Poe, MacArthur
		The Inland Route (IN)	1	Alanson
LRC (H6)	Chicago Harbor Cha.	1	Chicago	
SWD	SWL (M4)	McClellan-Kerr Arkansas River Navigation System (MK)	12	Norrell, 2, Joe Hardin, Emmett Sander, 5, David D. Terry, Murray, Toad Suck Ferry, Arthur V. Ormond, Dardanelle, Ozark, James W. Trimble
	SWT (M5)	McClellan-Kerr Arkansas River Navigation System (MK)	5	W.D. Mayo, Robert S. Kerr, Webbers Falls, Chouteau, Newt Graham
	SWG (M3)	Gulf Intra-coastal Waterway (GI)	4	Colorado River East, Colorado River West, Brazos East Gate, Brazos West Gate
SAD	SAM (K5)	Alabama-Coosa River (AL)	3	Claiborne, Millers Ferry, Robert F. Henry
		Black Warrior & Tombigee Rivers (BW)	6	Coffeerville, Demopolis, Selden, William Bacon Oliver, Holt, John Hollis Bankhead
		Tennessee Tombigbee Waterway (TT)	10	Howell Heflin, Tom Bevill, John C. Stennis, Aberdeen, Amory, Glover Wilkins, Fulton, John Rankin, G.V. Sonny Montgomery, Jamie L. Whitten
		Apalachicola, and Chattahoochee Flint Rivers (AP)	3	Jim Woodruff, George W. Andrews, Walter F. George
	SAJ (K3)	Canaveral Harbor (CN)	1	Canaveral
		Cross Florida Barge Canal (CF)	3	Henry Holland Buckman, Eureka, English
		Okeechobee Waterway (OK)	5	St. Lucie, Port Mayaca, Moore Have, Ortona, W.P. Franklin Lock and Control Structure
		Oklawaha River (OL)	1	Moss Bluff
	SAS (K6)	Savannah River (SV)	1	New Savannah Bluff
SAW (K7)	Cape Fear River (FR)	3	1, 2, William O. Huske	
NAD	NAN (E3)	Hudson River (HU)	1	Troy
	NAO (E4)	Atlantic Intra-Coastal Waterway (AI)	1	Great Bride Lock (Albemarle & Chesapeake Canal)
		Dismal Swamp Canal Route (DS)	2	Deep Creek, South Mills
NWD	NWS (G3)	Lake Washington Ship Canal (WS)	1	Hiram M. Chittenden
	NWP (G2)	Willamette River (WI)	2	Willamette Falls 1-4, Willamette Falls Guard
		Columbia River (CO)	3	Bonneville, The Dalles, John Day
	NWW (G4)	Columbia River (CO)	1	McNary
		Snake River (SN)	4	Ice Harbor, Lower Monumental, Little Goose, Lower Granite

2.2. Data

U.S. Army Corps of Engineers OMNI data compiled from 2000 through 2004 are used to conduct this analysis; vessel IDs and types, locations of lockage (i.e., lock, river, and district codes), travel directions, and times of lockages are extracted from the OMNI data.

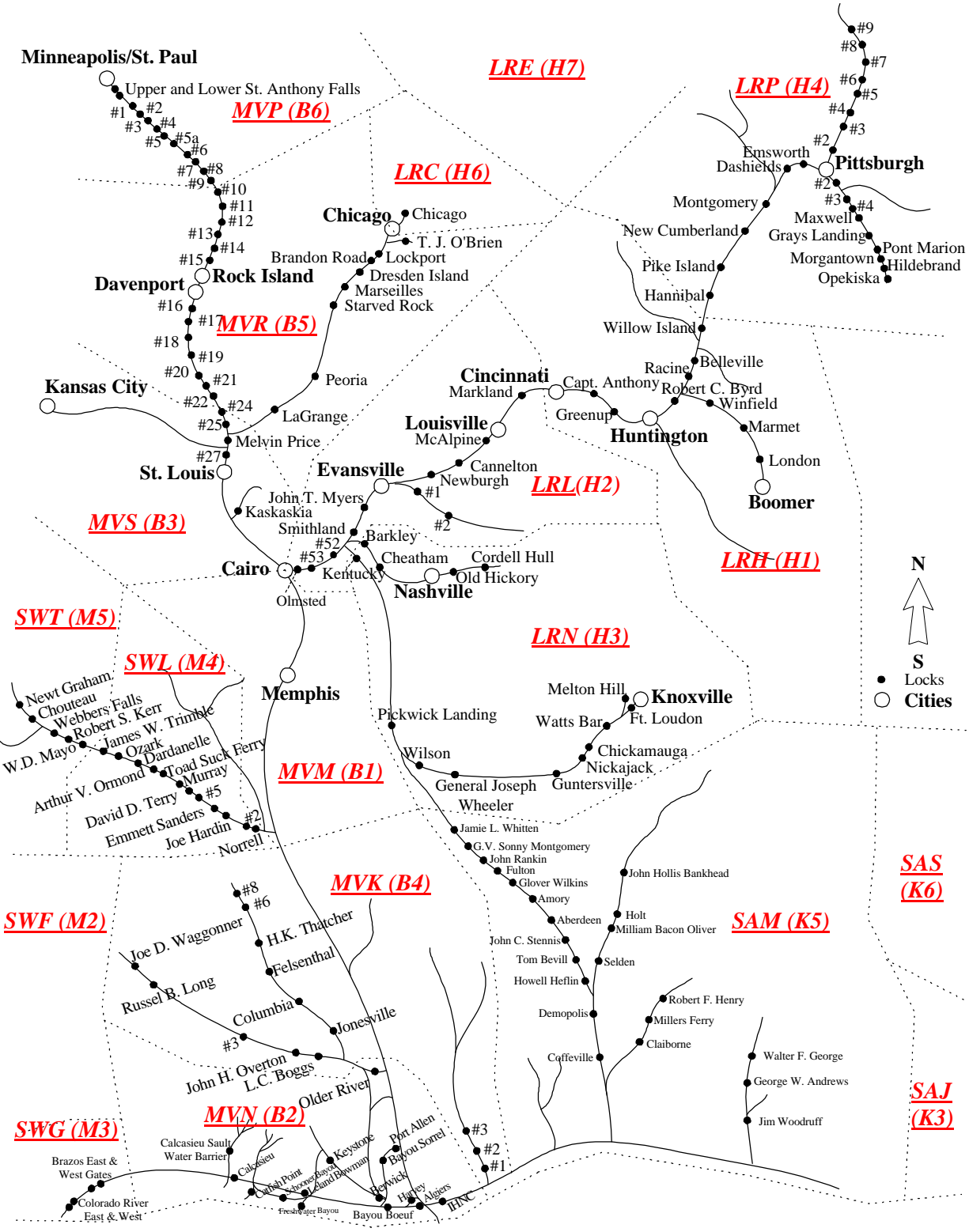


Figure 2. Lock Names in the Study Area²

² Locks which are shaded in Table 3 are not covered within Figure 2.

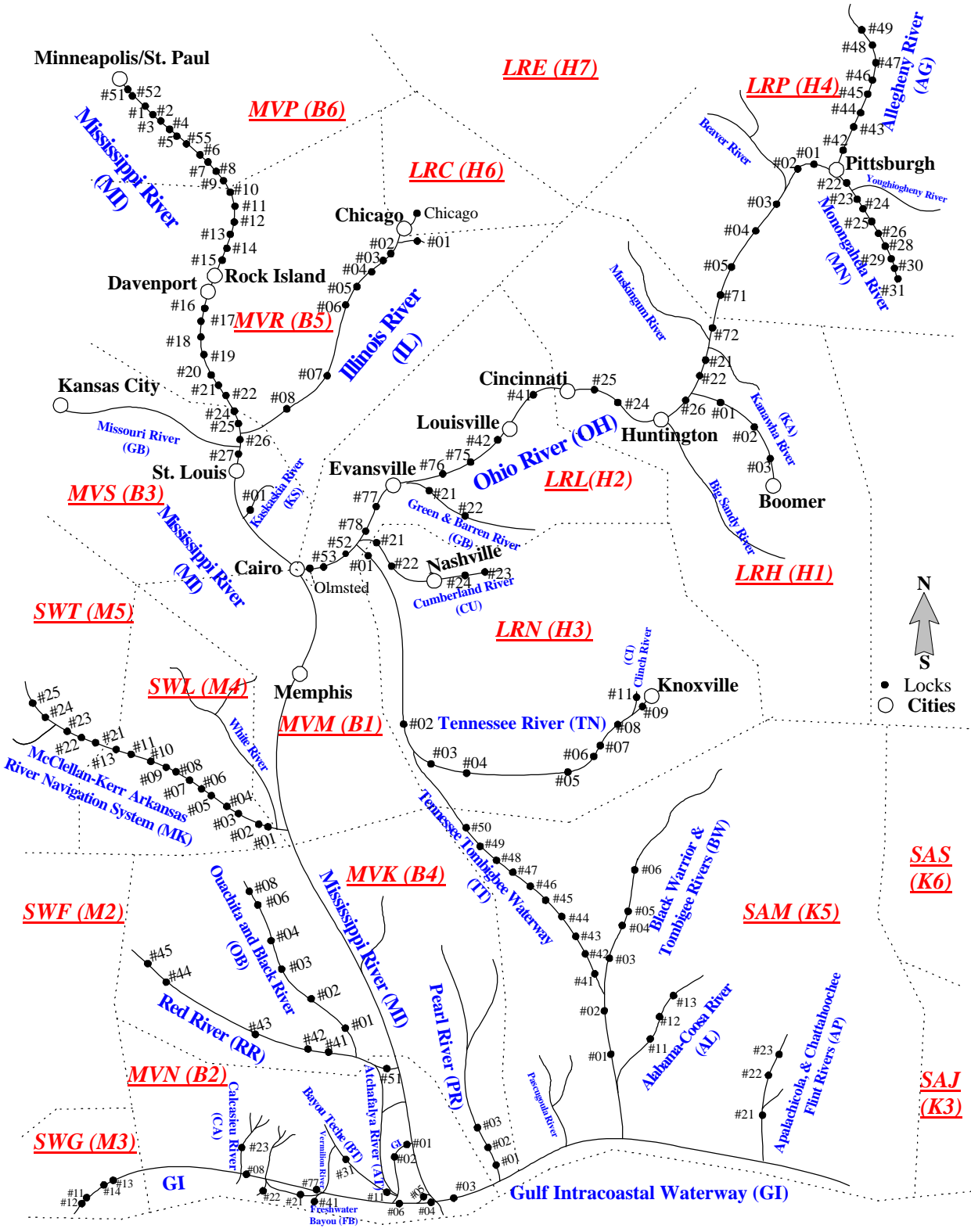


Figure 3. Lock Numbers in the Study Area³

³ Locks which are designated as in Figure 2

2.3. Definition of Towboat Lockages

We try to identify all towboats passing through locks in the study area to track movements of the unique towboats utilizing the UMR locks. However, it is noted that the tracking process may miss some vessels that are operating but are not traveling through locks. In this study, towboat lockages at a lock are defined as lockages by towboats, whether in tow or light, that pass through the lock. For example, if one towboat carrying several barges and three other towboats moving as light boats pass through a certain lock together, the number of towboat lockages for this movement is counted as four. However, counting and identifying towboats at a lock may be difficult since some light boats are locked together with a towboat carrying barges, without being clearly identified. In the current data recording system (such as LPMS and OMNI) some records show that x number of light boats are locked with a specific towboat; however, the information about those light boats is not recorded. The limitations and quality of the data recording system are well summarized in a recent study by Lisney (2005).

2.4. Seasonal Variation of Towboat Lockages

As shown in Figure 4, towboat lockages are steadily distributed over 12 months for most districts in the study area; however, those for the districts in the northern part of the Mississippi Valley Division (MVD) (i.e., Saint Paul (MVP), Rock Island (MVR), and Saint Louis (MVS)) fluctuate. This indicates that monthly towboat lockages in districts in the northern MVD are seasonal; however, those at the other districts are largely uniform. It is noted that the UMR, Illinois, and Ohio are three major rivers which are closely connected in the northern MVD (particularly in the MVS) so that towboats can easily shift among those rivers. Thus, seasonal use of towboats on one of those three rivers may affect the other two.

Towboat operation in the UMR system is not stable; towboats enter the UMR system in the early spring and leave the system in late fall. According to Sweeney (2005) and the CTS at the University of Missouri–St. Louis (2005), towboats that choose to operate on the UMR system during the peak period exit the UMR during the winter because they can earn higher profits elsewhere. Those studies imply that the towboats are always busy; however, some towboats may not operate during the winter due either to freezing of the river or lack of demand. In order to identify the fraction of the towboats that continue to operate during the winter, three distinct UMR time frames are specified based on its monthly towboat traffic over 12 months. Based on the specified periods, we determine the unique towboats which contribute most UMR lockages during the peak period and then try to track them during the off-peak. Additionally, there are no recorded towboat lockages in the Buffalo (LRB), Chicago (LRC), Detroit (LRE), and New York (NAN) districts despite the presence of locks, as shown in Figure 4. This suggests that traffic in those districts is mostly recreational; hence, we disregard those districts in the study area.

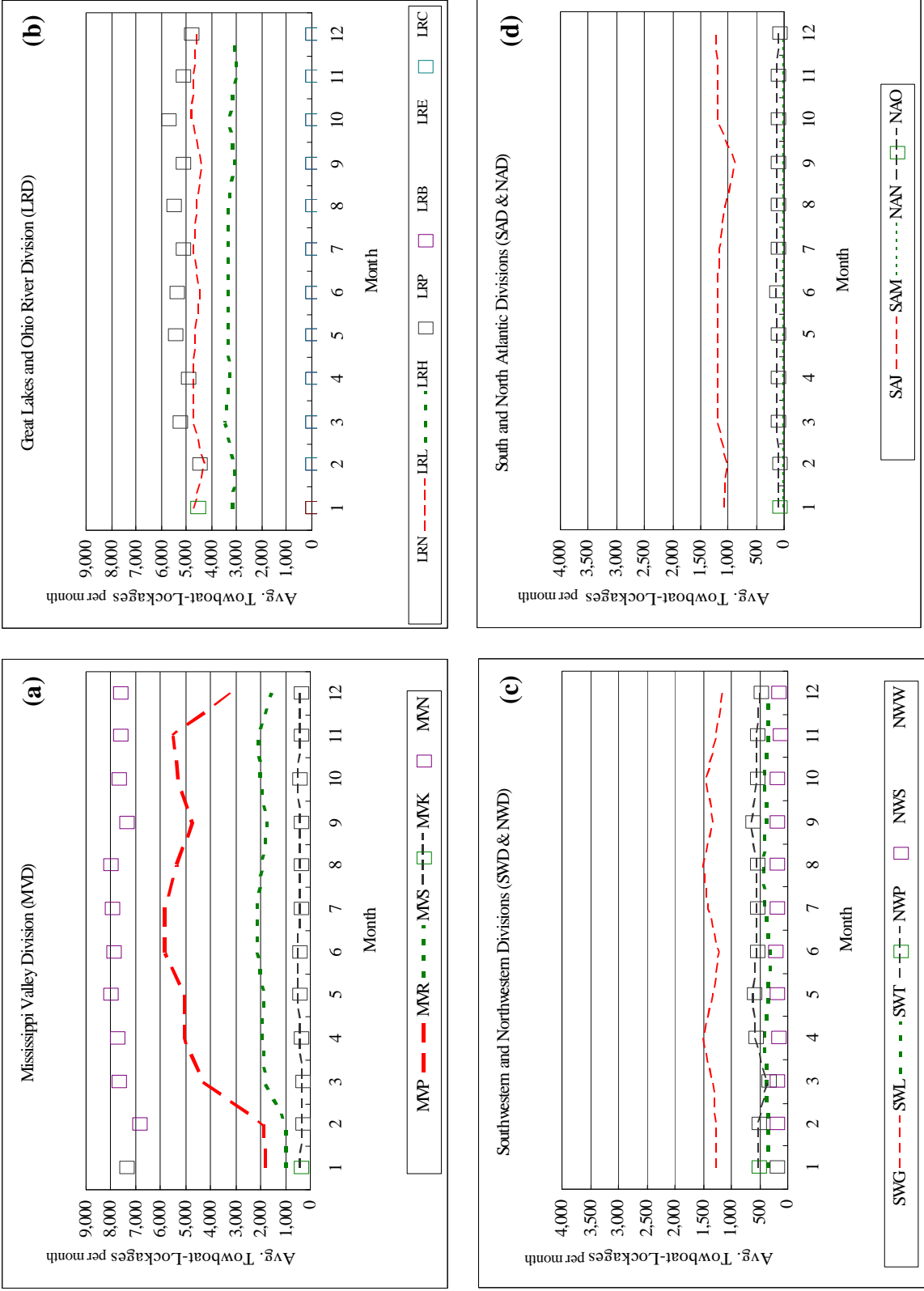


Figure 4. Average Monthly Towboat Lockages by Districts(2000-2004)

Figure 5 presents average monthly towboat lockages over 12 months for the three distinct rivers (the UMR, Illinois, and Ohio) during 2000-2004. As shown in Figure 5, the average monthly towboat lockages in the UMR system fluctuate seasonally while there is no significant seasonal variation in the Ohio and Illinois. In the UMR system, towboats generate steadily many lockages in April through November and steadily few lockages during January and February. Furthermore, distinct transition stages are evident between the peak and off-peak periods. We subdivide the UMR towboat traffic into three different stages (Peak, Off-Peak, and Transition) and summarize them in Table 4. It has been observed that 808 unique towboats operate in the UMR in a year, on average. Among them only 52% (419 towboats) operate during the off-peak while 96% (778 towboats) operate during the peak. This statistic shows that many peak-period towboats on the UMR would cease their operation or move elsewhere during the off-peak of the UMR.

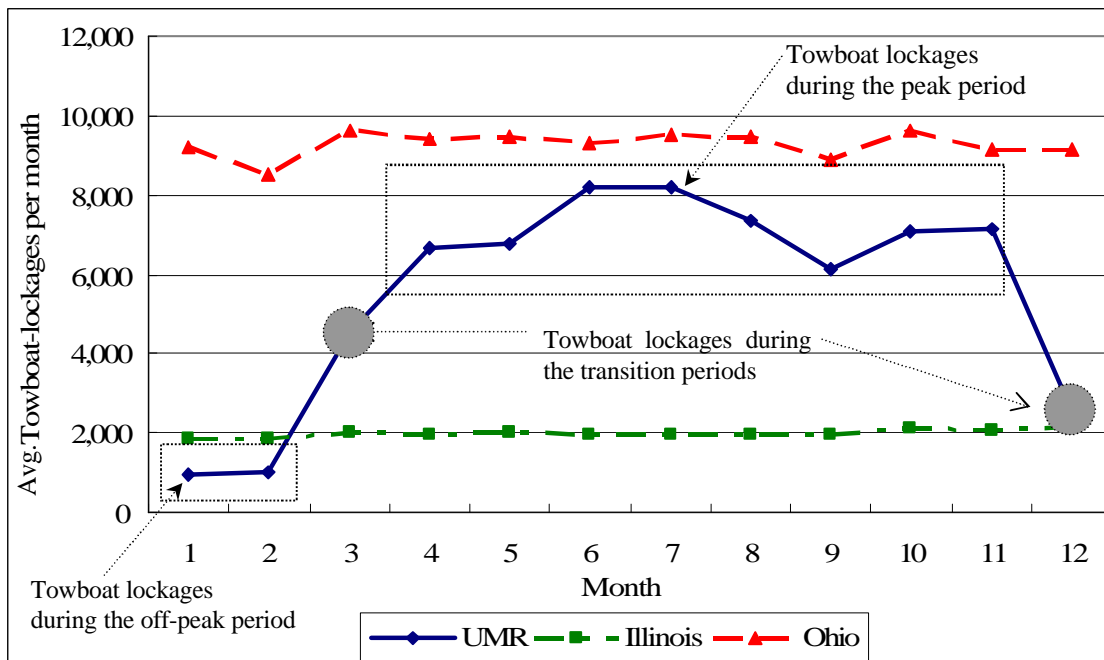


Figure 5. Average Monthly Towboat Lockages for the UMR, Illinois, and Ohio (2000-2004)

Table 4. Three Notable States of UMR Towboat Traffic over 12 Months

	Peak	Transition	Off-Peak	Entire
Period	Apr. through Nov.	Mar. and Dec.	Jan. through Feb.	Jan. through Dec.
Towboat Traffic	High and Steady	Fluctuating	Low and Steady	-
Number of Operating Tows, on Average	778	579	419	808

3. TOWBOAT MOVEMENTS

3.1. Identification of Unique Towboats Using the UMR Locks during the Peak

In section 2.4., we specified three distinct time frames for the UMR system (peak, off-peak, and transition periods). Now we try to determine unique towboats that normally operate in the UMR system during the peak and that contribute most peak-period UMR lockages. In order to identify the unique towboats having such characteristics, we define the unique towboats required to account for 90% of peak-period UMR towboat lockages.

Figure 6 shows cumulatively the average towboat lockages generated by each unique towboat using the UMR locks during the peak period. The busiest towboats (starting with #1) are on the left. It is noted that among the 778 unique towboats using the UMR locks during the peak period (refer to Table 4), the top 203 towboats generate 90% of the peak-period UMR towboat lockages. These towboats are tracked during the off-peak period in the next section, using the observed lockage information from the UMR and other rivers.

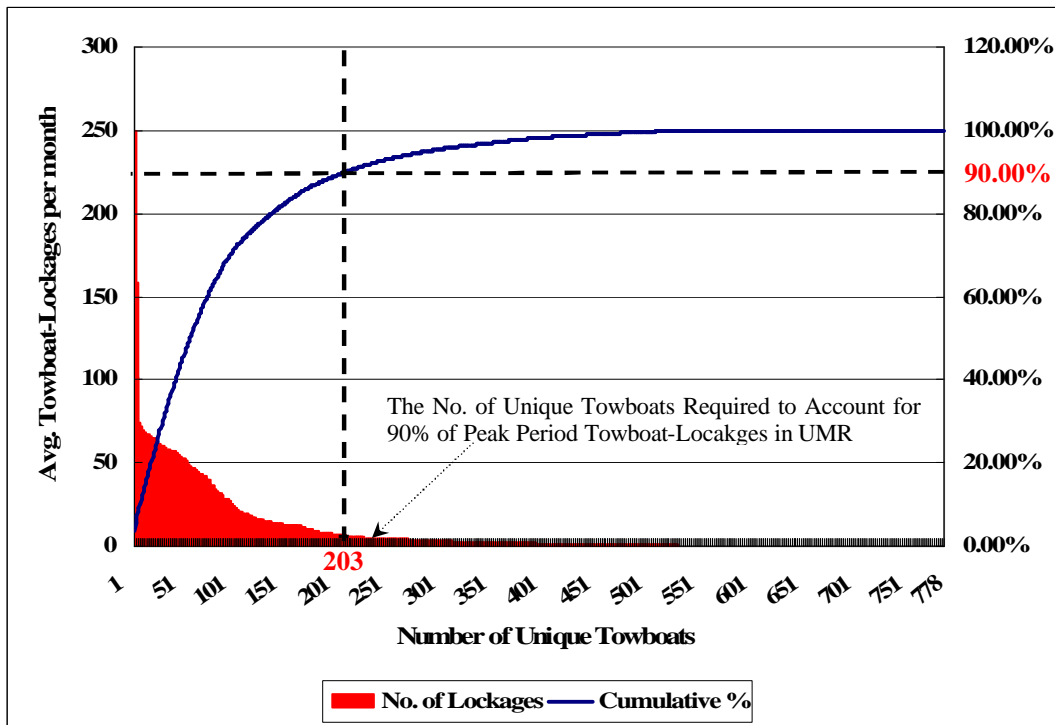


Figure 6. Average Monthly Towboat Lockges Generated by the Unique Towboats Using the UMR Locks during the Peak Period (2000-2004)

3.2. Tracking of Towboats during the UMR Off-peak (Jan. and Feb.)

In this section the unique towboats in the 90% group (203 in total) are tracked individually during the UMR off-peak. The tracked information for each unique towboat, including its observed off-peak lockages (average monthly) in different river systems, is presented in every line of Table 5. It is noted that during the off-peak period, the unique towboats are never observed outside the rivers presented in Table 5. In addition, numbers presented in the leftmost column of Table 5 specify the ranks of the busiest unique towboats during the UMR peak based on their observed lockages (in the second left column in Table 5). The shaded cells in Table 5 indicates whether each unique towboat is observed in corresponding rivers. This shows that the unique towboats are mostly observed in the UMR, Illinois, and Ohio systems during the off-peak and slightly in the Tennessee River (TN), McClellan-Kerr Arkansas River Navigation System (MK), and Gulf Intra-coastal Waterway (GI). More interestingly: (i) the top three unique towboats, which generate considerable UMR lockages during the peak, are not observed at any locks in the study area during the off-peak; furthermore, (ii) UMR lockages by most unique towboats decrease significantly during the off-peak (refer to left second and fourth columns in Table 5). Presumably, these are two of the main reasons why total UMR towboat lockages decrease significantly during the off-peak.

Decrease overall

Table 5. Tracking Results for the 90% Towboats during the UMR Off-Peak (2000-2004)

Rank 4 of the Unique Tows	Average Monthly Towboat Lockages Generated by the 90% Unique Towboats															Unit: Towboat Lockages/month
	During the UMR Peak		During the UMR Off-peak													
	In the UMR	Outside the UMR	In the UMR (% of the peak)	Outside the UMR 5												Total
				IL	OH	TN	CU	GB	MN	MK	OD	OB	GI	TT		
1	250	0	0 (0%)	0	0	0	0	0	0	0	0	0	0	0	0	0
2	158	0	0 (0%)	0	0	0	0	0	0	0	0	0	0	0	0	0
3	102	0	0 (0%)	0	0	0	0	0	0	0	0	0	0	0	0	0
4	74	1	12 (16%)	7	0	0	0	0	0	0	0	0	0	0	0	7
4	74	1	8 (11%)	17	1	0	0	0	0	0	0	0	0	0	0	18
6	72	2	11 (15%)	19	0	0	0	0	0	0	0	0	0	0	0	19
6	72	4	10 (14%)	18	0	0	0	0	0	0	0	0	0	0	0	18
8	70	0	6 (9%)	11	0	0	0	0	0	0	0	0	0	0	0	11
8	70	3	12 (17%)	17	0	0	0	0	0	0	0	0	0	0	0	17
10	68	2	3 (4%)	8	16	0	0	0	0	0	0	0	0	0	0	24
11	67	1	12 (18%)	6	0	0	0	0	0	0	0	0	0	0	0	6
11	67	0	6 (9%)	12	2	0	0	0	0	0	0	0	0	0	0	14
11	67	1	12 (18%)	9	0	0	0	0	0	0	0	0	0	0	0	9
14	66	2	0 (0%)	0	26	2	0	0	0	0	0	0	0	0	0	28
14	66	2	3 (5%)	6	13	0	0	0	0	0	0	0	0	0	0	19
16	65	2	1 (2%)	2	23	0	0	0	0	0	0	0	0	0	0	25
16	65	3	13 (20%)	18	0	0	0	0	0	0	0	0	0	0	0	18
16	65	3	2 (3%)	5	25	0	0	0	0	0	0	0	0	0	0	30
16	65	3	6 (9%)	7	0	0	0	0	0	0	0	0	0	0	0	7
20	64	0	11 (17%)	0	0	0	0	0	0	0	0	0	0	0	0	0
21	63	6	15 (22%)	15	7	0	0	0	0	0	0	0	0	0	0	22
22	62	1	2 (3%)	4	0	0	0	0	0	0	0	0	0	0	0	4

⁴ The busiest unique towboats during the UMR peak (starting with # 1) are on the top.

⁵ Refer to Table 3 for river codes. The unique tows are never observed in the other rivers absent from Table 5.

Rank of the Unique Tows	Average Monthly Towboat Lockages Generated by the 90% Unique Towboats														Unit: Towboat Lockages/month	
	During the UMR Peak		During the UMR Off-peak													
	In the UMR	Outside the UMR	In the UMR (% of the peak)	Outside the UMR											Total	
				IL	OH	TN	CU	GB	MN	MK	OD	OB	GI	TT		
22	62	6	6 (10%)	8	0	0	0	0	0	0	0	0	0	0	0	8
22	62	6	1 (2%)	3	26	1	0	0	0	0	0	0	0	0	0	30
25	61	5	2 (3%)	3	22	2	0	0	0	0	0	0	0	0	0	27
25	61	3	10 (15%)	11	0	0	0	0	0	0	0	0	0	0	0	11
27	60	4	2 (3%)	3	27	0	0	0	0	0	0	0	0	0	0	30
27	60	3	0 (0%)	0	37	0	0	0	0	0	0	0	0	0	0	37
29	59	10	15 (25%)	16	0	0	0	0	0	0	0	0	0	0	0	16
29	59	1	2 (3%)	3	0	0	0	0	0	0	0	0	0	0	0	3
31	58	3	7 (12%)	13	0	0	0	0	0	0	0	0	0	0	0	13
31	58	6	3 (5%)	7	20	0	0	0	0	0	0	0	0	0	0	27
31	58	6	0 (0%)	0	20	0	0	0	0	0	0	0	0	0	0	20
31	58	4	1 (2%)	3	28	0	0	0	0	0	0	0	0	0	0	31
35	57	0	1 (2%)	4	0	0	0	0	0	0	0	0	0	0	0	4
35	57	5	11 (19%)	19	0	0	0	0	0	0	0	0	0	0	0	19
35	57	7	4 (7%)	5	16	0	0	0	0	0	0	0	0	0	0	21
35	57	8	15 (25%)	14	2	0	0	0	0	0	0	0	0	0	0	16
35	57	6	3 (5%)	6	16	3	0	0	0	0	0	0	0	0	0	25
40	56	10	3 (5%)	3	18	2	0	0	0	0	0	0	0	0	0	23
40	56	7	5 (9%)	15	0	0	0	0	0	0	0	0	0	0	0	15
42	55	7	1 (2%)	3	30	0	0	0	0	0	0	0	0	0	0	33
42	55	5	3 (5%)	5	13	0	0	0	0	0	0	0	0	0	0	18
44	54	6	12 (22%)	9	0	0	0	0	0	0	0	0	0	0	0	9
45	53	1	1 (2%)	2	1	0	0	0	0	0	0	0	0	0	0	3
45	53	11	12 (23%)	15	4	0	0	0	0	0	0	0	0	0	0	19
47	52	8	8 (15%)	3	5	0	0	0	0	0	0	0	0	0	0	8
47	52	3	5 (10%)	3	0	0	0	0	0	0	0	0	0	0	0	3
47	52	6	2 (4%)	5	30	0	0	0	0	0	0	0	0	0	0	35
50	51	3	0 (0%)	0	0	0	0	0	0	0	0	0	0	0	0	0
51	50	3	4 (8%)	4	0	0	0	0	0	0	0	0	0	0	0	4
52	49	8	18 (35%)	14	0	0	0	0	0	0	0	0	0	0	0	14
53	48	7	3 (6%)	5	20	1	0	0	0	0	0	0	0	0	0	26
53	48	12	6 (13%)	10	0	0	0	0	0	0	0	0	0	0	0	10
55	47	12	3 (6%)	4	0	0	0	0	0	0	0	0	0	0	0	4
55	47	9	2 (4%)	6	16	0	0	0	0	0	0	0	0	0	0	22
55	47	8	5 (11%)	9	5	1	0	0	0	0	0	0	0	0	0	15
55	47	11	6 (13%)	6	14	1	0	0	0	0	0	0	0	0	0	21
59	46	7	7 (15%)	6	22	0	0	0	0	0	0	0	0	0	0	28
59	46	10	1 (2%)	5	0	0	0	0	0	0	0	0	0	0	0	5
61	44	11	3 (7%)	11	21	0	0	0	0	0	0	0	0	0	0	32
61	44	4	0 (0%)	0	1	0	0	0	0	2	0	0	0	0	0	3
63	43	3	14 (30%)	14	0	0	0	0	0	0	0	0	0	0	0	14
63	43	12	3 (7%)	2	11	0	0	0	0	0	0	0	0	0	0	13
63	43	12	4 (9%)	2	25	0	0	0	0	0	0	0	0	0	0	27
66	42	2	2 (5%)	3	3	0	0	0	0	0	0	0	0	0	0	6
66	42	15	6 (14%)	13	12	0	0	0	0	0	0	0	0	0	0	25
66	42	16	1 (2%)	1	25	0	0	0	0	0	0	0	0	0	0	26
69	41	13	5 (12%)	3	8	1	0	0	0	0	0	0	0	0	0	12
70	40	3	3 (8%)	1	0	0	0	0	0	0	0	0	0	0	0	1
70	40	6	2 (5%)	2	0	0	0	0	0	0	0	0	0	0	0	2
70	40	7	9 (23%)	17	5	0	0	0	0	0	0	0	0	0	0	22
73	38	12	2 (5%)	7	12	2	0	0	0	0	0	0	0	0	0	21
74	37	8	1 (3%)	3	7	0	0	0	0	0	0	0	0	0	0	10
75	36	4	2 (6%)	2	8	0	0	0	0	0	0	0	0	0	0	10
75	36	5	1 (3%)	0	15	0	0	0	0	0	0	0	0	0	0	15
77	34	0	0 (0%)	0	0	0	0	0	0	0	0	0	0	0	0	0
78	33	14	14 (39%)	13	0	0	0	0	0	0	0	0	0	0	0	13
78	33	5	3 (9%)	2	2	0	0	0	0	0	0	0	0	0	0	4
80	32	0	0 (0%)	0	0	0	0	0	0	0	0	0	0	0	0	0
80	32	11	1 (3%)	0	17	0	0	0	0	0	0	0	0	0	0	17
80	32	0	0 (0%)	0	0	0	0	0	0	0	0	0	0	0	0	0
80	32	5	1 (3%)	1	0	0	0	0	0	0	0	0	0	0	0	1
84	31	15	5 (16%)	8	9	0	0	0	0	0	0	0	0	0	0	17

Rank of the Unique Tows	Average Monthly Towboat Lockages Generated by the 90% Unique Towboats														Unit: Towboat Lockages/month		
	During the UMR Peak		During the UMR Off-peak														
	In the UMR	Outside the UMR	In the UMR (% of the peak)	Outside the UMR											Total		
				IL	OH	TN	CU	GB	MN	MK	OD	OB	GI	TT			
84	31	9	6 (19%)	6	9	0	0	0	0	0	0	0	0	0	0	0	15
86	29	4	7 (24%)	11	0	0	0	0	0	0	0	0	0	0	0	0	11
86	29	7	3 (10%)	2	5	0	0	0	0	0	0	0	0	0	0	0	7
88	28	0	4 (14%)	1	0	0	0	0	0	0	0	0	0	0	0	0	1
88	28	20	4 (14%)	7	17	1	0	0	0	0	0	0	0	0	0	0	25
88	28	7	0 (0%)	0	14	0	0	0	0	0	9	0	0	0	0	0	23
91	27	15	0 (0%)	0	0	0	0	0	0	0	0	0	0	0	13	0	13
91	27	0	0 (0%)	0	0	0	0	0	0	0	0	0	0	0	0	0	0
93	25	0	0 (0%)	0	0	0	0	0	0	0	0	0	0	0	0	0	0
93	25	0	18 (72%)	0	0	0	0	0	0	0	0	0	0	0	0	0	0
93	25	14	2 (8%)	6	23	0	0	0	0	0	0	0	0	0	0	0	29
96	24	17	0 (0%)	0	26	0	0	0	0	0	0	0	0	0	0	0	26
97	23	0	0 (0%)	0	0	0	0	0	0	0	0	0	0	0	0	0	0
97	23	24	0 (0%)	0	29	0	0	0	0	0	0	0	0	0	0	0	29
99	22	21	1 (5%)	4	16	0	0	0	0	0	0	0	0	0	0	0	20
100	21	33	1 (5%)	4	48	0	0	0	0	0	0	0	0	0	0	0	52
101	20	9	1 (5%)	1	10	0	0	0	0	0	0	0	0	0	2	0	13
101	20	19	6 (30%)	19	0	0	0	0	0	0	0	0	0	0	0	0	19
103	20	23	2 (10%)	2	27	0	0	0	0	0	0	0	0	0	0	0	29
104	19	8	0 (0%)	0	9	0	0	0	0	0	4	0	0	0	0	0	13
104	19	0	0 (0%)	0	0	0	0	0	0	0	0	0	0	0	0	0	0
104	19	14	2 (11%)	1	6	1	0	0	0	0	0	0	0	0	0	0	8
104	19	3	0 (0%)	0	0	0	0	0	0	0	0	0	0	0	0	0	0
104	19	3	2 (11%)	0	4	0	0	0	0	0	0	0	0	0	0	0	4
104	19	17	4 (21%)	8	15	1	1	0	0	0	0	0	0	0	0	0	25
110	18	10	0 (0%)	0	0	0	0	0	0	0	0	0	0	0	0	0	0
110	18	0	0 (0%)	0	0	0	0	0	0	0	0	0	0	0	0	0	0
110	18	0	0 (0%)	0	0	0	0	0	0	0	0	0	0	0	0	0	0
113	17	0	0 (0%)	0	0	0	0	0	0	0	0	0	0	0	0	0	0
113	17	5	4 (24%)	7	4	0	0	0	0	0	0	0	0	0	0	0	11
113	17	9	5 (29%)	5	3	1	0	0	0	0	1	0	0	0	0	0	10
113	17	2	5 (29%)	4	0	0	0	0	0	0	0	0	0	0	0	0	4
117	16	7	1 (6%)	0	3	0	0	0	0	0	0	0	0	0	0	0	3
117	16	1	1 (6%)	1	2	0	0	0	0	0	0	0	0	0	0	0	3
117	16	0	0 (0%)	0	0	0	0	0	0	0	0	0	0	0	0	0	0
117	16	1	0 (0%)	0	4	0	0	0	0	0	0	0	0	0	0	0	4
117	16	25	3 (19%)	15	1	2	0	0	0	0	0	0	0	0	2	0	20
117	16	5	3 (19%)	4	6	0	0	0	0	0	0	0	0	0	0	0	10
117	16	16	3 (19%)	6	0	0	0	0	0	0	0	0	0	0	0	0	6
124	15	11	4 (27%)	2	6	3	0	0	0	0	0	0	0	0	0	0	11
124	15	8	5 (33%)	3	6	0	0	0	0	0	0	0	0	0	0	0	9
124	15	30	4 (27%)	13	11	0	0	0	0	0	0	0	0	0	0	0	24
124	15	0	15 (100%)	0	0	0	0	0	0	0	0	0	0	0	0	0	0
124	15	5	0 (0%)	0	12	0	0	0	0	0	2	0	0	0	0	0	14
124	15	0	0 (0%)	0	0	0	0	0	0	0	0	0	0	0	0	0	0
124	15	13	1 (7%)	1	15	0	0	0	0	0	0	1	1	1	0	0	19
124	15	0	5 (33%)	0	0	0	0	0	0	0	0	0	0	0	0	0	0
132	14	10	1 (7%)	3	16	0	0	0	0	0	0	0	0	0	0	0	19
132	14	1	0 (0%)	0	3	0	0	0	0	0	0	0	0	0	0	0	3
132	14	16	1 (7%)	1	6	0	0	0	0	0	0	0	0	0	0	0	7
132	14	0	0 (0%)	0	0	0	0	0	0	0	0	0	0	0	0	0	0
132	14	25	0 (0%)	0	24	6	2	0	0	0	0	0	0	0	0	0	32
132	14	6	3 (21%)	4	2	0	0	0	0	0	0	0	0	3	0	0	9
132	14	19	3 (21%)	0	3	3	0	0	0	0	4	0	0	0	0	0	10
132	14	0	0 (0%)	0	0	0	0	0	0	0	0	0	0	0	0	0	0
132	14	15	1 (7%)	0	3	0	0	0	0	0	0	0	0	0	0	0	3
132	14	0	16 (114%)	0	0	0	0	0	0	0	0	0	0	0	0	0	0
142	13	14	0 (0%)	0	6	0	0	0	0	0	0	0	0	0	0	0	6
142	13	24	3 (23%)	12	0	0	0	0	0	0	0	0	0	0	0	0	12
142	13	12	0 (0%)	1	3	0	0	0	0	0	0	0	0	0	0	0	4
142	13	18	3 (23%)	4	15	0	0	0	0	0	0	0	0	0	0	0	19

Rank of the Unique Tows	Average Monthly Towboat Lockages Generated by the 90% Unique Towboats														Unit: Towboat Lockages/month		
	During the UMR Peak		During the UMR Off-peak														
	In the UMR	Outside the UMR	In the UMR (% of the peak)	Outside the UMR											Total		
				IL	OH	TN	CU	GB	MN	MK	OD	OB	GI	TT			
142	13	0	0 (0%)	0	0	0	0	0	0	0	0	0	0	0	0	0	0
147	12	2	0 (0%)	0	0	0	0	0	0	0	0	0	0	0	1	0	1
147	12	0	0 (0%)	0	0	0	0	0	0	0	0	0	0	0	0	0	0
147	12	0	0 (0%)	0	0	0	0	0	0	0	0	0	0	0	0	0	0
147	12	0	0 (0%)	0	0	0	0	0	0	0	0	0	0	0	0	0	0
147	12	0	0 (0%)	0	0	0	0	0	0	0	0	0	0	0	0	0	0
147	12	0	0 (0%)	0	0	0	0	0	0	0	0	0	0	0	0	0	0
147	12	4	0 (0%)	0	0	0	0	0	0	0	0	0	0	0	0	0	0
147	12	12	2 (17%)	0	6	0	0	0	0	0	0	0	0	0	0	0	6
147	12	19	3 (25%)	1	4	2	0	0	0	1	0	0	0	0	0	0	8
147	12	14	0 (0%)	0	9	0	0	0	0	0	0	0	0	0	0	0	9
147	12	0	0 (0%)	0	0	0	0	0	0	0	0	0	0	0	0	0	0
147	12	0	0 (0%)	0	0	0	0	0	0	0	0	0	0	0	0	0	0
160	11	8	3 (27%)	5	8	0	0	0	0	0	0	0	0	0	0	0	13
160	11	16	1 (9%)	1	0	4	0	0	0	0	0	0	0	10	0	0	15
160	11	5	0 (0%)	0	0	0	0	0	0	0	0	0	0	0	0	0	0
160	11	1	2 (18%)	3	0	0	0	0	0	0	0	0	0	0	0	0	3
160	11	0	0 (0%)	0	0	0	0	0	0	0	0	0	0	0	0	0	0
165	10	15	3 (30%)	5	6	0	0	0	0	8	0	0	0	0	0	0	19
165	10	25	2 (20%)	5	15	4	0	0	1	0	0	0	0	3	0	0	28
165	10	23	8 (80%)	20	0	0	0	0	0	0	0	0	0	0	0	0	20
165	10	0	0 (0%)	0	0	0	0	0	0	0	0	0	0	0	0	0	0
165	10	21	0 (0%)	0	2	0	0	0	0	3	0	0	0	9	0	0	14
165	10	30	0 (0%)	1	20	6	0	0	2	0	0	0	0	1	0	0	30
171	9	27	3 (33%)	0	13	10	0	0	0	1	0	0	0	1	0	0	25
171	9	18	0 (0%)	2	5	0	0	0	0	1	2	2	7	0	0	0	19
171	9	27	0 (0%)	0	18	8	0	0	1	0	0	0	1	0	0	0	28
171	9	4	0 (0%)	0	0	0	0	0	0	0	0	0	0	0	0	0	0
171	9	27	0 (0%)	0	38	0	0	0	0	0	0	0	0	0	0	0	38
171	9	3	1 (11%)	0	2	0	0	0	0	0	0	0	0	0	0	0	2
171	9	1	0 (0%)	0	0	0	0	0	0	0	0	0	0	0	0	0	0
178	8	25	2 (25%)	1	7	1	0	0	0	0	0	0	0	5	0	0	14
178	8	1	1 (13%)	0	4	0	0	0	0	0	0	0	0	0	0	0	4
178	8	17	0 (0%)	0	4	0	0	0	0	0	0	0	0	7	0	0	11
178	8	15	0 (0%)	0	9	0	0	0	0	0	0	0	0	5	0	0	14
178	8	0	2 (25%)	0	0	0	0	0	0	0	0	0	0	0	0	0	0
178	8	12	2 (16%)	3	0	0	0	0	0	0	0	0	0	9	2	0	14
178	8	15	0 (0%)	0	7	0	0	0	0	5	0	0	0	0	0	0	12
178	8	16	0 (0%)	0	2	1	0	0	0	0	0	0	0	8	6	0	17
178	8	10	0 (0%)	0	4	0	0	0	0	0	0	0	0	7	0	0	11
178	8	24	7 (88%)	12	0	0	0	0	0	1	0	0	0	0	0	0	13
178	8	28	0 (0%)	0	35	0	0	0	0	0	0	0	0	0	0	0	35
178	8	16	1 (13%)	1	4	0	0	0	0	0	0	0	0	6	0	0	11
178	8	37	0 (0%)	0	33	0	0	0	0	0	0	0	0	0	0	0	33
191	7	6	13 (186%)	0	3	0	0	2	0	0	0	0	0	0	0	0	5
191	7	31	6 (86%)	14	12	0	0	0	0	0	0	0	0	0	0	0	26
191	7	1	19 (271%)	0	0	0	0	0	0	0	0	0	0	0	0	0	0
191	7	9	2 (29%)	2	3	0	0	0	0	1	0	0	0	4	0	0	10
191	7	25	2 (29%)	2	11	4	2	0	0	5	0	0	0	5	0	0	29
191	7	0	0 (0%)	0	0	0	0	0	0	0	0	0	0	0	0	0	0
191	7	0	0 (0%)	0	0	0	0	0	0	0	0	0	0	0	0	0	0
191	7	8	2 (29%)	0	13	0	0	0	0	2	0	0	0	0	0	0	15
191	7	0	0 (0%)	0	0	0	0	0	0	0	0	0	0	0	0	0	0
191	7	29	7 (100%)	18	0	0	0	0	0	0	0	0	0	0	0	0	18
191	7	38	7 (100%)	14	12	0	0	0	0	0	0	0	0	0	0	0	26
191	7	5	1 (14%)	0	3	1	0	0	0	0	0	0	0	0	0	0	4
203	7	0	4 (67%)	0	0	0	0	0	0	0	0	0	0	0	0	0	0
Total	6,444	1,702	676 (10%)	804	1,410	75	5	2	4	50	3	3	110	8		2,474	

Decrease significantly

Increase

In order to identify off-peak (winter) states of the unique towboats inside and outside the UMR system, four types of off-peak lockage levels are specified based on the judgment rules listed below.

- **Negligible:** at most 2 observed off-peak lockages per month on average
- **Light:** 3 to 6 observed off-peak lockages per month on average
- **Moderate:** 7 to 29 observed off-peak lockages per month on average
- **Heavy:** at least 30 observed off-peak lockages per month on average

It is noted here that according to Table 5 (left second column), every unique towboat in the 90% group generates at least 7 UMR towboat lockages (monthly average) during the peak period. Based on the minimum peak-period lockages in the UMR system, the off-peak lockages of unique towboats are classified into the above four levels. The unique towboats with less than 7 observed off-peak lockages are classified as having a “light” lockage level in the system. Moreover, the unique towboats with no or very few observed off-peak lockages (at most 2 per month) are categorized as having a “negligible” lockage level while “moderate” and “heavy” levels are assigned to those unique towboats having 7 to 29 and more than 30 off-peak lockages, respectively. Unique towboats off-peak states are summarized in Table 6.

Table 6. Off-peak States of the 90% Unique Towboats

Level Code	Off-Peak Lockage Level at the UMR System	Off-Peak Lockage Level at the Outside the UMR	Fraction of the Unique Towboats % (No.)	
A	Negligible	Negligible	21.2% (43)	58% (117)
		Light	9.4% (19)	
		Moderate	20.7% (42)	
		Heavy	6.4% (13)	
B	Light	Negligible	2.0% (4)	26% (53)
		Light	3.0% (6)	
		Moderate	20.7% (42)	
		Heavy	0.5% (1)	
C	Moderate	Negligible	2.5% (5)	16% (33)
		Light	1.0% (2)	
		Moderate	12.8% (26)	
		Heavy	0% (0)	
D	Heavy	Negligible	0% (0)	0% (0)
		Light	0% (0)	
		Moderate	0% (0)	
		Heavy	0% (0)	
Total			100% (203)	

As shown in Table 6, it has been observed that about 58% of the unique towboats practically do not use the UMR locks during the off-peak. Among them about 37% (43 unique tows) are also not observed at any locks outside the UMR during the off-peak (i.e., about 21% of the unique towboats are never observed anywhere in the study area during the off-peak). It is noted, however, that many unique towboats (about 27% of the unique tows) classified in level A operate actively at locks outside the UMR during the off-peak although their UMR off-peak lockage level is negligible. In addition, Table 6 shows that during the off-peak, about 26% (classified in level B) of the unique towboats reduce their UMR operation; instead, most of them (about 81% of the 26%) operate actively outside the UMR. These results are interpreted to indicate that considerable numbers of the 90% unique towboats cease operation or shift to outside UMR during the off-peak. Finally, it has been observed that only about 16% of the unique towboats operate actively in the UMR system as much as during the off-peak as during the peak and most of them also operate outside the system. No heavily operated unique towboats are observed at locks both inside and outside the UMR during the off-peak (e.g., the top three unique towboats are never observed at any locks in the system during the off-peak).

Figure 7 shows the only districts visited by the 90% towboats during the UMR off-peak. The towboats operate actively in districts in the upper Mississippi Valley Division (MVD) and Great Lakes and Ohio River Division (LRD) during the off-peak and travel slightly to some rivers in New Orleans (MVN), Galveston (SWG), Little Rock (SWL), Tulsa (SWT), Mobile (SAM) districts. It is noted that many unique towboats of the 90% group must often pass through the Mississippi (MI) segment in the Memphis District (MVM), which has no locks.

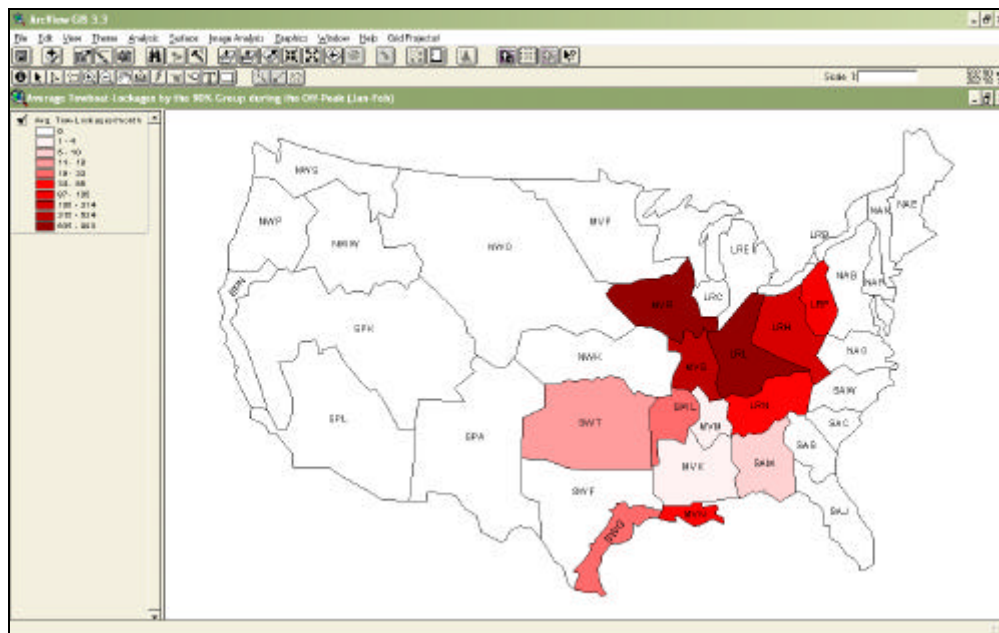


Figure 7. Districts Visited by the 90% Unique Towboats during the UMR Off-peak

3.3. Lock Use by Towboats in the Study Area

In order to identify the impact of the UMR seasonal variation on the other waterways, we determine total towboat lockages as well as the lockages attributable to the 90% unique towboats by locks in the U.S. waterway system. Tables 7 through 10 show the towboat use of locks by rivers. It is noted that there are no observed lockages by the 90% towboats in the North Atlantic Division (NAD) and Northwestern Division (NWD) for 2000-2004; thus, it seems that the UMR seasonality does not affect these areas.

Towboat Lockages in the UMR and Illinois Systems

As shown in the two rightmost columns for the UMR locks in Table 7, there is no significant difference in changes of the UMR towboat lockages generated by all vs. the 90% unique towboats in between the peak and off-peak; both drastically decrease during the off-peak. In particular, the towboat lockages significantly decrease upstream of Lock #25 during the off-peak; however, heavy towboat lockages still observed at Locks #27 and #26 (though the lockages at those locks also decrease significantly during the off-peak). Based on such findings, we conclude that many unique towboats, which normally operate in the UMR during the peak, hardly operate upstream of Lock #25 and would shift to other rivers (e.g., lower Mississippi, Illinois, and Ohio) or cease operating until the UMR thaws (refer to Table 6). Figure 8 presents the UMR lock use by all towboats and the 90% unique towboats for the peak and off-peak periods.

Three key findings are identified from the lock use on the Illinois system, as presented in Table 7 and Figure 9. During the UMR off-peak (i) towboat lockages attributable to the 90% unique towboats increase at every Illinois lock; however, (ii) total towboat lockages at almost every lock in the Illinois decrease overall, except at Lock #01 and the lower Illinois (Locks #07 and #08). In addition, (iii) Lock #01 is hardly used by the 90% unique towboats either in the peak or off-peak of the UMR. Such findings can be interpreted to indicate that among the unique towboats engaging in most peak-period UMR lockages, some towboats shift to the Illinois and operate during the UMR freeze; however, they do not travel to Lock #01⁶. They operate mostly from Lock #08 upstream to Lock #05 during the UMR off-peak and significantly contribute to the increase of off-peak towboat lockages on the lower Illinois (Locks #07 and #08); their contributions to the off-peak towboat lockages at such locks are about 58% and 70%, respectively. However, an interesting question arising here is why do the off-peak towboat lockages at Locks #02 through #06 decrease overall despite an increase there of the off-peak lockages by the 90% unique towboats? A possible answer is that some towboats which normally operate on the Illinois are replaced with towboats shifting from the UMR during

⁶ Lock #01 in the Illinois system may be too small or too unimportant (at all times).

winters. We leave this important question to future studies.

Table 7. Lock Use by Towboats in the UMR and Illinois Systems (2000-2004)

unit: Towboat-Lockages/month

River	Lock	During the Peak (Apr. to Nov.)			During the Off-Peak (Jan. to Feb.)			% Change of Towboat-Lockages Between the Peak and Off-Peak	
		towboat-Lockages		% of Total Attributable to the 90% group	towboat-Lockages		% of Total Attributable to the 90% group	% Change of Total	% Change of Tow-Lockages by the 90%
		Total	By the 90% group		Total	By the 90% group			
UMR	MVP(#51)	165	164	99%	0	0	-	-100.00%	-100.00%
	MVP(#52)	160	160	100%	0	0	-	-100.00%	-100.00%
	MVP(#01)	156	146	94%	0	0	-	-100.00%	-100.00%
	MVP(#02)	118	111	94%	0	0	-	-100.00%	-100.00%
	MVP(#03)	129	122	95%	0	0	-	-100.00%	-100.00%
	MVP(#04)	121	115	95%	0	0	-	-100.00%	-100.00%
	MVP(#05)	123	117	95%	0	0	-	-100.00%	-100.00%
	MVP(#55)	130	124	95%	0	0	-	-100.00%	-100.00%
	MVP(#06)	150	143	95%	0	0	-	-100.00%	-100.00%
	MVP(#07)	155	148	95%	0	0	-	-100.00%	-100.00%
	MVP(#08)	150	143	95%	0	0	-	-100.00%	-100.00%
	MVP(#09)	160	153	96%	0	0	-	-100.00%	-100.00%
	MVP(#10)	193	185	96%	0	0	-	-100.00%	-100.00%
	MVR(#11)	222	208	94%	0	0	-	-100.00%	-100.00%
	MVR(#12)	212	201	95%	0	0	-	-100.00%	-100.00%
	MVR(#13)	215	204	95%	0	0	-	-100.00%	-100.00%
	MVR(#14)	293	279	95%	2	1	50%	-99.32%	-99.64%
	MVR(#15)	359	343	96%	3	3	100%	-99.16%	-99.13%
	MVR(#16)	313	300	96%	3	2	67%	-99.04%	-99.33%
	MVR(#17)	276	264	96%	3	2	67%	-98.91%	-99.24%
	MVR(#18)	288	268	93%	3	3	100%	-98.96%	-98.88%
	MVR(#19)	279	260	93%	3	3	100%	-98.92%	-98.85%
	MVR(#20)	295	279	95%	6	6	100%	-97.97%	-97.85%
	MVR(#21)	297	274	92%	10	9	90%	-96.63%	-96.72%
	MVR(#22)	283	266	94%	12	12	100%	-95.76%	-95.49%
	MVS(#24)	293	269	92%	16	16	100%	-94.54%	-94.05%
	MVS(#25)	316	289	91%	18	17	94%	-94.30%	-94.12%
MVS(#26)	614	442	72%	372	262	70%	-39.41%	-40.72%	
MVS(#27)	710	461	65%	521	340	65%	-26.62%	-26.25%	
IL	MVR(#01)	190	2	1%	219	0	0%	15.26%	-100.00%
	MVR(#02)	257	49	19%	195	54	28%	-24.12%	10.20%
	MVR(#03)	256	53	21%	197	60	30%	-23.05%	13.21%
	MVR(#04)	249	63	25%	180	73	41%	-27.71%	15.87%
	MVR(#05)	229	74	32%	186	93	50%	-18.78%	25.68%
	MVR(#06)	245	83	34%	208	116	56%	-15.10%	39.76%
	MVR(#07)	296	117	40%	325	187	58%	9.80%	59.83%
	MVR(#08)	263	131	50%	311	219	70%	18.25%	67.18%

Decrease overall Increase

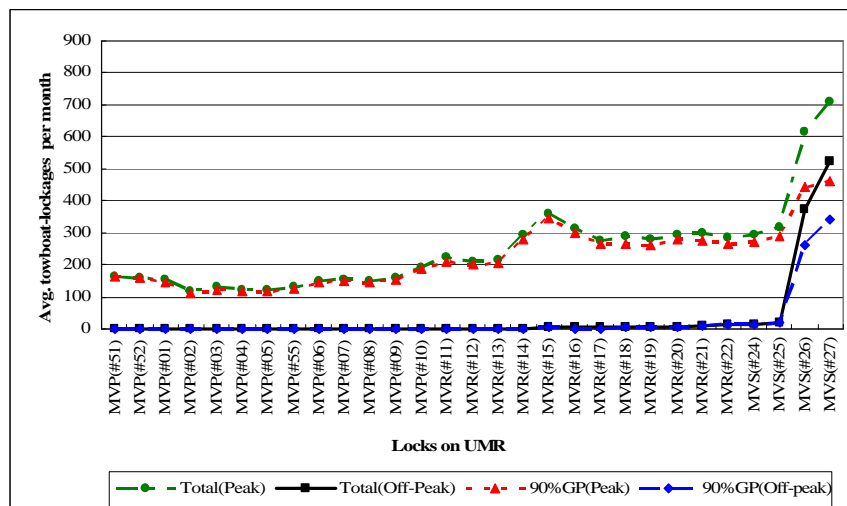


Figure 8. UMR Towboat Lockages during the Peak and Off-peak (2000-2004)

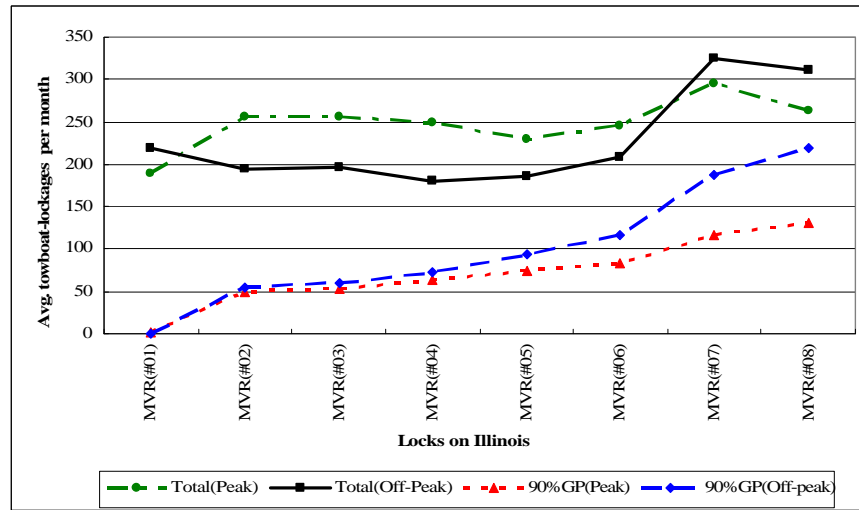


Figure 9. Illinois Towboat Lockages during the UMR Peak and Off-peak (2000-2004)

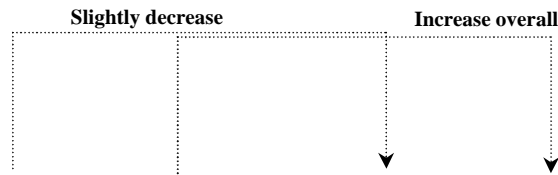
Towboat Lockages in the Ohio and Its Tributaries

During the UMR off-peak, towboat lockages attributable to the 90% unique towboats increase overall at every Ohio lock. This can be interpreted to indicate that among the unique towboats using the UMR locks, some towboats that normally operate on both the UMR and Ohio shift to the Ohio and generate more lockages during the off-peak while avoiding the freezing of the UMR; they operate mostly from Lock #53 upstream to Lock #24 downstream (refer to Table 8 and Figure 10 for the Ohio locks). However, it is clearly noted that total towboat lockages at every Ohio lock are stable in between the UMR peak and off-peak periods although the 90% unique towboats affect more Ohio lockages during the off-peak. This raises some important questions such as: (i) why are the total towboat lockages at every Ohio lock stable despite increase of the towboat lockages by the 90% unique towboats during the off-peak period? (ii) Do some towboats that normally operate on the Ohio cease operation so that they are replaced by the shifted towboats from the UMR during the off-peak? We leave such questions to future studies.

As shown in Figure 11, total towboat lockages at every Tennessee (TN) lock are also stable regardless of season and the contribution of the 90% unique towboats to the total lockages of the systems is insignificant and stable during both the UMR peak and off-peak periods. This indicates that the impact of the unique towboats, which operate in between the UMR and Tennessee systems, to the Tennessee is generally steady and low in spite of the seasonality in the UMR. For other Ohio tributaries, the 90% unique towboats hardly travel to there during both the UMR peak and off-peak periods; furthermore, total towboat lockages on most rivers slightly decrease during the UMR off-peak (see Table 8). Additionally, it should be noted that total

towboat lockages on the upper Allegheny (AG) (upstream of Lock #44) significantly decrease during the winter. It seems traffic on the upper Allegheny is also seasonal as in the UMR case since this river also freezes in winter.

Table 8. Lock Use by Towboats in the Ohio and Its Tributaries (2000-2004)



unit: Towboat-Lockages/month

River	Lock	During the Peak (Apr. to Nov.)			During the Off-Peak (Jan. to Feb.)			% Change of Towboat-Lockages Between the Peak and Off-Peak	
		towboat-Lockages		% of Total Attributable to the 90% group	towboat-Lockages		% of Total Attributable to the 90% group	% Change of Total	% Change of Tow-Lockages by the 90%
		Total	By the 90% group		Total	By the 90% group			
OH	LRL(#53)	610	108	18%	595	146	25%	-2.46%	35.19%
	LRL(#52)	844	109	13%	791	147	19%	-6.28%	34.86%
	LRL(#78)	607	78	13%	615	136	22%	1.32%	74.36%
	LRL(#77)	491	74	15%	503	131	26%	2.44%	77.03%
	LRL(#76)	520	70	13%	494	124	25%	-5.00%	77.14%
	LRL(#75)	414	62	15%	381	110	29%	-7.97%	77.42%
	LRL(#42)	438	61	14%	426	106	25%	-2.74%	73.77%
	LRL(#41)	404	52	13%	386	92	24%	-4.46%	76.92%
	LRH(#25)	439	46	10%	422	80	19%	-3.87%	73.91%
	LRH(#24)	549	44	8%	540	80	15%	-1.64%	81.82%
	LRH(#26)	434	28	6%	404	48	12%	-6.91%	71.43%
	LRH(#22)	379	24	6%	344	38	11%	-9.23%	58.33%
	LRH(#21)	358	22	6%	329	35	11%	-8.10%	59.09%
	LRH(#72)	351	20	6%	336	32	10%	-4.27%	60.00%
	LRP(#71)	383	20	5%	365	31	8%	-4.70%	55.00%
	LRP(#05)	423	17	4%	407	29	7%	-3.78%	70.59%
	LRP(#04)	377	15	4%	363	26	7%	-3.71%	73.33%
	LRP(#03)	423	5	1%	389	8	2%	-8.04%	60.00%
LRP(#02)	430	2	0%	365	4	1%	-15.12%	100.00%	
LRP(#01)	470	2	0%	394	4	1%	-16.17%	100.00%	
TN	LRN(#01)	274	25	9%	265	20	8%	-3.28%	-20.00%
	LRN(#02)	212	28	13%	190	18	9%	-10.38%	-35.71%
	LRN(#03)	159	13	8%	154	10	6%	-3.14%	-23.08%
	LRN(#04)	145	12	8%	136	10	7%	-6.21%	-16.67%
	LRN(#05)	94	12	13%	80	8	10%	-14.89%	-33.33%
	LRN(#06)	71	8	11%	57	6	11%	-19.72%	-25.00%
	LRN(#07)	56	6	11%	36	2	6%	-35.71%	-66.67%
	LRN(#08)	41	6	15%	27	2	7%	-34.15%	-66.67%
	LRN(#09)	23	6	26%	16	2	13%	-30.43%	-66.67%
CI	LRN(#11)	0	0	-	0	0	-	-	-
CU	LRN(#21)	109	5	5%	68	3	4%	-37.61%	-40.00%
	LRN(#22)	120	6	5%	92	2	2%	-23.33%	-66.67%
	LRN(#24)	69	0	0%	66	0	0%	-4.35%	-
	LRN(#23)	0	0	-	0	0	-	-	-
GB	LRL(#21)	170	4	2%	172	2	1%	1.18%	-50.00%
	LRL(#22)	101	0	0%	110	0	0%	8.91%	-
KA	LRH(#01)	245	0	0%	226	0	0%	-7.76%	-
	LRH(#02)	372	0	0%	354	0	0%	-4.84%	-
	LRH(#03)	139	0	0%	156	0	0%	12.23%	-
MN	LRP(#22)	404	2	0%	357	2	1%	-11.63%	0.00%
	LRP(#23)	655	6	1%	580	2	0%	-11.45%	-66.67%
	LRP(#24)	466	0	0%	392	0	0%	-15.88%	-
	LRP(#25)	350	0	0%	316	0	0%	-9.71%	-
	LRP(#26)	158	0	0%	140	0	0%	-11.39%	-
	LRP(#28)	152	0	0%	132	0	0%	-13.16%	-
	LRP(#29)	45	0	0%	13	0	0%	-71.11%	-
	LRP(#30)	10	0	0%	10	0	0%	0.00%	-
LRP(#31)	10	0	0%	12	0	0%	20.00%	-	
AG	LRP(#42)	126	0	0%	114	0	0%	-9.52%	-
	LRP(#43)	121	0	0%	107	0	0%	-11.57%	-
	LRP(#44)	127	0	0%	43	0	0%	-66.14%	-
	LRP(#45)	90	0	0%	18	0	0%	-80.00%	-
	LRP(#46)	18	0	0%	8	0	0%	-55.56%	-
	LRP(#47)	17	0	0%	6	0	0%	-64.71%	-
	LRP(#48)	84	0	0%	0	0	-	-100.00%	-
LRP(#49)	0	0	-	0	0	-	-	-	

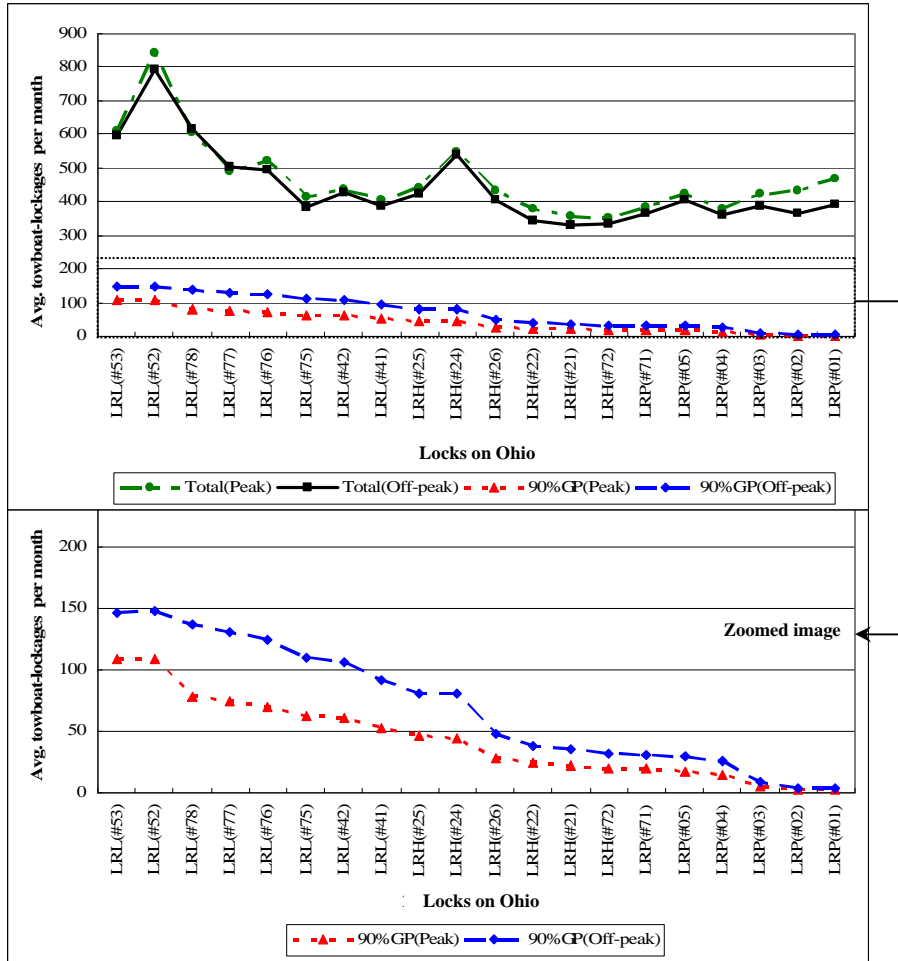


Figure 10. Ohio Towboat Lockages during the UMR Peak and Off-peak (2000-2004)

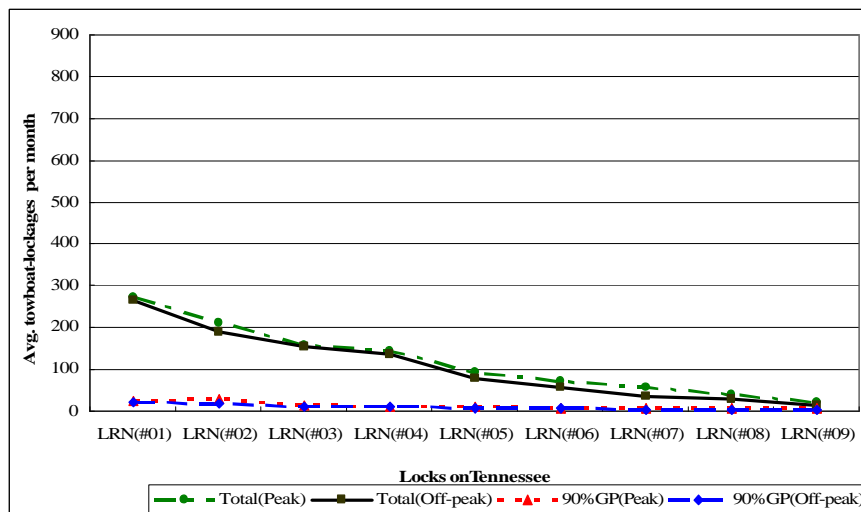


Figure 11. Tennessee Towboat Lockages during the UMR Peak and Off-peak (2000-2004)

Towboat Lockages on the Lower MVD and Southwester Division (SWD)

As shown in Figure 12 and Table 9, total towboat lockages at every Gulf Intra-coastal Waterway (GI) lock decrease overall during the UMR off-peak, except at Lock #01, and the fraction of the total lockages attributable to the 90% unique towboats is negligible (below 2%) during both the UMR peak and off-peak periods. These results indicate that towboats using the Gulf Intra-coastal Waterway reduce their operation during the winter; furthermore, among them some towboats which normally operate in between the UMR and Gulf Intra-coastal Waterway slightly affect Gulf Intra-coastal Waterway lockages with almost stable but insignificant rates during both the UMR peak and off-peak periods. Thus, it seems that the UMR seasonality hardly affects the Gulf Intra-coastal Waterway system. The same interpretation given for the Gulf Intra-coastal Waterway is also applicable to the McClellan-Kerr Arkansas River Navigation System (MK) since total towboat lockages of the McClellan-Kerr Arkansas River Navigation System also slightly decrease during the off-peak and lockages generated by the 90% unique towboats are low and fairly stable (less than 5 lockages per month on average) during both the peak and off-peak periods. Finally, the 90% unique towboats are never observed on the Red River (RR), Pearl River (PR), Atchafalaya River (AT), Bayou Tech (BT), Freshwater Bayou (FB), and Calcasieu River (CA).

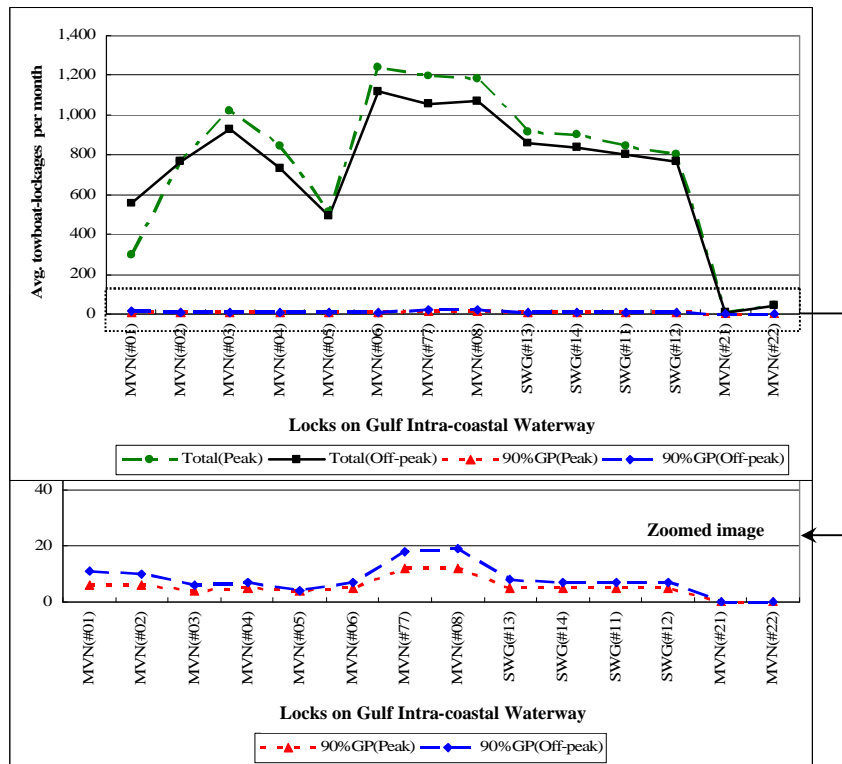


Figure 12. Towboat Lockages on Gulf Intra-coastal Waterway during the UMR Peak and Off-peak (2000-2004)

Table 9. Lock Use by Towboats in the Lower MVD and SWD (2000-2004)

unit: Towboat-Lockages/month

River	Lock	During the Peak (Apr. to Nov.)			During the Off-Peak (Jan. to Feb.)			% Change of Towboat-Lockages Between the Peak and Off-Peak	
		towboat-Lockages		% of Total Attributable to the 90% group	towboat-Lockages		% of Total Attributable to the 90% group	% Change of Total	% Change of Tow-Lockages by the 90%
		Total	By the 90% group		Total	By the 90% group			
GI	MVN(#01)	292	6	2.05%	558	11	1.97%	91.10%	83.33%
	MVN(#02)	767	6	0.78%	764	10	1.31%	-0.39%	66.67%
	MVN(#03)	1,021	4	0.39%	930	6	0.65%	-8.91%	50.00%
	MVN(#04)	842	5	0.59%	729	7	0.96%	-13.42%	40.00%
	MVN(#05)	511	4	0.78%	492	4	0.81%	-3.72%	0.00%
	MVN(#06)	1,236	5	0.40%	1,116	7	0.63%	-9.71%	40.00%
	MVN(#77)	1,196	12	1.00%	1,054	18	1.71%	-11.87%	50.00%
	MVN(#08)	1,180	12	1.02%	1,070	19	1.78%	-9.32%	58.33%
	SWG(#13)	915	5	0.55%	859	8	0.93%	-6.12%	60.00%
	SWG(#14)	901	5	0.55%	834	7	0.84%	-7.44%	40.00%
	SWG(#11)	844	5	0.59%	799	7	0.88%	-5.33%	40.00%
	SWG(#12)	804	5	0.62%	766	7	0.91%	-4.73%	40.00%
	MVN(#21)	6	0	0.00%	9	0	0.00%	50.00%	-
	MVN(#22)	39	0	0.00%	40	0	0.00%	2.56%	-
MK	SWL(#01)	90	3	3.33%	91	5	5.49%	1.11%	66.67%
	SWL(#02)	90	4	4.44%	89	5	5.62%	-1.11%	25.00%
	SWL(#03)	78	3	3.85%	74	5	6.76%	-5.13%	66.67%
	SWL(#04)	79	3	3.80%	76	4	5.26%	-3.80%	33.33%
	SWL(#05)	73	3	4.11%	66	3	4.55%	-9.59%	0.00%
	SWL(#06)	73	3	4.11%	64	2	3.13%	-12.33%	-33.33%
	SWL(#07)	64	2	3.13%	57	2	3.51%	-10.94%	0.00%
	SWL(#08)	64	2	3.13%	60	2	3.33%	-6.25%	0.00%
	SWL(#09)	61	2	3.28%	55	2	3.64%	-9.84%	0.00%
	SWL(#10)	64	2	3.13%	57	2	3.51%	-10.94%	0.00%
	SWL(#11)	38	2	5.26%	36	1	2.78%	-5.26%	-50.00%
	SWL(#13)	42	2	4.76%	34	1	2.94%	-19.05%	-50.00%
	SWT(#21)	78	5	6.41%	74	4	5.41%	-5.13%	-20.00%
	SWT(#22)	80	4	5.00%	73	4	5.48%	-8.75%	0.00%
	SWT(#23)	75	4	5.33%	71	4	5.63%	-5.33%	0.00%
SWT(#24)	70	3	4.29%	68	3	4.41%	-2.86%	0.00%	
SWT(#25)	69	3	4.35%	65	3	4.62%	-5.80%	0.00%	
OD	MVN(#51)	578	2	0.35%	233	3	1.29%	-59.69%	50.00%
OB	MVK(#01)	93	0	0.00%	66	2	3.03%	-29.03%	100.00%
	MVK(#02)	69	0	0.00%	53	1	1.89%	-23.19%	100.00%
	MVK(#03)	16	0	0.00%	14	0	0.00%	-12.50%	-
	MVK(#04)	16	0	0.00%	14	0	0.00%	-12.50%	-
	MVK(#06)	0	0	-	0	0	-	-	-
	MVK(#08)	0	0	-	0	0	-	-	-
RR	MVK(#41)	74	0	0.00%	72	0	0.00%	-2.70%	-
	MVK(#42)	71	0	0.00%	71	0	0.00%	0.00%	-
	MVK(#43)	38	0	0.00%	35	0	0.00%	-7.89%	-
	MVK(#44)	25	0	0.00%	22	0	0.00%	-12.00%	-
	MVK(#45)	16	0	0.00%	11	0	0.00%	-31.25%	-
AT	MVN(#11)	55	0	0.00%	48	0	0.00%	-12.73%	-
BT	MVN(#31)	0	0	-	0	0	-	-	-
FB	MVN(#41)	42	0	0.00%	38	0	0.00%	-9.52%	-
CA	MVN(#23)	40	0	0.00%	29	0	0.00%	-27.50%	-
PR	MVK(#31)	0	0	-	0	0	-	-	-
	MVK(#32)	0	0	-	0	0	-	-	-
	MVK(#33)	0	0	-	0	0	-	-	-

Towboat Lockages in the SAD, NAD, and NWD

Table 10 presents the lock use by towboats on rivers in the South Atlantic Division (SAD), North Atlantic Division (NAD), and Northwestern Division (NWD). As stated previously, the 90% unique towboats are never observed on such rivers during either the UMR peak or off-peak periods, except on the Tennessee Tombigbee Waterway (TT).

Table 10. Lock Use by Towboats in the SAD, NAD, and NWD (2000-2004)

unit: Towboat-Lockages/month

River	Lock	During the Peak (Apr. to Nov.)			During the Off-Peak (Jan. to Feb.)			% Change of Towboat-Lockages Between the Peak and Off-Peak	
		towboat-Lockages		% of Total Attributable to the 90% group	towboat-Lockages		% of Total Attributable to the 90% group	% Change of Total	% Change of Tow-Lockages by the 90%
		Total	By the 90% group		Total	By the 90% group			
BW	SAM(#01)	0	0	-	0	0	-	-	-
	SAM(#02)	223	2	0.90%	217	0	0.00%	-2.69%	-100.00%
	SAM(#03)	0	0	-	0	0	-	-	-
	SAM(#04)	0	0	-	0	0	-	-	-
	SAM(#05)	108	0	0.00%	105	0	0.00%	-2.78%	-
	SAM(#06)	0	0	-	0	0	-	-	-
TT	SAM(#41)	132	1	0.76%	131	1	0.76%	-0.76%	0.00%
	SAM(#42)	80	0	0.00%	68	1	1.47%	-15.00%	-
	SAM(#43)	75	0	0.00%	65	1	1.54%	-13.33%	-
	SAM(#44)	66	0	0.00%	56	1	1.79%	-15.15%	-
	SAM(#45)	66	0	0.00%	56	1	1.79%	-15.15%	-
	SAM(#46)	66	0	0.00%	56	1	1.79%	-15.15%	-
	SAM(#47)	64	0	0.00%	56	1	1.79%	-12.50%	-
	SAM(#48)	64	0	0.00%	55	0	0.00%	-14.06%	-
	SAM(#49)	63	1	1.59%	54	0	0.00%	-14.29%	-100.00%
	SAM(#50)	99	1	1.01%	99	1	1.01%	0.00%	0.00%
AL	SAM(#11)	4	0	0.00%	4	0	0.00%	0.00%	-
	SAM(#12)	0	0	-	0	0	-	-	-
	SAM(#13)	0	0	-	0	0	-	-	-
AP	SAM(#21)	13	0	0.00%	17	0	0.00%	30.77%	-
	SAM(#22)	0	0	-	0	0	-	-	-
	SAM(#23)	1	0	0.00%	0	0	-	-100.00%	-
CN	SAJ(#21)	103	0	0.00%	67	0	0.00%	-34.95%	-
CF	SAJ(#11)	0	0	-	0	0	-	-	-
	SAJ(#12)	0	0	-	0	0	-	-	-
	SAJ(#13)	0	0	-	0	0	-	-	-
OK	SAJ(#01)	29	0	0.00%	36	0	0.00%	24.14%	-
	SAJ(#05)	11	0	0.00%	9	0	0.00%	-18.18%	-
	SAJ(#02)	12	0	0.00%	11	0	0.00%	-8.33%	-
	SAJ(#03)	12	0	0.00%	11	0	0.00%	-8.33%	-
	SAJ(#04)	12	0	0.00%	12	0	0.00%	0.00%	-
OL	SAJ(#31)	0	0	-	0	0	-	-	-
SV	SAS(#01)	0	0	-	0	0	-	-	-
FR	SAW(#01)	0	0	-	0	0	-	-	-
	SAW(#02)	0	0	-	0	0	-	-	-
	SAW(#03)	0	0	-	0	0	-	-	-
HU	NAN(#01)	7	0	0.00%	0	0	-	-100.00%	-
AI	NAO(#11)	116	0	0.00%	98	0	0.00%	-15.52%	-
DS	NAO(#01)	0	0	-	0	0	-	-	-
	NAO(#02)	0	0	-	0	0	-	-	-
WS	NWS(#01)	198	0	0.00%	192	0	0.00%	-3.03%	-
WI	NWS(#11)	2	0	0.00%	1	0	0.00%	-50.00%	-
	NWS(#15)	2	0	0.00%	2	0	0.00%	0.00%	-
CO	NWS(#01)	213	0	0.00%	188	0	0.00%	-11.74%	-
	NWS(#02)	195	0	0.00%	167	0	0.00%	-14.36%	-
	NWS(#03)	167	0	0.00%	152	0	0.00%	-8.98%	-
	NWS(#24)	143	0	0.00%	129	0	0.00%	-9.79%	-
SN	NWS(#01)	95	0	0.00%	88	0	0.00%	-7.37%	-
	NWS(#02)	70	0	0.00%	68	0	0.00%	-2.86%	-
	NWS(#03)	67	0	0.00%	62	0	0.00%	-7.46%	-
	NWS(#04)	50	0	0.00%	48	0	0.00%	-4.00%	-

4. CONCLUSIONS

Throughout this analysis, it is shown that seasonality is prevalent and important in the UMR and affects some other rivers in the U.S. inland waterway system. The UMR traffic is unsteady due to freezing in winter as well as some seasonality in demand for transporting commodities. This study aims to identify the impact of the UMR seasonality on towboat use and shifts to other waterways. To accomplish this we perform several tasks, ultimately tracking the unique towboats that account for most peak- period towboat lockages in the UMR system, during the freezing of the UMR. It should be noted that the results presented in this report rely completely on the observed lockage information at all locks in the study area. The use of Waterborne Commerce Statistics Center (WCSC) data⁷, which are not limited to observations at locks, should be considered in future studies.

Key findings from the analysis are summarized below.

1. *The UMR seasonality is significant and driven by freezing during winter as well as seasonal variation in demand.*
 - A. *The UMR has numerous and stable towboat lockages during Apr. through Nov.*
 - B. *The UMR has few and stable towboat lockages during Jan. through Feb.*
 - C. *The towboat lockages of the UMR fluctuate in Dec. and Mar.*
 - D. *Towboats hardly operate upstream of UMR Lock #25 during the off-peak.*
 - E. *Towboat lockages at UMR Locks #27 and #26 significantly decrease during the off-peak (% change of towboat lockages on these locks between the peak and off-peak is 30%, on average; refer to Table 7).*
 - F. *The top three unique towboats, which serve a considerable fraction of the peak period UMR towboat lockages of the UMR, are never observed anywhere in the study area during the off-peak.*
 - G. *It is observed that in the winter (off-peak), about 58% of the unique towboats in the 90% group have practically no use of the UMR locks; moreover, about 21% of the unique towboats are not observed at any locks in the study area. (Refer to Table 6.)*
 - H. *It is observed that in winter, about 27% of the unique towboats operate actively outside the UMR and are practically absent from the UMR locks. (Refer to Table 6.)*
 - I. *It is observed that in winter, about 26% of the unique towboats reduce their UMR*

⁷ WCSC data are submitted to the U.S. Army Corps of Engineers by towboat operators, barge operators, and through cargo manifests and custom clearing for foreign data. They contain information about the amount and types of equipment using the waterway system, how the equipment moves around the system, and the types and amount of commodities moved by the equipment (4).

operation; instead, most of them (about 81% of the 26%) operate actively outside the UMR. (Refer to Table 6.)

J. It is observed that in winter, only about 16% of the UMR unique towboats operate actively as much during the off-peak as during the peak in the study area. (Refer to Table 6.)

K. No heavily operated unique towboats are observed inside and outside the UMR during the winter. (Refer to Table 6.)

- 2. The unique towboats which serve most peak-period towboat lockages of the UMR system operate largely in between the UMR, Illinois, and Ohio systems during the UMR off-peak.*
- 3. Total towboat lockages on the Illinois decrease overall during the UMR off-peak (the Illinois also freezes farther north); however, they increase on the lower Illinois (Locks #07 and #08) due to towboats shifting from the UMR to avoid its freeze. Therefore, steady state demands are not realistic in modeling the Illinois.*
- 4. Total towboat lockages on the Ohio slightly decrease (the reduction is insignificant) during the UMR off-peak although some towboats shifted from the UMR have more lockages while avoiding the UMR freeze. This leads to some questions stated in section 3.3; however, steady state demands on the Ohio system seem acceptable in modeling that system.*
- 5. Total towboat lockages on the Gulf Intra-coastal Waterway decrease during the off-peak of the UMR but it seems that the UMR's seasonality hardly affects the use of the GI locks.*
- 6. Total towboat lockages on the Tennessee and McClellan-Kerr decrease slightly (the reduction is slight for both rivers) during the off-peak of the UMR and towboat lockages generated by the shifted towboats from the UMR are few and fairly stable all year round.*
- 7. No significant seasonal impact of the UMR is observed outside of the UMR, Illinois, and Ohio systems.*

Figures 13 through 15 exhibit average monthly towboat lockages by the 90% unique towboats at every lock in the study area during the peak and off-peak of the UMR.

ACKNOWLEDGEMENTS

We gratefully acknowledge the advice and support provided by Mr. Mark Lisney and Mr. Keith Hofseth of the USACE Institute for Water Resources throughout this study, the technical assistance provided by Dr. Shiaau-Lir Wang of the University of Maryland, and the valuable data provided by Ms. Shilpa Patel and Mr. David Lichy of the Institute for Water Resources.

REFERENCES

1. Sweeney, D.C. “A Discrete Event Simulation Model of a Congested Segment of the Upper Mississippi River Inland Navigation System”, Final Report for the U.S. Army Corps of Engineers, 2004
2. Mundy, R.A., Nauss, R.M., Rust, D.L., Smith, L.D., Sweeney, D.C., “Management Systems for Inland Waterway Traffic Control: **Volume 1** (IDENTIFICATION AND EVALUATION OF ALTERNATIVES FOR MANAGING LOCK TRAFFIC ON THE UPPER MISSISSIPPI RIVER)”, Final Report, CTS-UMSL, 2005
3. Mundy, R.A., Nauss, R.M., Rust, D.L., Smith, L.D., Sweeney, D.C., “Management Systems for Inland Waterway Traffic Control: **Volume 2** (VESSEL TRACKING FOR MANAGING TRAFFIC ON THE UPPER MISSISSIPPI RIVER)”, Final Report, CTS-UMSL, 2005
4. Lisney, M.W., “LPMS-OMNI and WCSC Data Quality, Final Report, US Army Corps of Engineers Institute for Water Resources, 2005

APPENDIX

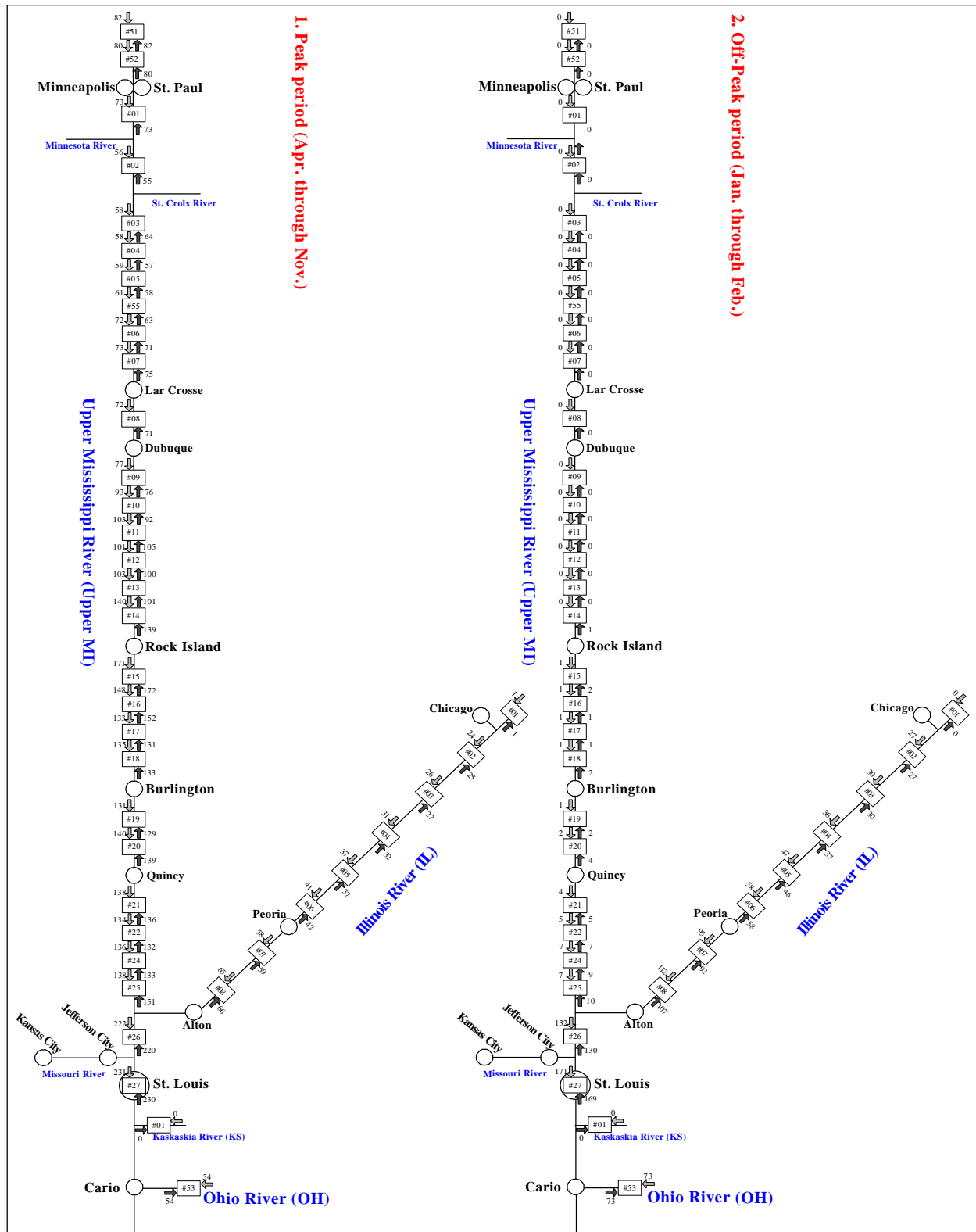


Figure 13. Average Monthly Towboat Traffic of the 90% Unique Towboats at the UMR and Illinois Locks during the UMR Peak and Off-peak (2000-2004)

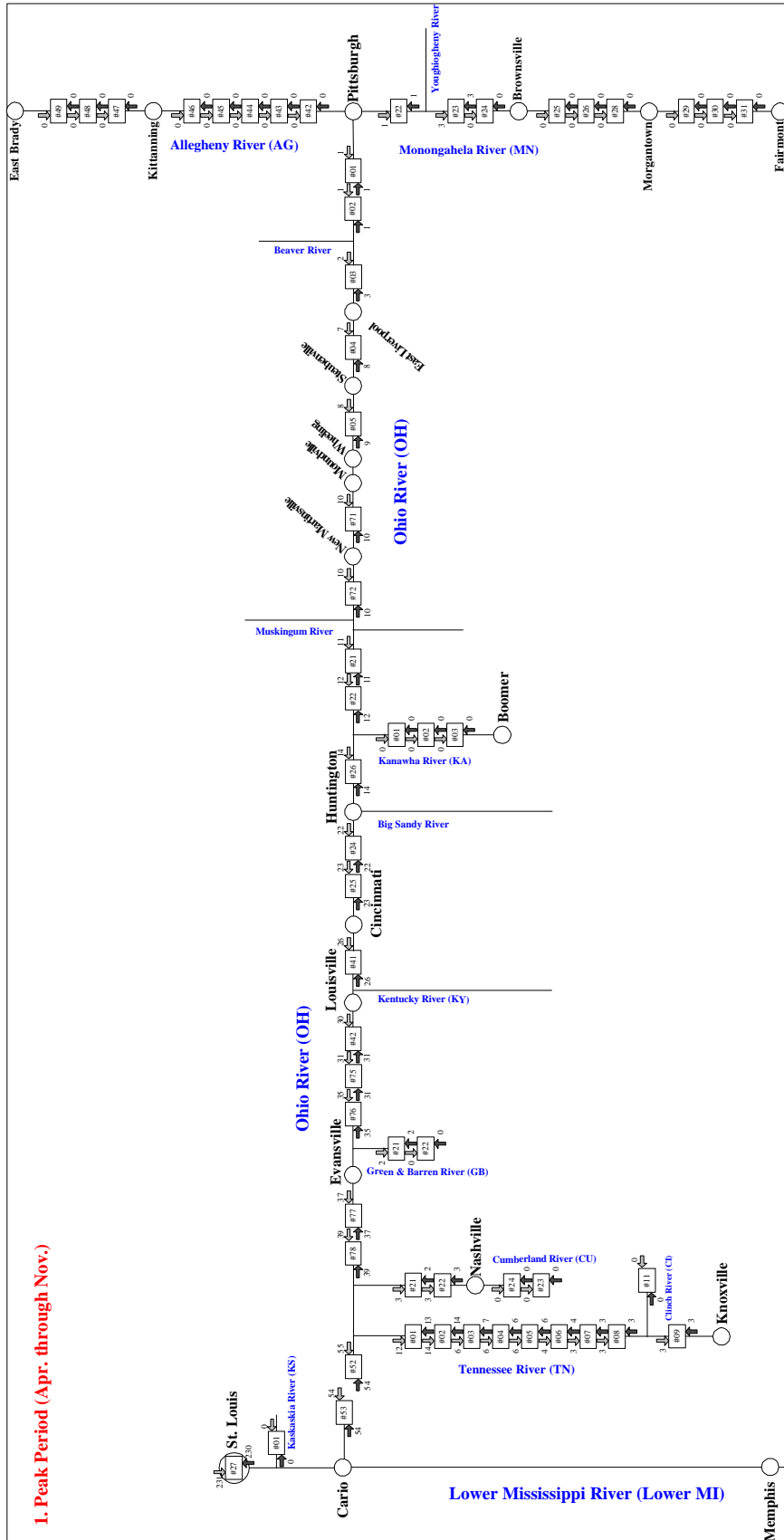


Figure 14 (a). Average Monthly Towboat Traffic of the 90% Unique Towboats at the Ohio Locks during the UMR Peak(2000-2004)

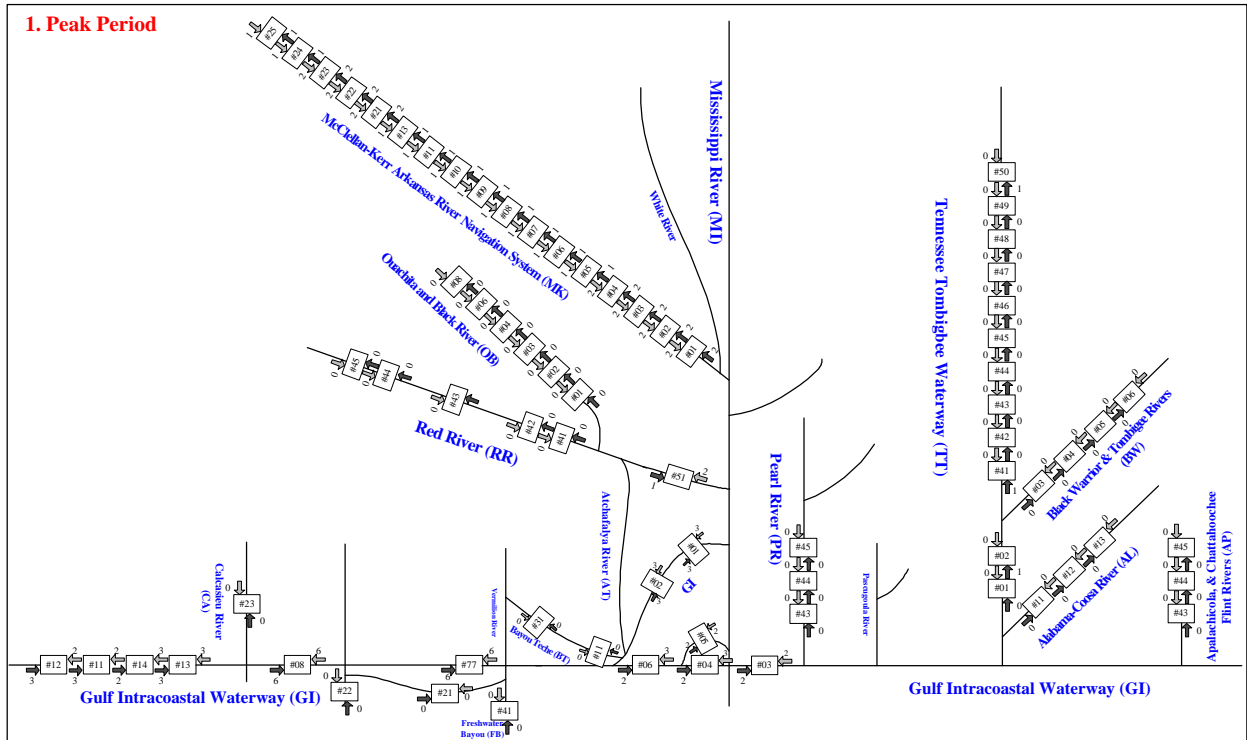


Figure 15 (a). Average Monthly Towboat Traffic of the 90% Unique Towboats in the Lower MVD, SWD, and SAD during the UMR Peak of the UMR (2000-2004)

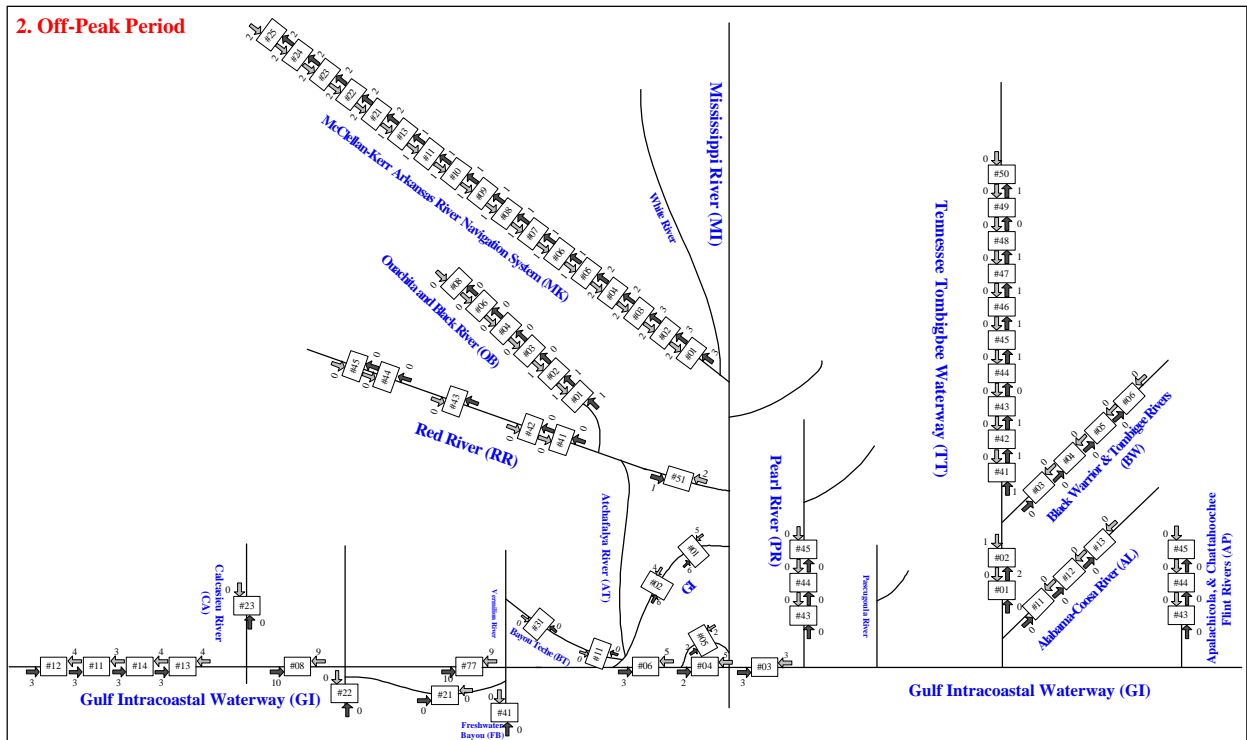


Figure 15 (b). Average Monthly Towboat Traffic of the 90% Unique Towboats in the Lower MVD, SWD, and SAD during the UMR Off-Peak (2000-2004)

Genetic Algorithms for Selecting and Scheduling Waterway Projects

By Shiaaulir Wang and Paul Schonfeld

*Department of Civil and Environmental Engineering
University of Maryland, College Park*

April 2006

Table of Contents

Abstract	5
Introduction	5
Optimization	5
Simulation-Based Optimization Model.....	6
Genetic Algorithms	7
Characteristics.....	7
Design of GAs.....	8
Genetic Operators.....	10
Crossover Operators.....	10
Mutation Operators.....	11
Project Scheduling Problems.....	11
Problems of Scheduling Waterway Improvement Projects.....	14
Inland Waterway Simulation Model.....	14
Integrated Waterway Simulation and Optimization.....	15
SIMOPT	16
SIMOPT Model Assumptions	16
Model Features.....	17
Network Examples.....	18
Test Network 1 (Artificial Network).....	18
Test Network 2 (Upper Mississippi River).....	18
Model Testing	19
Simulation Inputs	19
Optimization Inputs.....	20
Optimized Results	21
NaSS.....	23
Model Extensions for NaSS.....	24
Enhanced Work on Genetic Algorithms.....	25
Project Construction Time	25
Project Multiplicity.....	27
Time Efficiency.....	31
Model Test (Enhanced SIMOPT)	33
Test Network.....	33
Input Parameters.....	34
Testing Results.....	35
Verification of GA Optimization Model.....	41
Conclusions and Future Work	43
Summary and Conclusions	43
Future Work.....	44
Appendix	46
GA Phase 1 Scope of Work.....	46
References	47

List of Tables

Table 1 Lock Control Settings for SIMOPT	20
Table 2 Lock Expansion Plans for SIMOPT	20
Table 3 Genetic Parameters for SIMOPT	21
Table 4 Test Results for SIMOPT	22
Table 5 Simulation Parameters in SIMOPT Extension.....	35
Table 6 Optimization Parameters in SIMOPT Extension.....	35
Table 7 Project Information for Case 1.1 (Baseline without Construction Times)	36
Table 8 Project Information for Case 1.2 (Considering Construction Times)	36
Table 9 Optimized Results for Case 1 (Considering Construction Times).....	36
Table 10 Additional Optimized Results for Case 1 (Considering Construction Times)...	37
Table 11 Project Information for Case 2 (Considering Mutually Exclusive Projects)	39
Table 12 Optimized Results for Case 2 (Considering Mutually Exclusive Projects).....	39
Table 13 Additional Optimized Results for Case 2 (Considering Mutually Exclusive Projects).....	40
Table 14 Results for Case 3 (Avoiding Duplicated Simulation Runs)	41

List of Figures

Figure 1 Interaction between Simulation and Optimization.....	7
Figure 2 GA Procedure	9
Figure 3 Relations of Budget Flow, Cumulative Cost, Project Sequence, and Project Schedule	13
Figure 4 Structure of SIMOPT Problem	14
Figure 5 Integration of Waterway Simulation and GA Optimization.....	16
Figure 6 SIMTOP Test Network – Artificial Network.....	18
Figure 7 SIMOPT Test Network – Network of Upper Mississippi River	19
Figure 8 Cost and Network Analysis of SIMOPT Project Implementation.....	22
Figure 9 Benefits of Projects with Control Considerations in SIMOPT.....	23
Figure 10 Structure of Chromosome for Considering Project Construction Time	25
Figure 11 Capacity Changes during the Simulation	26
Figure 12 Paired Representation of Chromosome for Mutually Exclusive Projects.....	28
Figure 13 Illegitimacy Generated from Mutation Operator for Paired Representation....	29
Figure 14 Possible Mutation Operator for Paired Representation.....	29
Figure 15 Path Representation of Chromosome for Mutually Exclusive Projects.....	30
Figure 16 Proposed Refining Technique to Create Feasible Solutions for Mutually Exclusive Projects.....	30
Figure 17 Structure of Chromosome Defined in SIMOPT	31
Figure 18 Modified Structure of Chromosome for Mutually Exclusive Projects	31
Figure 19 Deque Data Structure	32
Figure 20 Sequence Comparison	33
Figure 21 Refined Sequence.....	33
Figure 22 Test Network for SIMOPT Extension.....	34
Figure 23 GA Search Performance	38
Figure 24 Histograms of Sampled Solutions	42
Figure 25 Fitted Gamma and Lognormal Distributions	43

Abstract

A testbed waterway model (SIMOPT) that combines simulation and optimization has been developed at the University of Maryland. It employs genetic algorithms to solve the problem of evaluating, selecting, sequencing and scheduling waterway improvement projects. It provides a promising demonstration of simulation-based optimization.

Since the developments of simulation and optimization components are largely separable, this testbed model can be used to quickly test optimization improvements without running more detailed and longer-running simulations. The improved optimization models are intended to work with the next generation NaSS waterway simulation model which is developed under the NETS program of the Corps of Engineers. As a testbed, SIMOPT is modified here to consider project construction time and capacity reductions during construction, avoid duplicate evaluations and consider mutually exclusive projects at any locks.

Introduction

A problem of great concern to the U. S. Army Corps of Engineers (USACE) is the selection, sequencing and scheduling of the waterway improvement projects, which include chamber construction, expansion, rehabilitation, or maintenance. If numerous projects are considered, a massive combinatorial optimization problem results. This problem is very difficult to solve with conventional optimization approaches. Thus, an investment optimization model based on genetic search algorithms is proposed to solve this large and complex combinatorial problem.

Solving an optimization problem requires evaluation as well as optimization. As a complex and probabilistic system, a waterway network can be analyzed through a detailed simulation model. Thus a simulation-based optimization model is explored for selecting and scheduling waterway projects.

The following sections focus on the issues of optimization, simulation-based optimization modeling and project scheduling. The SIMOPT model is presented to demonstrate the capabilities of a simulation-based optimization model in scheduling waterway improvement projects. It is expected that the optimization methods developed and tested with SIMOPT can then be applied with the next generation NaSS waterway simulation model.

Optimization

Optimization is a mathematical process that searches for the solution which best satisfies a stated objective. Any optimization problem can be formulated with an objective function to be minimized or maximized, and subject to constraints of budgets, capacities,

construction times or facility closure times. Various optimization algorithms are available for solving different levels of optimization problems. Calculus, enumerative search, mathematical programming and branch and bound algorithms may be used to solve exactly some optimization problems which are sufficiently small or well behaved . Heuristic optimization methods such as simulated annealing, tabu search, genetic algorithms and swarm intelligence may be tried for problems that are relatively large of have numerous local optima.

If the decision variables are discrete, the optimization problem is a combinatorial optimization problem, whose optimal solution is found from the enumeration, combination and permutation of several discrete elements. Since it is practically very hard to identify the global optimum as number of decision variables becomes large, rather than finding the perfect “optimum solution”, we seek a very good (or “near-optimal”) solution. In solving a complex optimization problem, the objective function must be repeatedly evaluated. This function might be computed or estimated with a simple equation, a queuing model, and other methods. If the system analyzed is complex enough and subject to probabilistic variations, it is difficult to evaluate it or its objective function without a detailed simulation model.

Simulation-Based Optimization Model

For years, there has been considerable interest in combining simulation and optimization models. With a number of controllable decision variables and an objective function to be maximized or minimized, the optimization model runs the simulation model and eventually determines a combination of the decision variables that produces an optimal or near optimal solution.

A simulation model is commonly used for complex probabilistic systems. Since those systems are hard to evaluate analytically, the objective function is not fully specifiable. There are several advantages of applying simulation models:

- System performance can be estimated under specified operating conditions.
- Operations with alternative design and control characteristics can be compared.
- Experimental scenarios can be carefully controlled.
- Systems undergoing many changes over time can be studied.

A possible simulation-based optimization model is presented in Figure 1. The optimization module first instructs the simulation module to simulate some initial system configurations, i.e. combinations of decision variables for the system. The simulation model evaluates and computes the objective function for each analyzed configuration. Based on the above results, the optimization model selects new combinations of decision variables to be simulated, until further improvements become insignificant. That is, the outputs from these simulations are fed back into the optimization module, which then uses its built-in search algorithm to generate additional configurations to simulate, etc. The whole process is continued, while insuring that all constraints are satisfied, till the termination rule in the optimization module is reached.

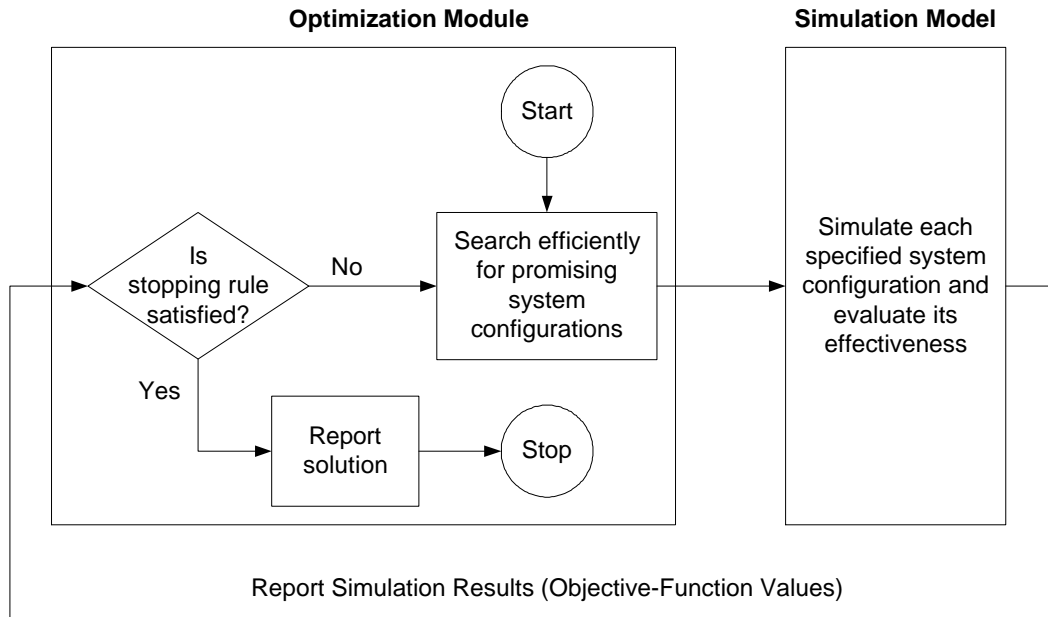


Figure 1 Interaction between Simulation and Optimization

However, although the operational steps are indeed workable, it is important to note that the results are not absolutely guaranteed to be optimal. The optimization results depend on how the options, parameters, and tolerances are specified. A good optimization model can efficiently reach a near-optimal configuration. The difference between the global optimum and the near optimal solution is usually insignificant in practice, considering the uncertainties in inputs and in functional relations.

Genetic Algorithms

Characteristics

An efficient optimization algorithm must satisfy two requirements in finding the global optimum: sufficiently explore the search space and exploit the knowledge gained at the previously visited points. (That search space includes the points representing the various combinations of decision variables.) Rooted in natural genetics and computer science, genetic algorithms (GAs) treat the problem as the environment, and consider a set of possible solutions to the problem as the population. A procedure that (somewhat) mimics the natural evolution is established to select individuals for reproducing offspring according to their “fitness” to the environment (i.e. the problem). Each individual (which constitutes a tentative solution to the problem) in the population is represented by a set of encoded genes called a chromosome. After several generations, the most adapted individuals will survive and have a higher chance of reproducing offspring. If the

algorithm is well designed, the population will converge to an optimal solution to the problem.

There are several characteristics distinguishing GAs from other conventional optimization techniques. At any stage in the search GAs work with a set of solutions rather than one single solution. This feature enables GAs to escape from local optima in their multi-directional global search. Besides, no specific function (i.e. formulated objective function) for the mathematical expression of a given problem is required in GAs. Thus GAs are able to handle any kind of objective function and constraints, and are especially suitable when the objective function is quite noisy (i.e. with numerous local optima). The GA search approach is at least partially probabilistic in the way population members are selected for future generations and in the frequency with which various operators are applied.

Design of GAs

Figure 2 shows the basic GA procedure in optimization search process. The application of GAs to a specific problem includes several steps.

1. Solution encoding
Originally, a potential solution to the problem is encoded into a binary string, called a chromosome, of a given length which depends on the required precision. In terms of problem characteristics, some other ways of representing solutions are necessary, such as integer coding for solving combinatorial optimization problem.
2. Initial population
Generally, the initial population is randomly generated. If good solutions can be included in the initial population, the optimization time can be reduced somewhat.
3. Fitness function
When GAs are applied, the fitness function is the objective function to be optimized. The fitness value of each individual solution from a population must be evaluated.
4. Selection
The individuals in the population are selected to reproduce offspring according to their fitness value. Typically, proportional selection chooses individuals by calculating their relative fitness values. If necessary, scaling and ranking schemes provide alternatives for measuring fitness other than using raw values directly
5. Genetic operators
Classic GAs provide two types of genetic operators – crossover and mutation. A crossover operator generates the offspring from two parents by swapping their genes at some randomly chosen position of the chromosomes. A mutation operator alters (according to some rules and/or probabilities) one or more genes of one selected parent chromosome in order to increase the population variability.
6. Population replacement
Replacement creates a new population for the next generation and is strongly related to the selection process. Two issues arise in this phase – sampling space and sampling

mechanism. Along with selection, both of them have a significant influence on selective pressure and thereby on genetic algorithm behavior.

7. Termination and convergence

Usually, the genetic system is terminated through a pre-specified number of generations. Another termination rule could be as follows: stop the search process after the solution of the best sequence remains unchanged for the last m generations.

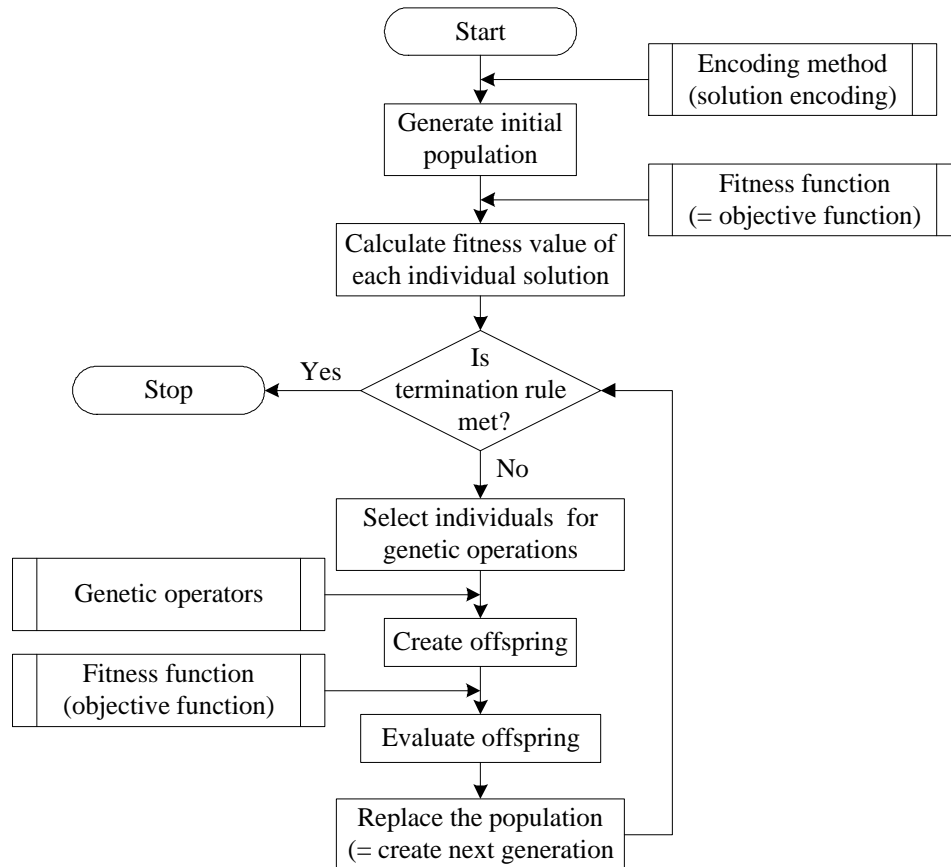


Figure 2 GA Procedure

For the integration of waterway simulation and optimization, a genetic algorithm is chosen to perform the optimization search. Several steps are included in an ordinary genetic algorithm:

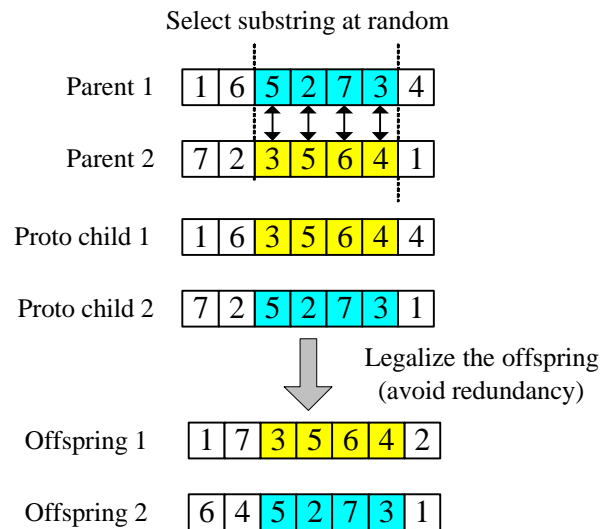
- Step 1: Create initial population of solutions (i.e., project sequences).
- Step 2: Evaluate those solutions (with a simulation model in this study).
- Step 3: Select the better individual solutions for genetic refinement.
- Step 4: Create new solutions using mutation, crossover, or other operators.
- Step 5: Evaluate new solutions.
- Step 6: Replace most or all previous solutions in the population.
- Step 7: Stop if the termination rule is satisfied. Otherwise, return to step 3

Genetic Operators

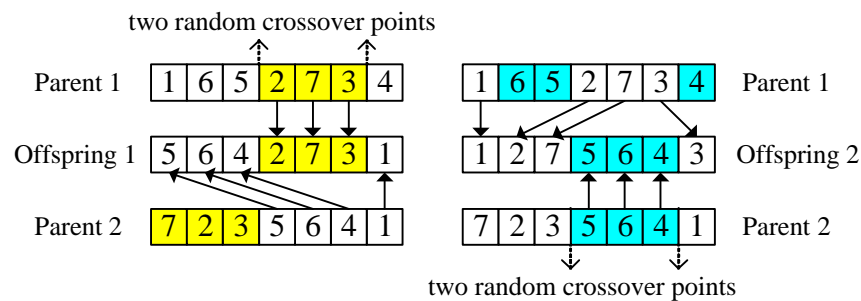
In general, there are two types of genetic operators: mutation operators and crossover operators. During the past decades, several operators have been proposed, widely discussed and served as standard operators for solving sequencing problems. Those are discussed below.

Crossover Operators

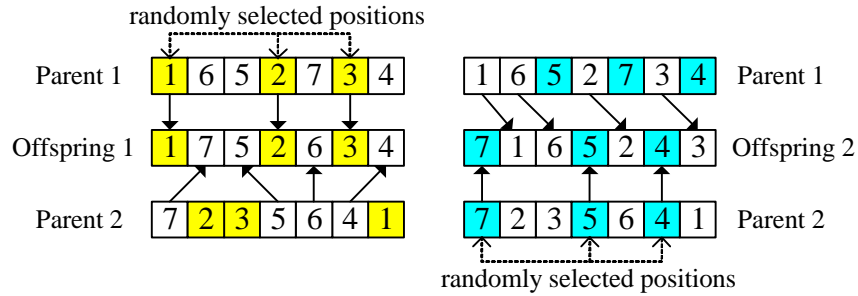
- Partial-Mapped Crossover (PMX)



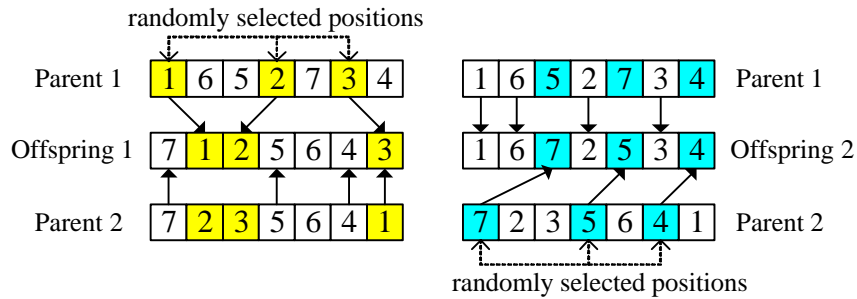
- Order Crossover (OX)



- Position-Based Crossover (PBX)

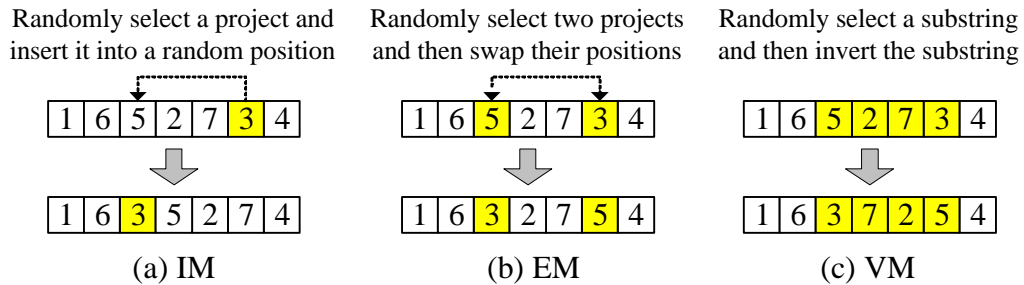


- Order-Based Crossover (OBX)



Mutation Operators

- Insertion Mutation (IM)
- Exchange Mutation (EM)
- Inversion Mutation (SM)



Project Scheduling Problems

Investment planning, also known as capital budgeting, is the process of determining which investments or candidate projects will be funded and pursued to meet the pre-specified objectives over a planning horizon. It includes the tasks of project evaluation, project selection, project sequencing and project scheduling.

With a constrained budget available for various investment combinations, project selection and sequencing is a large combinatorial optimization problem. The solution space increases more than exponentially with problem size, i.e., with the number of projects considered. Furthermore, project interdependence increases the difficulty of solving project scheduling problems. Project benefits and/or costs might depend on which other projects are implemented. Especially in transportation networks, there are traffic interactions between adjacent projects. Some capacity improvement projects may mostly shift elsewhere the bottlenecks and delays. Therefore, those interdependencies make the evaluation even more complex if the improvements from some projects affect the operations and benefits of other projects.

The literature includes various methods of evaluating schedules of interdependent projects, such as queuing metamodels, equilibrium traffic assignment, artificial neural networks and microscopic simulation models. Some optimization approaches are also explored in previous studies, such as swapping algorithms, branch and bound algorithms, Lagrange relaxation, simulated annealing and genetic algorithms.

If funds are limited (i.e., always insufficient for all worthwhile projects), funds should be used as soon as they become available to complete as soon as possible each project in a sequence. That is, as funds become available over time, and assuming that funding is never (at anytime throughout the simulated analysis period) sufficient to implement all justifiable projects, then, a sequence of projects uniquely determines the schedule (i.e., the implementation time of each project). Thus each project in the sequence is implemented as soon as the funding stream allows it. Hence, with a constrained budget over time, the optimal project sequence uniquely determines the optimal project schedules. Only those projects with implementation times before the end of analysis period are selected. The others are implicitly rejected, thus, determining the project selection.

As shown in Figure 3, for a given project sequence, the time at which each project is finished can be obtained by comparing the cumulative budgets and cumulative project costs. Then let o_i denote the i^{th} project to be implemented in chronological order and t_i^o denote the time at which o_i is finished. Then t_i^o can be determined by solving the equation $\sum_{j=1}^i c_j^o = \int_0^{t_i^o} b(t)dt$, where c_j^o is the capital cost of the j^{th} project to be implemented.

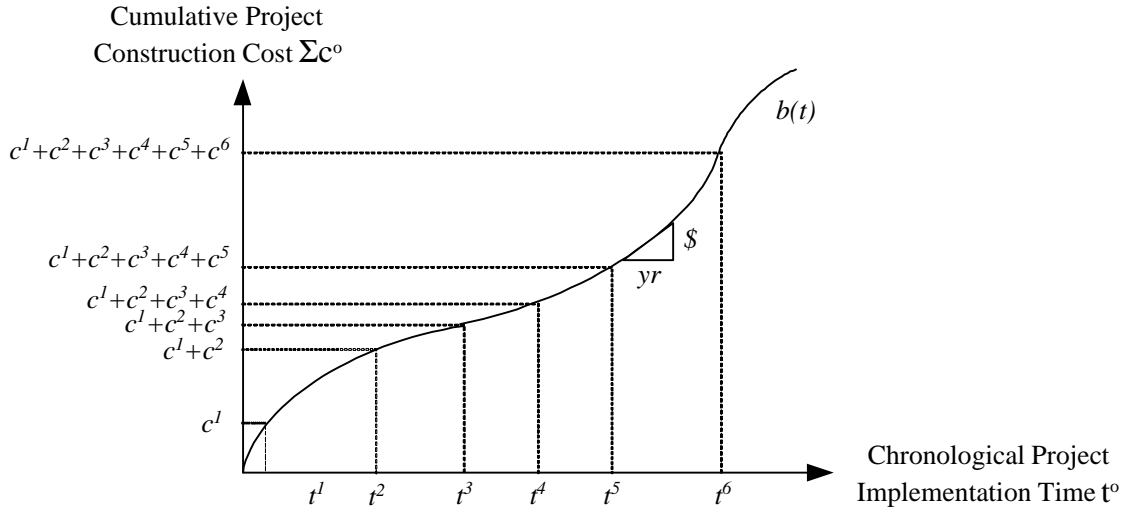


Figure 3 Relations of Budget Flow, Cumulative Cost, Project Sequence, and Project Schedule

If there are N lock improvement projects in N fixed lock locations, the project selection process chooses a subset of n projects from a set of N desirable projects in the most desirable order. Meanwhile, the project scheduling process determines the sequence for implementing projects as well as the timing for the selected projects. Given a sequence and timing of lock capacity expansions, the project evaluation process estimates the system performance, which is usually defined as system delay costs. The performance measures cannot be determined until a project portfolio is specified. When project interdependencies exist, any lock improvement may affect traffic characteristics at other locks. As a practical matter, if there were a large number N of lock improvement projects and only n projects will be selected due to budget constraints, the solution space for project selection and sequencing including all possible combinations and permutations would be

$$\sum_{n=0}^N \frac{N!}{n!(N-n)!} \times n! = \sum_{n=0}^N \frac{N!}{(N-n)!}$$

The above equation indicates that the size of the solution space increases more than exponentially with the number of candidate projects N . If N is not very small, a full enumeration search becomes infeasible for finding the optimal combination among all alternative project sets. For jointly considering project selection, sequencing and scheduling, the solution space is even larger. Through the budget constraints, the size of the project sequencing problem becomes $n!$, which is smaller than that of the original problem, and each of the $n!$ sequence corresponds to a feasible solution.

If the project size (or changed capacity) is lumpy rather than continuous at any project location, the solution space is increased by the factor of $\prod_{i=1}^n P_i$, where P_i is the number of possible projects at lock i . The project scheduling problem will then consider more combinations and permutations.

Problems of Scheduling Waterway Improvement Projects

Scheduling waterway improvement projects is considered as a combinatorial optimization problem. The objective function is set to minimize the system costs or maximize the net benefits over a multi-year period. There may be several constraints regarding budgets (possibly by region or type of expense), precedence, mutually exclusivity, minimum improvement steps, construction times, capacities, service quality, and geographic distributions. It is difficult to analytically model the probabilistic features of a waterway system. Hence, a simulation model is adopted for evaluating the system with each schedule. A conceptual approach for combining simulation and optimization models to solve our problem is shown in Figure 4.

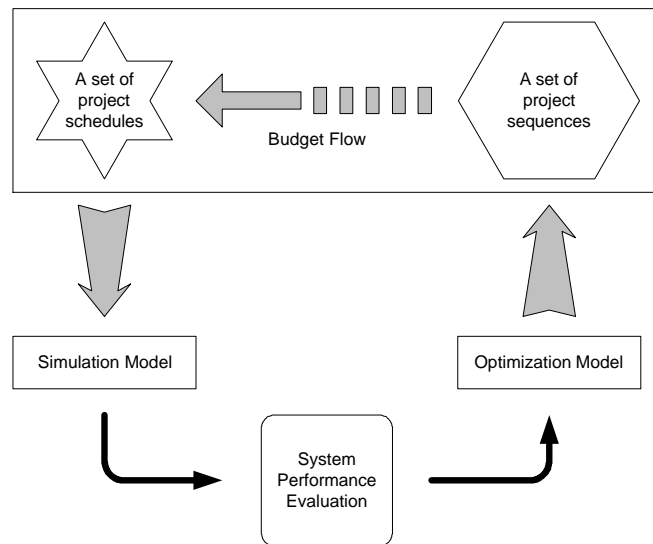


Figure 4 Structure of SIMOPT Problem

The inputs required for this combined simulation-optimization model should be information on improvement projects, system network configuration and network relevant variables. The outputs for these two interacting modules should be performance measures from the simulation model and project schedule (implementation timetable of the selected projects) from the optimization model.

Inland Waterway Simulation Model

Due to the probabilistic features in waterway traffic, a microscopic, discrete-event simulation model is preferred to model the inland waterway operation. The purpose of using a waterway simulation model is to evaluate the performance of inland waterways with specified system characteristics, as well as analyze short-term system variability and control alternatives. In the long run, the system evolution can also be assessed.

Coding is a major aspect of building a complex simulation model. One of the most important features of such a system simulation model is its portability. With portability, a model can be easily reused for other geographic areas or networks. With different levels of details for different study purposes, such a simulation model could have wide applicability for various purposes, such as forecasting, design, control, project selection and scheduling, maintenance planning and scheduling, reliability analysis.

Some major factors should be considered in inland waterway simulation model:

- Probabilistic aspects of waterway traffic, lockage times, travel times, stalls, etc.
- Demand variability
 - Demand sensitivity to service levels
 - Demand sensitivity to construction and closures
 - Demand sensitivity to improvement projects
- Operational lock control alternatives
 - Lock control strategies
 - Chamber interference at multiple-chamber locks
 - Chamber assignment for multiple-chamber locks

Integrated Waterway Simulation and Optimization

The inland waterway simulation model is designed as a discrete-event simulation model. It includes various “network operation events”. In addition to those events in the simulation kernel, “project construction events” have been added to update some system variables during the simulation. Those project construction events come from the project implementation schedule whose sequence is generated by the GA. The schedule is then determined based on budget constraints. The project implementation schedule is then fed into the simulation model and evaluated by the simulation model. The integration of simulation model and optimization model is shown in Figure 5. Two blocks show the two separate models for simulation and optimization. They are connected by the information they exchange about decision variables of the project implementation schedule.

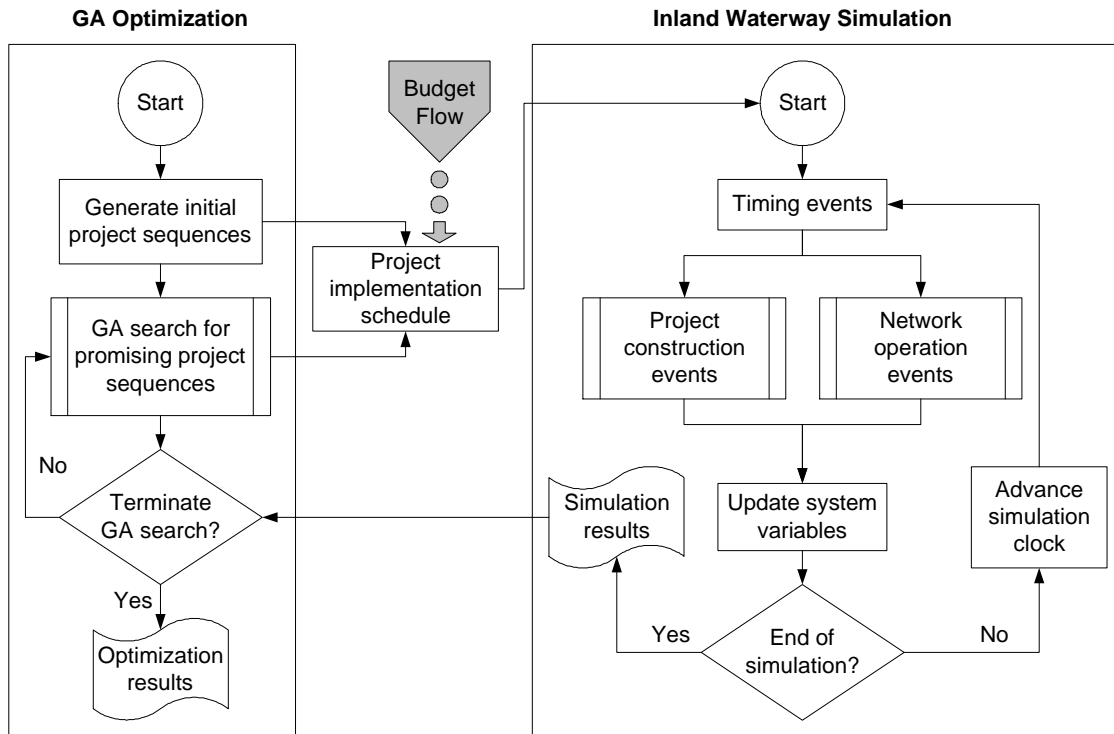


Figure 5 Integration of Waterway Simulation and GA Optimization

SIMOPT

SIMOPT was developed at the University of Maryland and presented to USACE's Institute for Water Resources (IWR) in a meeting on July 27-29, 2005. It serves as a proof of concept model that can be tested and manipulated to help identify problems that may arise in future when a much more complex simulation model is combined with optimization. As a testbed, SIMOPT can run a simulation alone or combine it with a genetic algorithm to optimize project scheduling. After some discussion and refinements, the latest version of SIMOPT was delivered to USACE in late September 2005, accompanied by the SIMOPT presentation file, which mainly serves as a simple user guide for SIMOPT.

SIMOPT Model Assumptions

The simplifying assumptions in the original SIMOPT include the following:

- Simulation Model
 - Each tow maintains a constant number of barges through the entire trip, even if it is necessary to disassemble barges while passing through the locks. That is, a tow's size is assigned when that tow is generated, and there is no reflecting during its trip.

- Each tow maintains a constant speed between its origin and destination ports, either upstream or downstream.
- There is always enough equipment, such as towboats and barges, for waterway shipments wherever needed in the network.
- The queue storage space at each lock is unlimited for both directions.
- Components of lockage process are simplified with a single service time distribution.
- Optimization Model
 - The implementation (i.e., mainly construction) costs of projects are independent and additive. Whenever the cumulative budget reaches the required construction cost for an additional, that project implementation is completed.
 - The budget is accumulated continuously as a function of time over the planning horizon.
 - The implementation of one project does not yet depend on the existence of the other projects.
 - The increase in lock capacity is indicated by the increased service rate (i.e., the inverse of service time).
 - A capacity is specified without affecting the number of chambers.
 - Lock capacity increases instantaneously after a lock improvement project is completed. After the project selection and sequencing are completed the project completion times can be uniquely determined.
 - There is one and only one improvement project at each lock location. No other alternatives are yet considered.
 - Budget constraints are always binding, i.e., there are never enough funds for all justifiable projects.

Model Features

SIMOPT is built with an inland waterway simulation model (Wang 2001) and a GA search algorithm. The simulation model incorporated in SIMOPT is designed to be a portable, data-driven model which can be applied on various waterway tree networks without re-coding the computation kernel. The optimization model employed in SIMOPT is deliberated with genetic algorithm, especially in solving sequencing problems.

SIMOPT has a simple user interface. It allows users to specify required input files, which should be prepared ahead of running the SIMOPT model, and some other basic parameters such as the duration of the simulation period and the number of simulation replications needed to reduce the variance of the combined stochastic processes of simulation and optimization.

Demonstrations of SIMOPT have exhibited the following features of this model:

- Run Simulation
 - Performance of designed simulation scenario

- Project Evaluation
 - Evaluation of single projects
 - Evaluation of any given project sequence
 - Evaluation of lock control policies
- Run Optimization
 - Optimization of project selection, sequencing and scheduling

Network Examples

Two network examples are provided with the latest version of SIMOPT. One is a simple, artificial test network (shown in Figure 6) and the other is a section of the actual US inland waterway network, the Upper Mississippi River (shown in Figure 7). The latter case is shown in greater detail in Wang’s dissertation (referred as “Case Study”).

Test Network 1 (Artificial Network)

This artificial network includes 5 ports (5×5 O/Ds) and 7 locks (3 two-chamber locks and 4 one-chamber locks). Improvement projects are applied at locks to expand capacity, by doubling capacities at single-chamber locks and expanding the capacities at two-chamber locks. This artificial network is used to show how the network configuration inputs are prepared for the simulation module, which was developed with a data-driven approach. Details of the development of simulation model development are shown in Wang and Schonfeld’s 2003 TRB paper.

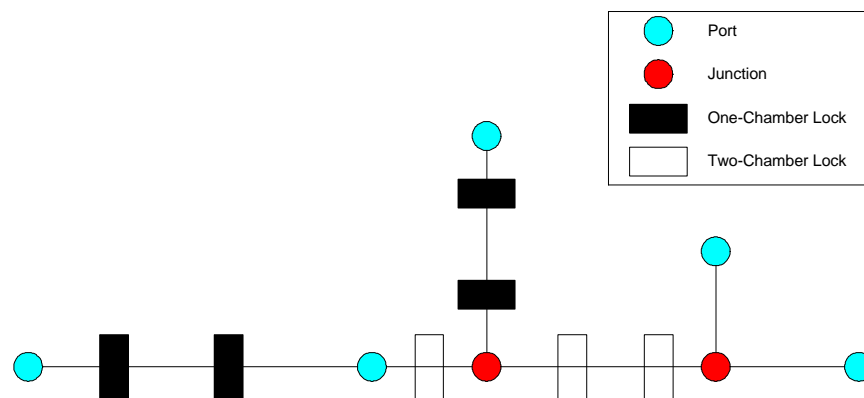


Figure 6 SIMTOP Test Network – Artificial Network

Test Network 2 (Upper Mississippi River)

The simulation model in SIMOPT is capable of simulating a large waterway network, such as Upper Mississippi River area and Ohio River area with 17 major ports and 74 locks. The distance between St. Louis and Cairo exceeds 100 miles, which is enough to eliminate lock interdependence. Therefore, the inland waterway network analyzed here is the Upper Mississippi region area which contains 3 rivers, 7 ports and 36 locks.

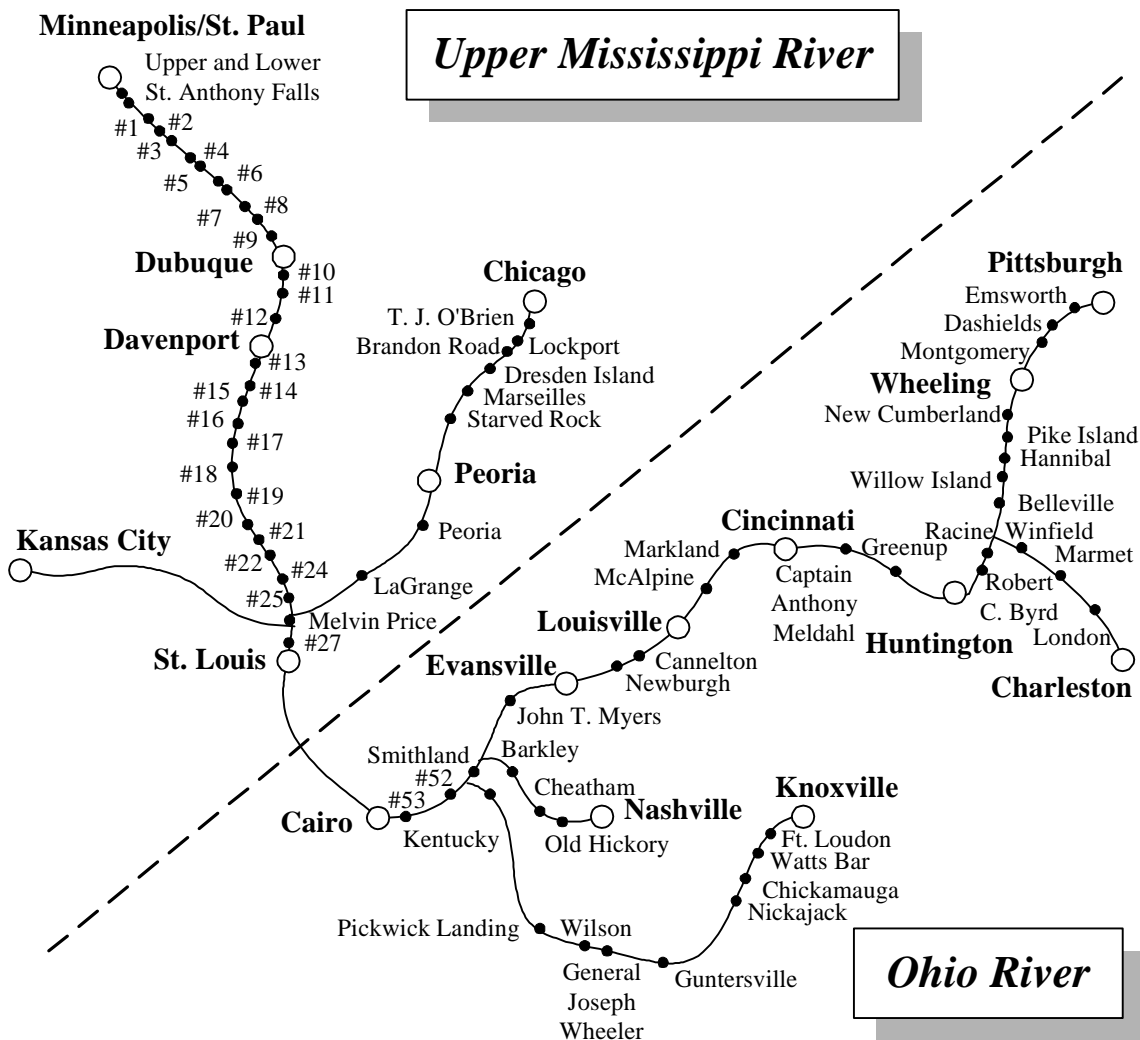


Figure 7 SIMOPT Test Network – Network of Upper Mississippi River

Model Testing

After examining the delays at current locks, locks #15, #16, #17, #18, #19, #20, #21, #22, #24, #25 are selected for improvement projects which double their capacities. Running the simulation model on such a large network, even once, takes considerable time. Besides, hundreds or thousands of evaluations might be necessary to approach the optimal or near optimal solution while using genetic algorithms. Therefore, due to limited computational resources, the simulation is accelerated (within 1.5 years) with high traffic growth and high budget rates.

Simulation Inputs

- O/D matrices

- Matrices of demand growth rates
- Matrices of demand elasticity
- Tow size distribution
- Speed distribution
- Service time distribution
- Link distances
- Number of chambers
- Chamber bias and lockage cuts
- Control alternatives (F → FCFS, S → SPF)
 - Case 1.1: network-wide FCFS
 - Case 1.2: network-wide FCFS w/ selected SPF

Table 1 Lock Control Settings for SIMOPT

Lock	Control	Lock	Control	Lock	Control	Lock	Control
Up. Falls	F	#8	F	#17	F	#27	F
Lo. Falls	F	#9	F	#18	F	LaGrange	F
#1	F	#10	F	#19	F	Peoria	F
#2	F	#11	F	#20	F	Starved Rock	F
#3	F	#12	F	#21	F	Marseilles	F
#4	F	#13	F / S	#22	F / S	Dresden Island	F
#5	F	#14	F	#24	F / S	Brandon Road	F
#6	F	#15	F	#25	F / S	Lockport	F
#7	F	#16	F / S	#26	F	T. J. O'Brien	F

Optimization Inputs

- Lock expansion plan

Table 2 Lock Expansion Plans for SIMOPT

Lock Site	Capacity	Cost (10 ⁶)	Current Lock Delays (barge-hrs)	Project Benefit (system total delay savings)
#13	2.0	2.5	3742780	1086416
#16	2.0	1.6	2501000	731052
#17	2.0	2.7	2120250	551020
#18	2.0	2.1	1987090	508484
#19	2.0	1.7	1765470	408528
#20	2.0	2.4	1733540	263210
#21	2.0	2.1	1795420	337892
#22	2.0	1.9	2098990	432320
#24	2.0	2.3	2940650	679700
#25	2.0	2.2	5130450	946204

- Genetic parameters

Table 3 Genetic Parameters for SIMOPT

<i>GA Parameters</i>	<i>Value</i>
Population Size	20
Mutation Rate	0.2
Crossover Rate	0.5
Selection	Elite
Sampling Mechanism	Stochastic
Selection Probability	Ranking Scheme
Sampling Space	Large w/ replacement
Termination	5 generations w/o improvement

Optimized Results

Intuitively, if locks are considered individually, the construction projects would be implemented according to the rank of their delay severities, that is #25→#13→#24→#16→#17→#22→#18→#19→#21→#20. Based on two sets of control alternatives designed in previous input tables, the optimized solutions for sequencing and scheduling 10 projects are shown in the following table.

As can be seen in the left side of table, if only physical construction projects are considered and all locks are operated with FCFS, i.e., without changes in lock control, then #22→#16→#25→#13→#18→#24→#19→#21→#20→#17 is the optimized project sequence. It differs from the one ranked according to individual lock delay severities. Also, the rank-based project sequence results in a total delay cost of $\$1.467 \times 10^9$. The optimized sequence found does have a lower system delay costs of $\$1.448 \times 10^9$. Further, SPF control improves efficiency and reduces the delays. Therefore, when combining improvement projects with more efficient control at selected locks, the network bottleneck will shift and lock congestion levels will change. The possibility of operating SPF only at selected locks leads to the project sequence shown on the right side of table. Those locks with better control alternatives can have their improvement projects implemented later. The resulting total delay cost is 1.344×10^9 .

Table 4 Test Results for SIMOPT

Project Sequence	Network-Wide FCFS		Selected SPF	
	Lock Location	Completion Time (Year)	Lock Location	Completion Time (Year)
1	# 22	0.13	# 13	0.17
2	# 16	0.23	# 16	0.27
3	# 25	0.38	# 18	0.41
4	# 13	0.55	# 19	0.53
5	# 18	0.69	# 17	0.71
6	# 24	0.84	# 20	0.87
7	# 19	0.95	# 22	0.99
8	# 21	1.09	# 25	1.14
9	# 20	1.25	# 21	1.28
10	# 17	1.43	# 24	1.43

The above table illustrates the effect of the optimized project implementation schedule on delay costs and on the volume to capacity (V/C) ratio at the remaining critical bottleneck in the network. Figure 8 indicate the accumulated total delay costs with and without projects over the assumed planning horizon of 1.5 years. The dashed lines indicate the implementation times of the 10 projects. At the end of year 1.5, these improvement projects can save almost 25% of total system delay costs. Figure 8 also presents the change of V/C ratio at the network's bottleneck. Along the time axis, the bottleneck physically shifts over the network as additional projects are implemented. In the current demand model, the elasticity of demand with respect to travel time is determined by a sensitivity coefficient which is specified based on judgment and experience with local conditions. With any positive demand elasticity, lock improvements that reduce delays will attract additional traffic, thus changing the V/C ratio in the network.

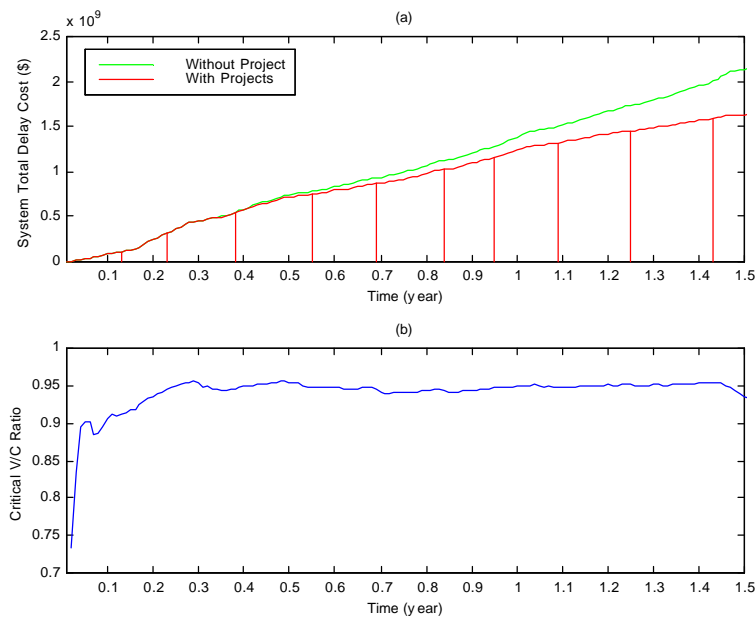


Figure 8 Cost and Network Analysis of SIMOPT Project Implementation

The upper part of Figure 9 compares the results of capital improvement projects and operational control alternatives. As can be seen, the curves intersect around year 0.6. That is, before year 0.6, SPF control can save more delays than capital improvements. The implementation of the first four projects might not be necessary if an effective control alternative is considered. Without projects, the construction costs are also avoided. Finally, the lower part of Figure 9 displays the total delay savings from implementing projects without and with SPF controls. It shows that the system performance can be further improved if more effective lock control and lock expansions are considered jointly.

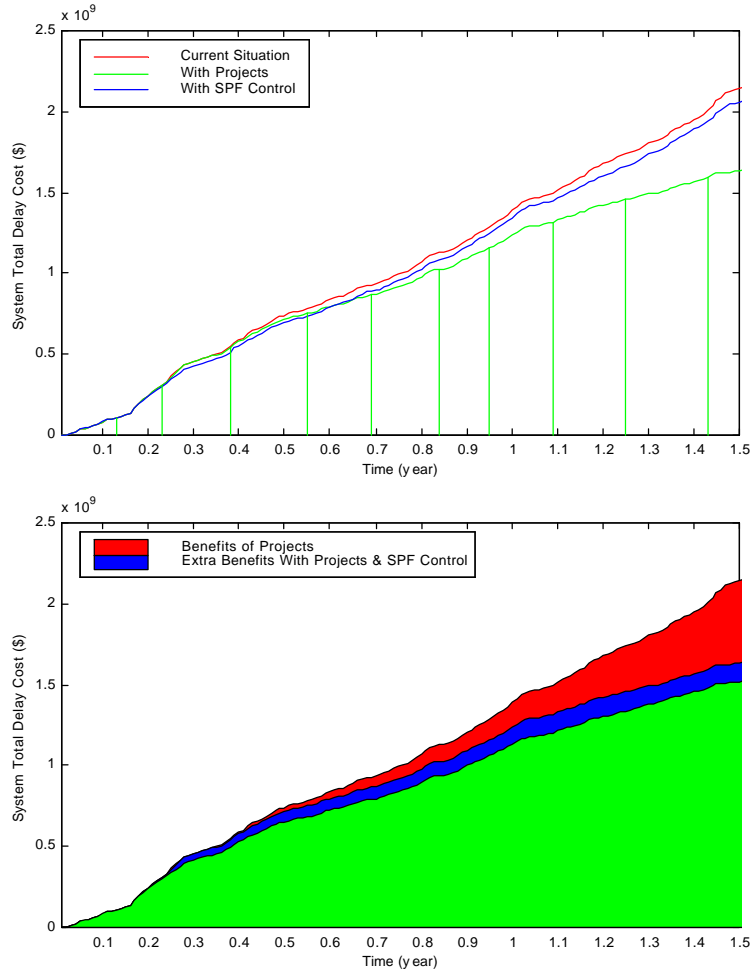


Figure 9 Benefits of Projects with Control Considerations in SIMOPT

NaSS

The Navigation Economics Technologies (NETS) research program is initiated by the US Army Corps of Engineers Institute for Water Resources (IWR) to organize the latest research findings to develop economic tools and techniques for navigation needs. One of

the efforts is to improve the analysis models directed primarily at inland navigation, for which the new NaSS (Navigation System Simulation) model is being developed.

Based on the experience with previously developed USACE models and applications, including the basin-level models WAM, ORNIM, and NavSym; and single lock model representations WAM, LCLM and LockSym, the system network model is a discrete event simulation model that generates commodity shipments between ports, moves vessels through reaches and locks, considers flow conservation, takes into account re-fleeting activities at some designated locations, and incorporates shippers response to scheduled or unscheduled closures. For the investment optimization, the SIMOPT model developed at the University of Maryland is used to explore genetic algorithm optimization in conjunction with a network simulation model. Such a model is flexible and adaptable to a wide variety of inland navigation problems addressed by the Corps.

Model Extensions for NaSS

The NaSS design document describes the model's characteristics including the network model, investment optimization model as well as auxiliary tools of data analyzer, result analyzer and data pre-processor. As discussed above, the investment optimization model can be fully separated from system network model in the development stage. After that, the integration of the simulation and optimization models should be a low-risk and straightforward problem. That is, while the optimization models are developed, they may be integrated with either the SIMOPT testbed or with an even simpler evaluation function.

Several needed enhancements to the GA optimization capabilities and simulation complexities were of interest. Thus, the original model assumptions in SIMOPT are reviewed and possible modifications are studied.

In developing future simulation model, the following features should be considered:

- Consider demand response to network improvements during simulation
- Consider demand diversion due to construction and service interruption
- Update system characteristics during the simulation
- Change lockage behavior if a parallel chamber is added
- Change lock control policies as congestion increases

A more detailed improvement plan could also include:

- Project construction times
- Capacity reductions during construction
- Number and size of chambers
- Maintenance cost
- Failure rates and durations before and after projects.

Some refined optimization features could be included:

- Add constraints (e.g., precedence, mutual exclusivity, available budgets, regional distribution of projects, complementarities among projects)

- Improve search algorithm by creating “smart” operators
- Develop prescreening rules to avoid unpromising solutions
- Avoid re-simulating previous solutions
- Develop parallel processing capabilities

Enhanced Work on Genetic Algorithms

According to the Scope of Work drafted for GA enhancement (see Appendix), several tasks are included in the current phase, including considering project construction time and its relevant effects, involving multiple alternatives at the same project location, and increasing the search efficiency in GA optimization process. The task of “optimal timing for projects absent budget constraints” is automatically bound with other tasks.

Project Construction Time

One of the basic assumptions in SIMOPT in solving the project selection / sequencing / scheduling problem is “lock capacity increases instantaneously after a lock improvement project is selected and completed”. There is no consideration of project construction time and any possible capacity reduction during the construction period. That is, the system increases lock capacity suddenly, whenever a project is implemented. Therefore, by reviewing the inputs given to the simulation model for project evaluation, the construction related information is simplified and added into data file of project information. As shown in Figure 10, in addition to project ID, project size (i.e., capacity expansion ratio) and project cost, two extra data items are included, namely construction duration and residual capacity ratio (Co. T and Res.).

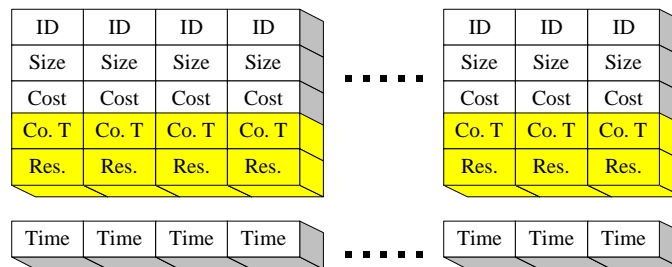
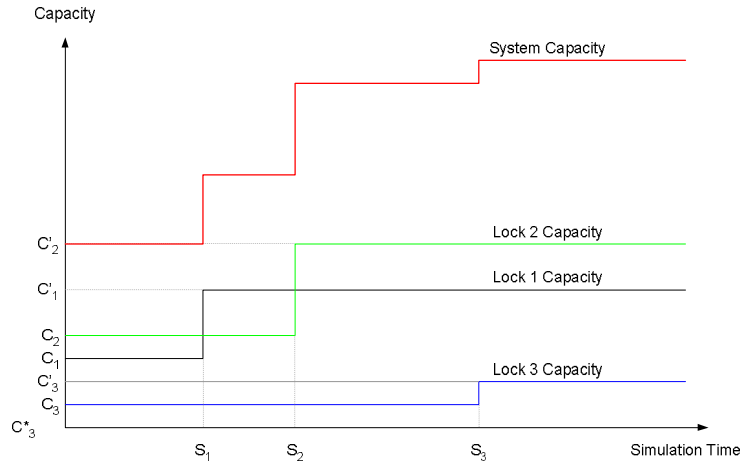
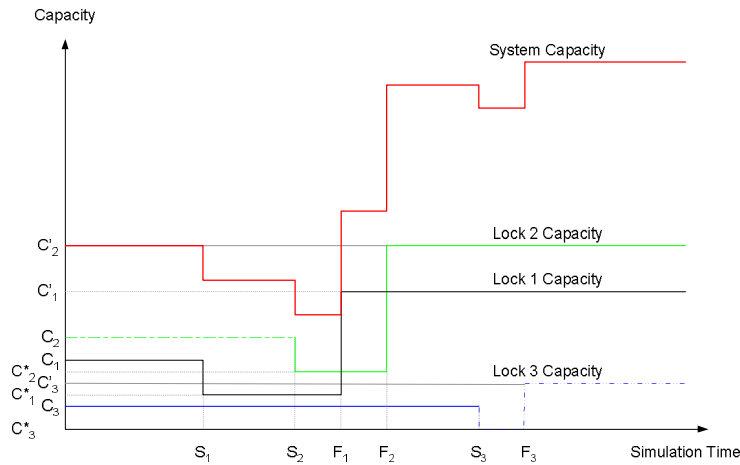


Figure 10 Structure of Chromosome for Considering Project Construction Time

An example is shown in the Figure 11. 3 lock improvement projects are for lock 1, 2, and 3 to increase lock capacities from C_1 , C_2 , and C_3 to C'_1 , C'_2 , and C'_3 , respectively. Figure 11 (a) shows the lock capacity changes in original SIMOPT without considering construction time and capacity reduction. After considering construction time and capacity reduction during the construction, Figure 11 (b) shows that the project construction will decrease the capacities from C_1 , C_2 and C_3 to C^*_1 , C^*_2 , and C^*_3 during the construction periods of S_1 to F_1 , S_2 to F_2 , S_3 to F_3 , respectively. After construction, the capacities are increased to the improvement levels of C'_1 , C'_2 , and C'_3 .



(a)



(b)

Figure 11 Capacity Changes during the Simulation

Some questions worth considering include the following:

- How will the optimization result (project sequencing) be affected if we consider the construction time and capacity reduction?
- How will the demand react to the increasing delays due to project construction? Should a full equilibrium model, or partial equilibrium model, or elasticity model be applied?
- How will the optimization result be affected if demand is or is not sensitive to the capacity and resulting delays?
- How will the optimization results be affected in comparison with the rank of lock congestion level which might intuitively generate the schedule of lock improvement projects?

In order to consider project construction time and capacity reduction in SIMOPT, some modifications in the simulation model are made. With the implementation schedule calculated from the budget flow and project costs, projects are chronologically introduced into the simulation program and implemented immediately whenever the cumulative

budgets reach the construction costs. In addition to the “start project” events in the original SIMOPT, “complete project” events are now added.

Some system variables are updated while the above two projects events are invoked. When an event of starting a project is invoked, lock capacity is reduced to its blockage level and the service rate decreases proportionally. At the same time, the completion time for project construction is calculated to determine when an event of completing a project will be invoked. Similarly, when an event of completing a project is invoked, lock capacity is increased to its expansion level as well as decreased the service time proportionally.

It is possible that the system might explode when a local capacity is reduced to zero or near zero during the construction time, if demand cannot respond to the level of service. In order to avoid infinite queues, an elastic demand model is involved during the simulation. That is, when an event of trip generation is invoked, the generation rate is updated based on the expected and real-time travel times. Let I_{ij} denote current generation rate for a O_i / D_j pair, r_{ij} denote the annual growth rate and k_{ij} denote the demand elasticity. If the expected travel time is w_{ij} and real-time travel time is z_{ij} , the generation rate is updated as $I_{ij} \cdot (1 + r_{ij})^{t_c - t_p} \cdot (z_{ij} / w_{ij})^{k_{ij}}$, where t_c is the clock time and t_p is the previous generation time.

If considering an alternate transportation mode, such as rail, to ease the possible traffic congestion due to the construction, full equilibrium or partial equilibrium models could be used. The shippers response to maintenance closures (i.e., capacity dropping to zero) when the railroads are the alternate mode to waterways has been modeled in Wang and Schonfeld’s 2006 TRB paper. Based on those concepts, the reaction of traffic demand to capacity reductions could be similarly treated with an equilibrium model.

Project Multiplicity

At any specific lock site, several expansion alternatives with discretely specified capacities may be considered. Two cases may arise for project multiplicity: only one project among those alternatives can be selected, or multiple alternatives could be selected but implemented at different times over the planning period. The first case is straightforward and project costs for different alternatives are independent. However, the project costs in the second case could be interdependent and revised based on the implementation sequence. That is, project cost might include the construction cost for building the new project and deconstruction cost for removing the old project at the same location. In the current phase, the first case is considered with at most one project being selected among the alternatives at each site.

If there are mutually exclusive projects at the same location, i.e. if only one can be selected, we may consider the inclusion of sizing decisions in the project scheduling

problem. While combining sizing and scheduling problem, the solution space of fully permuted sequences will be further enlarged through the inclusion of all project alternatives at each lock. That is, if there are N lock locations and m_i ($i = 1, \dots, N$) project alternatives for each lock, the total number of solution including all possible combinations and permutations would be $N! \prod_i m_i$. The project constraints must ensure that only one project at each location is selected among all available alternatives. Let X_i be a binary variable. If $X_i = 1$, the project is selected; if $X_i = 0$, the project is not selected. If i denotes the project alternatives, then the project constraints for any location can be formulated as $\sum_i X_i \leq 1$.

In order to consider project multiplicity, the definition of chromosome used in SIMOPT should be redefined or modified. Different ways to define a chromosome could represent the information about project multiplicity. One possible way of encoding project size and schedule is having both decision variables in the same sequence (as shown in Figure 12). That is, a new representation of sequence contains both lock ID (1, 2, 3... etc) and project alternative (A, B, C... etc).

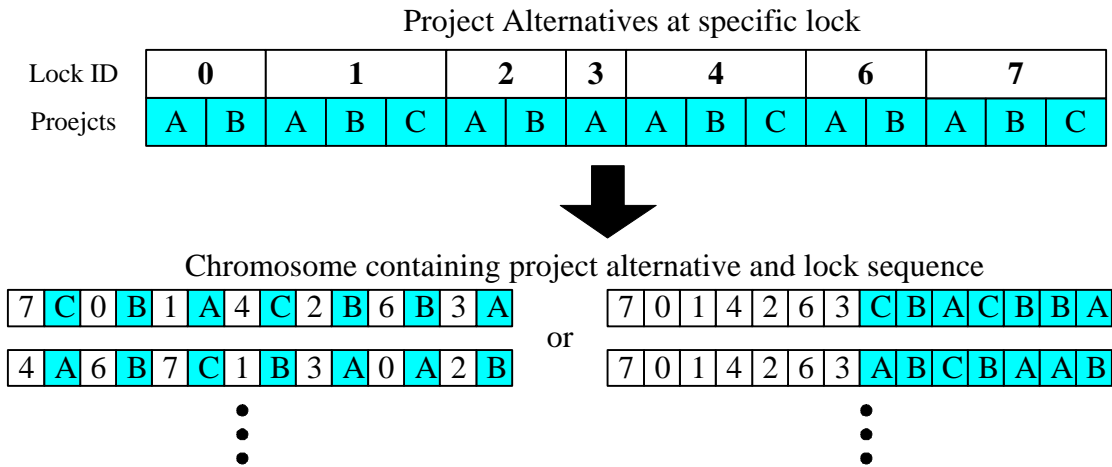


Figure 12 Paired Representation of Chromosome for Mutually Exclusive Projects

However, with this paired representation, both mutation and crossover operators must be redeveloped to avoid illegitimacy in the reproduction process, which creates offspring with invalid sequences or unavailable project alternatives. For example, as shown in Figure 13, an original EM operator developed in SIMOPT yields unavailable project alternative (that is, (a) some alternative is not available at some lock sites), or invalid sequence (that is, (b) unreasonable numbering sequence).

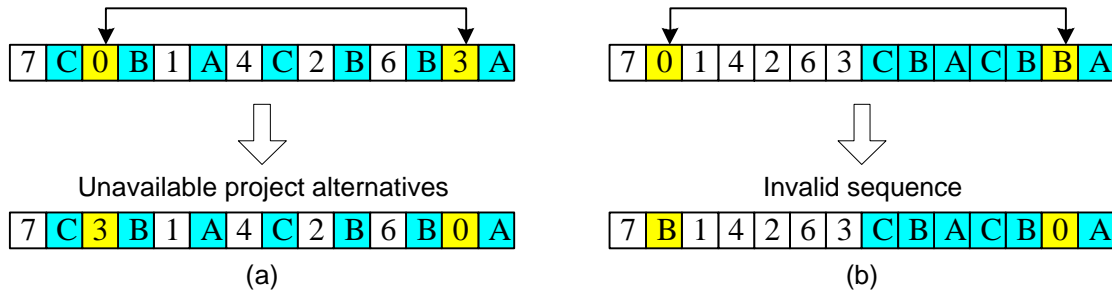


Figure 13 Illegitimacy Generated from Mutation Operator for Paired Representation

Therefore, a new EM operator should be able to swap the lock ID and project alternative together (as a pair) at the same time (as shown in Figure 14 (a)), or perform swapping twice for lock ID and project alternative with matching positions (as shown in Figure 14 (b)). It should also be able to randomize the project alternatives after any swapping (as shown in (c) and (d)). In other words, the genetic operators should be redesigned to be able to characterize legitimately the priority of project locations with corresponding project alternatives.

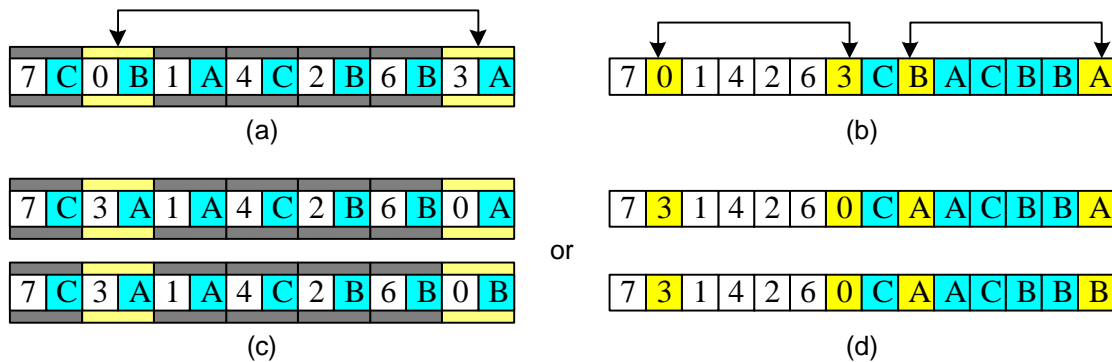


Figure 14 Possible Mutation Operator for Paired Representation

The other way of encoding these two variables together is keeping the same path representation used in SIMOPT but using project ID instead of lock ID in a sequence (as shown in Figure 15). With the original representation, the proposed GA operators in SIMOPT could still be applied on the mutation and crossover processes without any modification to produce the offspring. However, if considering only one alternative for each location, the sequences with full list projects are not the feasible solutions, in the sense that all alternatives will be implemented at different times (as shown in the middle part of the figure). Therefore, it is necessary to have a “refining” scheme embedded to create the feasible solutions for simulation evaluation. That is, instead of sequences with full lists of projects, a shorter sequence whose list of projects has only one project at each lock should be formed after the “refining” procedure (as shown in the lower part of Figure 15).

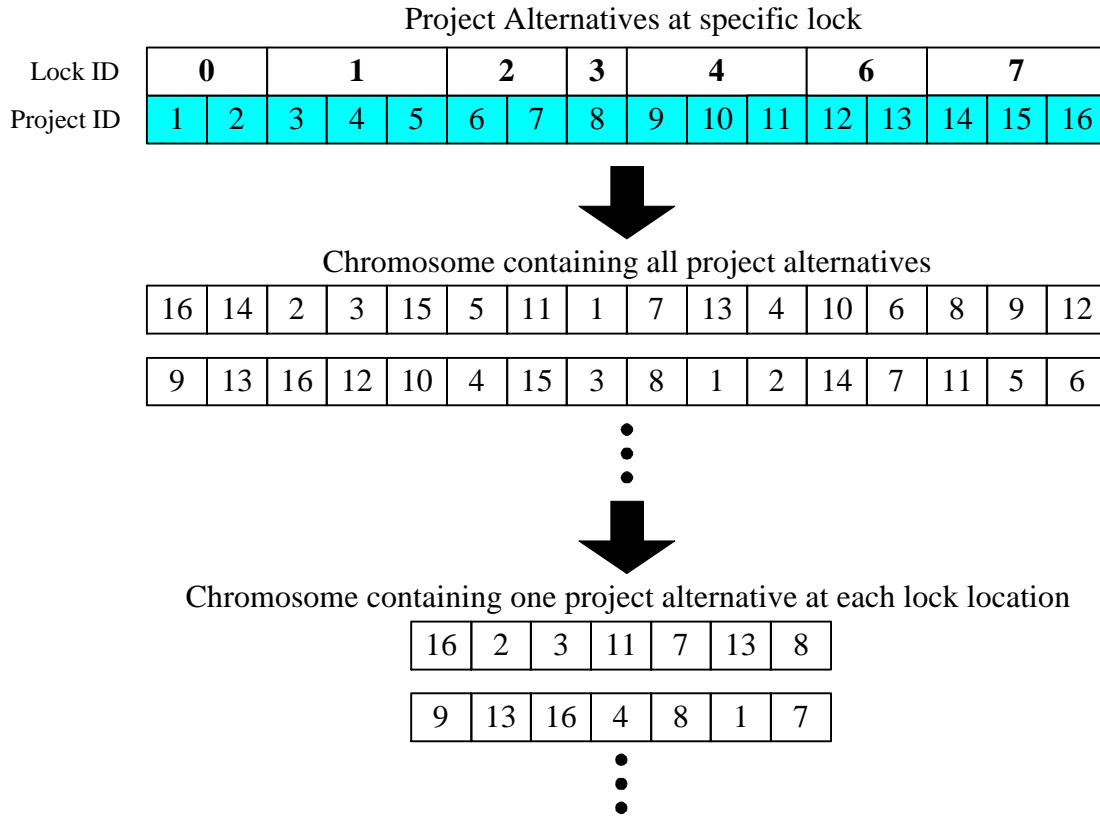


Figure 15 Path Representation of Chromosome for Mutually Exclusive Projects

The simplest way is to keep only one project at any lock and discarding the other projects at the same lock locations in any full-list sequence. As shown in Figure 16, whenever the first project alternative at one lock is selected, a “refining” technique will automatically discard the other project alternatives at the same lock. As noted, all the mutation and crossover operators are applied on the full-list chromosomes, not the refined chromosomes. Before starting any simulation evaluation, chromosome refining processes are performed on all produced offspring from any mutation or crossover operations.

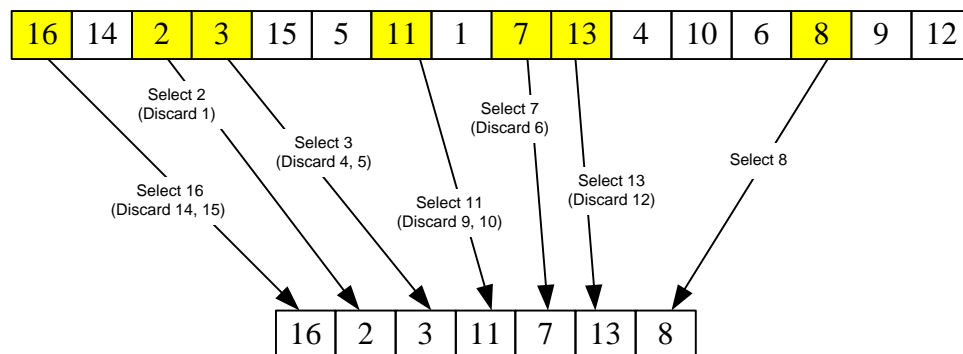


Figure 16 Proposed Refining Technique to Create Feasible Solutions for Mutually Exclusive Projects

In order to allow project multiplicity in SIMOPT, some modifications in the GA optimization model are made. In SIMOPT, the structure of the designed chromosome is shown in Figure 17. Each project initially includes information about project ID, project size and project cost. The project ID automatically indicates the project location. The implementation time for each project will be determined after the project sequence is generated and bounded with budget flow.

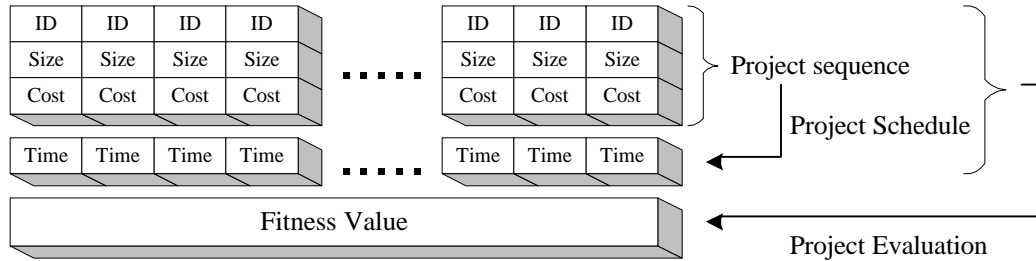


Figure 17 Structure of Chromosome Defined in SIMOPT

More information should be added into the chromosome definition when multiple alternatives are available at some lock locations. That is, in addition to project ID, lock ID should be provided (as shown in Figure 18, denoted as P.ID and L.ID). In this newly defined chromosome with multiple project alternatives per lock, lock ID is not unique anymore for each project but project ID is.

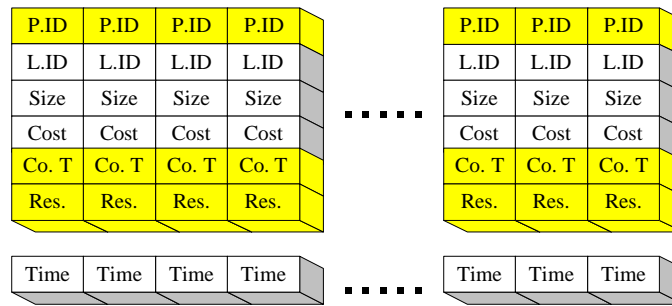


Figure 18 Modified Structure of Chromosome for Mutually Exclusive Projects

Time Efficiency

It is conceivable that some sequences that have been evaluated in previous generations are created again in the current generation. It is expected that combining the two stochastic processes of simulation and GA optimization will be time consuming. A significant time is required for evaluating each generated project sequence through simulation; especially numbers of replication is involved for variance reduction. Therefore, in order to reduce optimization search time, avoidance of duplicate simulation runs is considered.

A genetic approach is usually based on a memoryless evolutionary procedure. In contrast, another meta-heuristic approach called tabu search is designed with an adaptive memory which records solutions visited during the search. With this feature, the implementation of procedures can search the solution space economically and effectively. Thus inspired

by the idea provided in tabu search, the proposed GA is further modified as memorized evolutionary model. That is, the evaluated solutions in GA optimization are memorized in each generation. With the intension of avoiding duplications, it is a key step to search through memorized solutions before performing the simulation.

In order to avoid re-evaluating the same project sequences, each evaluated sequence and its evaluation results are recorded in a *deque* (short for “double-ended-queue”) data structure. If the newly generated sequence appears in the recorded solution pool, its evaluation result is directly assigned from memory rather than re-obtained simulation. Later, all newly generated sequences are pre-screened to identify those previously simulated ones before any time-consuming simulation is performed. Compared with the time for multiple simulation runs, it would be still worthwhile to spend time on checking throughout the recorded sequences.

In a *deque* data structure, the length of list is unlimited. It is also not necessary to declare a bulky memory space as for array data structure before starting the optimization process. Since a *deque* structure provides rapid insertions and deletions at its front or back of the structure, it is easy to add any newly evaluated solution onto the end of list. It also allows direct access to any stored element. Whenever an evaluated sequence has been found as the same sequence with the one being going to be evaluated, the stored fitness value can be directly assigned to the fitness result instead of duplicating simulation runs.

Thus, as shown in Figure 19, the evaluated sequences are stored in a *deque* and each element contains information about project sequences and their fitness values. During pre-screening, a newly generated sequence is compared with the recorded sequences, a “solution list”. As long as an exact sequence is found in the solution list, the recorded fitness value is directly assigned to the new generated sequence and the simulation evaluation is skipped. If no exact match is found among previously evaluated sequences, the new sequence is simulated and added into the solution list with its newly evaluated fitness value.

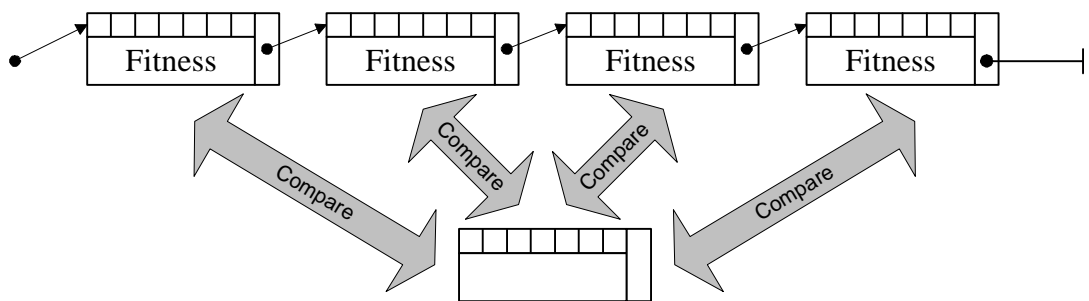


Figure 19 Deque Data Structure

The comparison between two sequences is performed project by project. The sequence comparing process is stopped whenever any of project elements is found different (as shown in Figure 20).

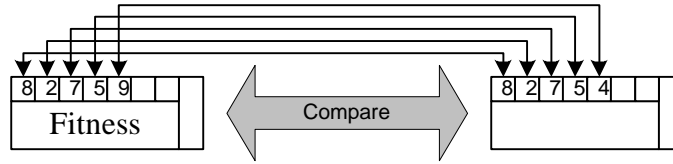


Figure 20 Sequence Comparison

It is noted that the comparison of sequences is straightforward if there are no mutually exclusive projects, since the full list of projects is the same as the full list of lock locations. However, with mutually exclusive projects, the comparison results could be different. Two types of sequences are created when considering mutually exclusive projects. Full sequences of project alternatives are generated from the offspring production process. Partial sequences with only one project per lock are “refined” for evaluation by simulation. To avoid duplication in the evaluation process, we should compare the refined partial sequences, rather than the full sequences. That is, as shown in Figure 21, after the “refining” process (performed in the case of mutually exclusive projects), different full sequences of project alternatives could become the same partial sequence with only one project per lock.

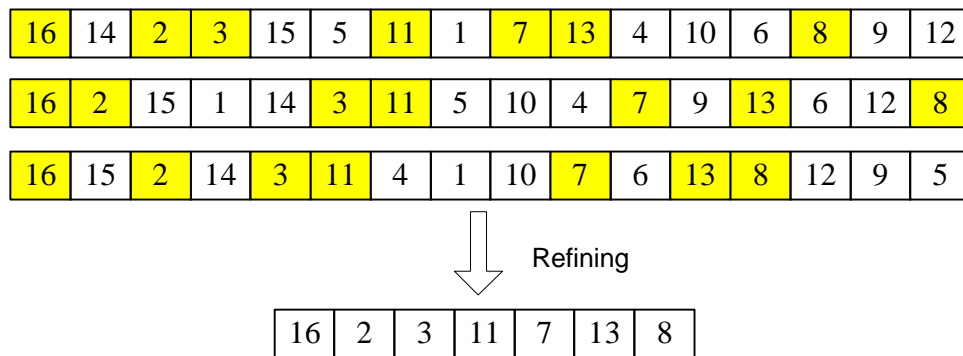


Figure 21 Refined Sequence

Therefore, in order to save simulation time even efficiently, it is better to have a solution list recording the “refined” partial sequences rather than the “original” full sequences.

Model Test (Enhanced SIMOPT)

Test Network

The test network used in SIMOPT demonstration is used here for testing any enhanced GA techniques proposed in this phase (as shown in Figure 22). There are 3 rivers, 5 ports, and 7 locks (4 single-chamber locks and 3 double-chamber locks). Locks are numbered with ID 0, 1, 2, 3, 4, 6, 7. Lock #5 and #8 are dummy locks (refer to the “SIMOPT” presentation, July 2005). Not all locks require improvement projects, but all improvement projects are at real locks.

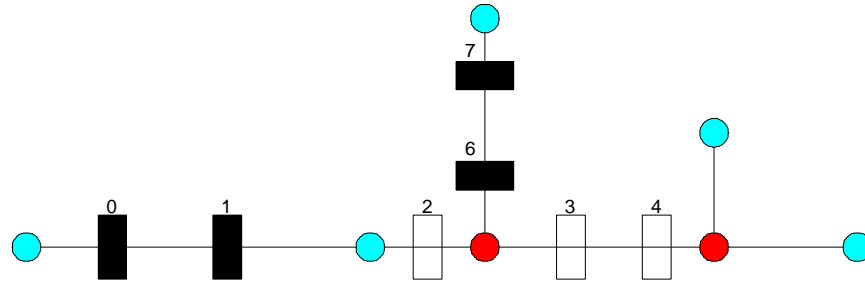


Figure 22 Test Network for SIMOPT Extension

Input Parameters

Input Statistics

- O/D matrix with trip generation rates
- Tow size distributions
- Chamber service time distributions
- Speed distributions

Lock Operation

- FIFO control
- Towboats priority (tow w/o barge)
- Lockage cuts
 - Main: always 1 cut
 - Auxiliary: 2 cuts for tows with more than 9 barges
- Chamber assignment
- Chamber bias (main chamber is preferred for tows with more than 7 barges)

Demand

- Annual growth rates for each O/D pair
- Elasticity for each OD pair

Base Case Run

- Lock congestion level (from highest V/C to lowest V/C): 7→1→6→0→2→4→3
- Average O/D travel time

System Parameters

- Simulation parameters

Table 5 Simulation Parameters in SIMOPT Extension

Time Value	450 \$ / barge-minute
Budget Rate	150×10^6 \$ / year
Demand Growth Rate	2.0% per year
Replications	10
Simulation Period	2.5 years
Warm-Up Period	1 year

- Optimization parameters

Table 6 Optimization Parameters in SIMOPT Extension

Population Size	50
Selection Probability	Ranking of fitness value
Sampling Mechanism	Elitist selection & stochastic sampling
Mutation Rate	0.07
Crossover Rate	0.3
Replacement	Replace worst parents
Termination	20 generations w/o improvement

Testing Results

All the test results are presented with three cases obtained with the recently modified SIMOPT: (1) Considering construction times, (2) Considering mutually exclusive projects, and (3) Avoiding duplicated simulation runs. In those test cases, it is assumed that the project construction starts at the time when required cost is accumulated. The current objective function is set to minimize the total cost which includes system total delay cost (barge-minute) and project construction cost. All the cases are run on a Pentium III machine with 3.6 GHz CPU and 1GB memory.

Case 1: Considering Construction Times

In this case, only one project is considered at each single lock. Project information is detailed in blockage duration for the construction and capacity reduction ratio during the construction time as well as project size (capacity expansion ratio) and project cost. Two scenarios are proposed. One (case 1.1) serves as the base case in which construction time is neglected, as in the original SIMOPT. (The implicit assumption is that construction is instantaneous.) The other (case 1.2) considers construction time and its relevant effects such as capacity reduction and demand response.

Inputs of Lock Improvement Projects

- Project ID
- Lock ID
- Project size – capacity expansion ratio
- Project cost (\$ M)

- Project duration – construction time(year)
- Project blockage – residual capacity ratio

Table 7 Project Information for Case 1.1 (Baseline without Construction Times)

Project ID	Lock ID	Size	Cost
1	7	2.0	17
2	1	2.0	16
3	6	2.0	23
4	0	2.0	19
5	2	1.1	22
6	4	1.3	21
7	3	1.1	25

Table 8 Project Information for Case 1.2 (Considering Construction Times)

Project ID	Lock ID	Size	Cost	Duration	Blockage
1	7	2.0	17	0.17	0.2
2	1	2.0	16	0.09	0.5
3	6	2.0	23	0.12	1.0
4	0	2.0	19	0.11	0.5
5	2	1.1	22	0.03	0.8
6	4	1.3	21	0.09	0.2
7	3	1.1	25	0.04	0.5

Optimized Project Sequences and Implementation Schedules

Since there are 7 projects to be sequenced in Table 7 or Table 8, the solution space is $7! = 5,040$. For testing purposes, this is not a huge number. The optimized project sequences and their implementation schedules are shown in Table 9 and Table 10. The optimized results are quite different for the two scenarios. While considering construction time and capacity reduction, the total cost increases considerably due to increasing traffic delays during the construction period. That is, inclusion of construction time and the capacity reduction during construction in the simulation is important and significantly affects the optimization results.

Table 9 Optimized Results for Case 1 (Considering Construction Times)

Construction Time / Capacity Reduction	Optimized Sequence (Lock Location)	Total Cost
NO	1→0→7→6→2→4→3	319,707,226
YES	1→6→7→2→4→3→0	1,225,828,520

Table 10 Additional Optimized Results for Case 1 (Considering Construction Times)

w/o Construction Time and Capacity Reduction				w/ Construction Time and Capacity Reduction			
Project No.	Lock	Time Table (Yr)		Project No.	Lock	Time Table (Yr)	
		Build	Open			Build	Open
2	1	0.11	0.11	2	1	0.11	0.2
4	0	0.23	0.23	3	6	0.26	0.38
1	7	0.35	0.35	1	7	0.37	0.54
3	6	0.5	0.5	5	2	0.52	0.55
5	2	0.65	0.65	6	4	0.66	0.75
6	4	0.79	0.79	7	3	0.83	0.87
7	3	0.95	0.95	4	0	0.95	1.06
Computation time = 10792 sec Number of generations = 21				Computation time = 23158 sec Number of generations = 58			

GA Search Performance

Based on case 1.2, Figure 23 shows as an example of GA search performance. The best sequence in each generation is always saved, so the solution can never get worse over successive generations. However, the rate of improvement decreases over successive generations until further improvement become very unlikely. From the first generation to the termination, there is an approximately 60% improvement in the optimized solutions.

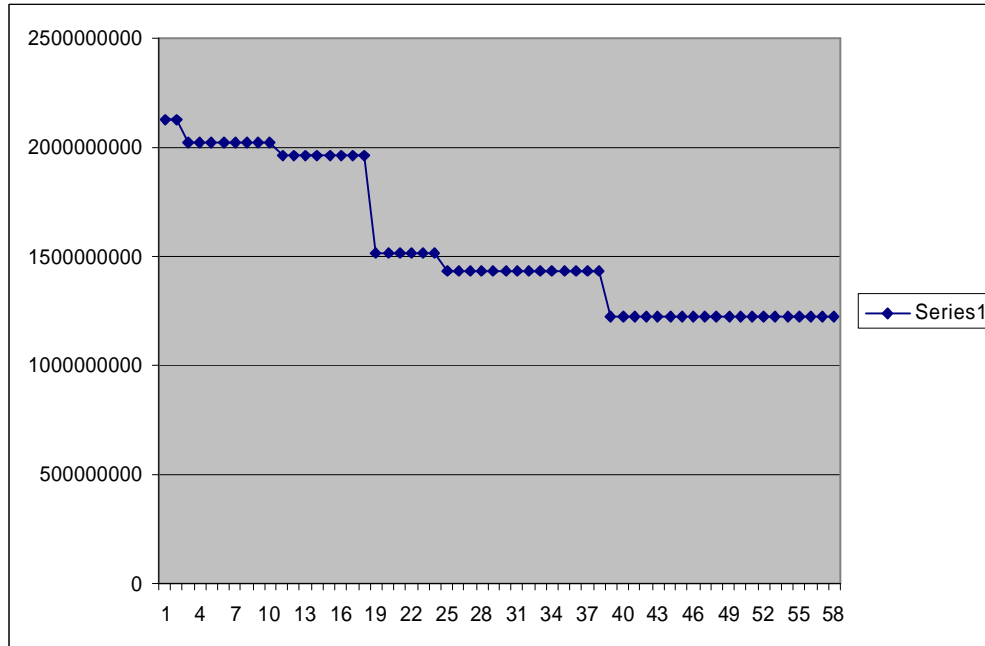


Figure 23 GA Search Performance

Case 2: Considering Mutually Exclusive Projects

In this case, multiple projects are considered at some lock locations. However, at most one of the alternative projects for each location will be selected in any implementation sequence. Construction time and capacity reduction during the construction period are considered. Similarly, two scenarios (case 2.1 and case 2.2) are proposed for case 2: with or without considering mutually exclusive projects. Case 2.1 is actually the previous case 1.2.

Inputs of Lock Improvement Projects

- Project ID
- Lock ID
- Project size – capacity expansion ratio
- Project cost (\$ M)
- Project duration – construction time(year)
- Project blockage – residual capacity ratio

Table 11 Project Information for Case 2 (Considering Mutually Exclusive Projects)

Project ID	Lock ID	Size	Cost	Duration	Blockage
1	7	1.5	10	0.10	1.0
2	7	1.8	13	0.13	0.8
3	7	2.0	17	0.17	0.2
4	1	1.5	10	0.05	1.0
5	1	2.0	16	0.09	0.5
6	6	2.0	23	0.12	1.0
7	0	1.5	15	0.10	1.0
8	0	2.0	19	0.11	0.5
9	2	1.1	22	0.03	0.8
10	4	1.1	15	0.01	1.0
11	4	1.2	17	0.05	0.5
12	4	1.3	21	0.09	0.2
13	3	1.1	25	0.04	0.5

Optimized Project Sequences and Implementation Scheduled

Here, there are 13 projects: 3 alternatives at lock #7, 2 alternatives at lock #1, 1 alternative at lock #6, 2 alternatives at lock #0, 2 alternatives at lock #2, 3 alternatives at lock #4, and 1 alternative at lock #3. The solution space is $7! \times 3! \times 2! \times 2! \times 3! = 725,760$. That is, much less than $13! = 6,227,020,800$. The optimized project sequences and implementation schedules are shown in following tables.

Table 12 Optimized Results for Case 2 (Considering Mutually Exclusive Projects)

Construction Time / Capacity Reduction	Mutually Exclusive Projects	Optimized Sequence (Lock Location)	Total Cost
YES	NO	1→6→7→2→4→3→0	1,225,828,520
YES	YES	7→0→1→6→4→3→2	344,908,155

Table 13 Additional Optimized Results for Case 2 (Considering Mutually Exclusive Projects)

w/o Mutually Exclusive Projects				w/ Mutually Exclusive Projects			
Project No.	Lock	Time Table (Yr)		Project No.	Lock	Time Table (Yr)	
		Build	Open			Build	Open
2	1	0.11	0.2	1	7	0.07	0.17
3	6	0.26	0.38	7	0	0.37	0.47
1	7	0.37	0.54	4	1	0.56	0.61
5	2	0.52	0.55	6	6	0.82	0.94
6	4	0.66	0.75	10	4	0.92	0.93
7	3	0.83	0.87	13	3	1.09	1.13
4	0	0.95	1.06	9	2	1.23	1.26
Computation time = 23158 sec Number of generations = 58				Computation time = 41766 sec Number of generations = 24			

Case 3: Avoiding Duplicated Simulation Runs

In this case, newly produced sequences are prescreened to avoid re-simulating previous ones. Therefore, two scenarios are proposed to compare the differences of required genetic search times.

The first scenario serves as base case without any pre-screening action for the evaluated solutions before the simulation. The second scenario considers the pre-screening process to avoid duplicated simulation runs, but may require some search time in the pre-screening process. In order to perform the pre-screening process, the search comparison is conducted after a full list of projects is refined as a feasible sequence, in which only one project is selected at each lock. Instead of comparing sequences whenever a full list of project alternatives is generated, this will eliminate all the possible simulation duplications, since different full lists of sequences might result in the same project lists after the “refining” procedure.

Computation Times for Optimization Search

Most inputs in this case are the same as in the second case. In order to generate more varieties, the population size is increased to 100 in this case. Search time for pre-screening process is expected to increase when the number of recorded solutions increases. After generations in GA's, the number of recorded solutions could be so large that considerable time is spent searching through the whole list for sequence comparison. The additional “solution search process” might reduce the time-saving effect from the

pre-screening step. However, in a simulation-based optimization model, the pre-screening time seems negligible compared to the time for multiple simulation replications. The optimized solution found in this case is shown as project sequence 4→7→1→6→10→13→9 with total cost of \$342,086,655. This result differs slightly from the result in case 2.2 due to some changes in input parameters, such as the population size of 100.

Comparative results for GA search time are shown in Table 14. With pre-screening, the GA search time decreases by approximately 20%. If the number of generations increases, time savings from pre-screening should increase.

Table 14 Results for Case 3 (Avoiding Duplicated Simulation Runs)

Construction Time / Capacity Reduction	Mutually Exclusive Project	Pre-screening Solutions	# of Generations	GA Search Time (sec)
YES	YES	NO	21	129641
YES	YES	YES (refined list)	21	104604

Verification of GA Optimization Model

In such a complex combinatorial problem, it is not easy to find the exact optimal solution; at least no existing methods can guarantee finding the global minimum. Verifying the goodness of the solution optimized by the proposed algorithm is also difficult. Therefore, in order to statistically test the effectiveness of the algorithm, an experiment is designed to evaluate 20,000 randomly generated solutions to the problem with a sampling process.

Using case 2.2 with mutually exclusive projects as an example, the solution space contains 725,760 ($= 7! \times 3! \times 2! \times 2! \times 3!$) solutions. 20,000 solutions cover approximately 3% of the solution space. From those observations, the best fitness value in this sample is 0.34521×10^9 , while the worst one is 9.8882×10^9 . The sample mean is 2.3769×10^9 and the standard deviation is 1.7497×10^9 .

Since the sample is randomly generated, the fitted distribution should approximate the actual distribution of fitness values for all possible solutions in the search space. The distribution for those 20,000 sampled solutions is shown in Figure 24 with different histogram scalars, namely 20 and 100. From Figure 24(a), there is one higher peak around value of 1.0×10^9 and one lower peak around value of 5.5×10^9 . From Figure 24 (b), two higher peaks around the values of 0.5×10^9 and 1.2×10^9 can be observed. Based on the plotted histograms, the best fitting distribution with uneven bell shape might be the gamma distribution or the lognormal distribution.

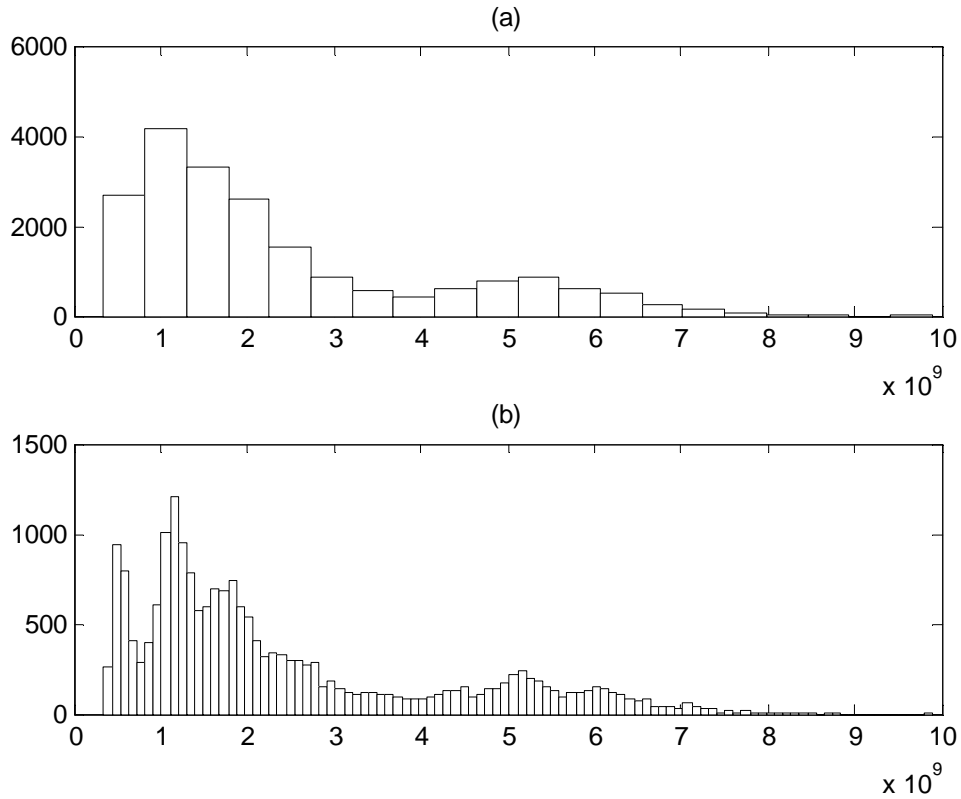


Figure 24 Histograms of Sampled Solutions

Figure 25 shows those 20,000 sample solutions fitted with gamma distribution, gamma (a, β), in which a and b are the shape and scale parameters, and lognormal distribution, LN (μ, s^2), in which μ and s^2 are sample mean variance. The values of a and b for the fitted gamma distribution are 2.0757 and 1.1451×10^9 , and the values of μ and s^2 for fitted lognormal distribution are 21.3292 and 0.7307, respectively. As can be seen, there is a large “spike” close to $x = 0$, which is covered better by the lognormal distribution.

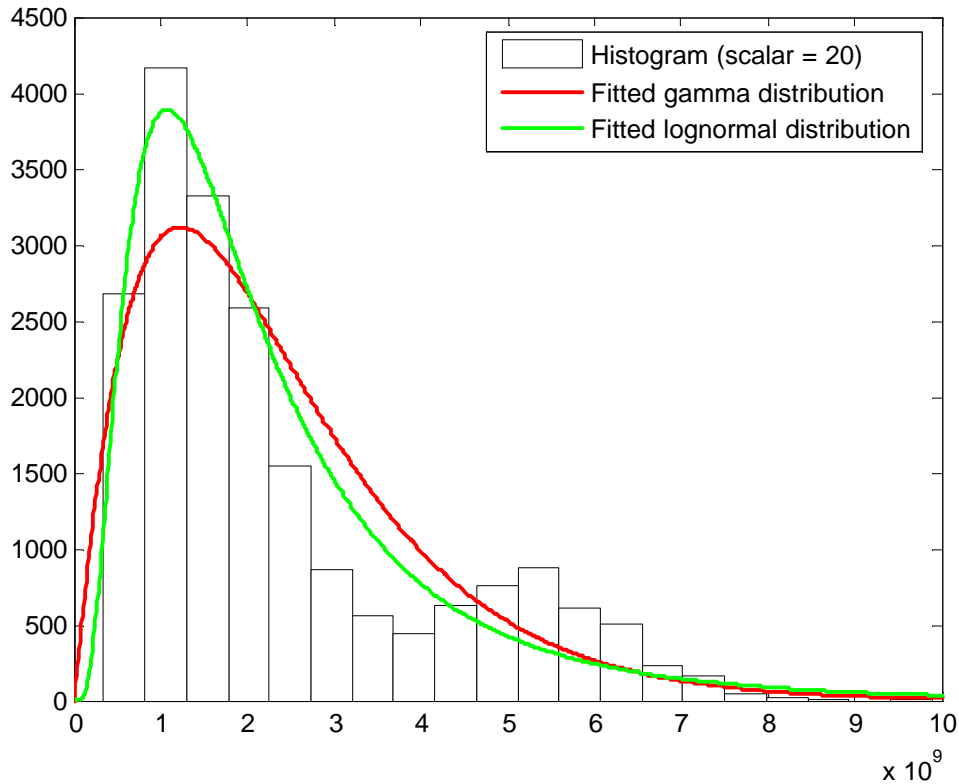


Figure 25 Fitted Gamma and Lognormal Distributions

Compared with the optimized solutions found in case 2 (best fitness value = 0.3449×10^9) and case 3 (best fitness value = 0.3420×10^9), the best solution with fitness value of 0.34521×10^9 is approximately 0.1% higher (i.e. worse) than the GA search results. That is, the optimized solution found in proposed GA search still 0.1% less than the best solution found from the random search experiment. Those optimized solutions, though not necessarily optimal, are still very good when compared with other random solutions in the solution space. That practically shows the reliability and validity of the proposed search algorithm.

Conclusions and Future Work

Summary and Conclusions

Optimization based on evaluating objective functions with simulation is becoming feasible, but the computation time is a crucial factor. Since the optimization method can be fully separated from the simulation model, the development efforts for these two processes can proceed concurrently. Thus, using the SIMOPT testbed, enhancements of the simulation-based optimization models are developed and tested.

When considering project construction time and capacity reduction during the construction, the “events” of starting and completing the projects are defined to update the system capacity during the simulation. The simulation model also considers the possibility of queue “explosion” if lock capacity decreases significantly during construction periods. Traffic demand is thus designed to be sensitive to the service level and adjusted automatically during the trip generation. For the optimization model, extra project information related to construction is added into the GA chromosome. Results show how the construction time and associated capacity reduction significantly affect the optimized sequence.

When considering mutually exclusive projects, the GA chromosome definition should be modified. In order to apply the same genetic operators developed in SIMOPT, the newly defined chromosome contains a full list of mutually exclusive projects. However, solutions with full lists of projects are not feasible when we allow at most one project per lock. Therefore, a “refining” technique is applied to create feasible solutions with lists of projects having at most one project per lock. The modified SIMOPT is able to solve the problem of sequencing and scheduling mutually exclusive projects.

To reduce running time in a simulation-based optimization model, any newly evaluated solution is recorded in a “solution list”. Whenever a new sequence is produced from mutation or crossover operations, a pre-screening process is first performed to check throughout the solution list. If that solution is also found in the list, its simulation is omitted and its fitness value is directly assigned from the saved records. By avoiding duplicated simulation runs, the test case shows that the optimization search time is reduced by approximately 20% over 21 generations. Even larger percentage reductions are expected if the number of generations is increased.

At the end, a verification process is conducted to show the validity and reliability of the proposed GA search algorithm. Random solutions are generated from a sampling process and fitted with gamma or lognormal distributions. Compared with the those generated solutions, the optimized results found by the proposed GA search algorithm are still 0.1% better than the minimum value found from the random search experiment.

Future Work

A key component of NaSS is the investment optimization module, which is currently tested with Genetic Algorithm (GA) optimization. This investment optimization module is used to identify project modifications that are worthy of implementation, their order of implementation, and optimal implementation timing. There are good reasons for choosing GA instead of other optimization algorithms. First, GA’s provide great flexibility for creative ideas, for example in the selection method, mutation/crossover rules, problem specific operators, and immigration and replacement between generations. Secondly, GA’s are naturally suitable for running on parallel processors. With parallel computing, the optimization time could be significantly reduced. Also, the GA’s developed for

network-level optimization also seem adaptable for optimizing lock-level enhancement projects.

Additional ways of enhancing the GA optimization algorithms are available. The scope of work for the next phase includes additional development of genetic algorithms, and their application to project selection, sequencing and scheduling.

In GA's, search performance could possibly be affected by the mix of different genetic operators. To exploit the problem structure, some "smart" operators might be created specifically for waterway project scheduling. Some prescreening rules could also be developed to avoid simulating solutions that are unpromising or violate constraints.

Since the optimization model can be developed separately from the network simulation model, it is possible to integrate them with a simple "evaluator" to save the time in running simulation-based optimization. The simple evaluator could be any approximate simulator or even an algebraic function.

In the problem of project selection, sequencing and scheduling, additional complexities may arise, such as multiple alternatives at the same location which may be implemented at different times, project precedence relations, further budget constraints (e.g. regional limits, new construction vs. maintenance), budgets related to taxes on traffic levels found during simulations, and tradeoffs between construction times and costs. Such complexities could all be addressed in future model developments.

Appendix

GA Phase 1 Scope of Work

In the Design Document development phase, a “testbed” simulation-optimization model was used to demonstrate the feasibility of using simulation and GA optimization to determine optimal solutions to problems requiring simulation as the objective function evaluation tool. During that demonstration, several needed enhancements to the GA optimization capabilities were identified. The following tasks describe those activities which are related to enhancing the capabilities of the GA optimization model.

Task 1 Genetic algorithm

Task 2 Evaluation / Simulation model

2.1 Store results and prescreen alternatives to avoid repeated simulation near previous searches

Task 3 Project selection / sequencing / scheduling

3.1 Include construction time during simulation

3.2 Consider capacity reduction during construction period

3.3 Consider multiple alternatives at the same location / mutually exclusive projects

3.4 Consider optimal timing for projects absent budget constraints

Task 4 Continued participation on NaSS team

4.1 Continue to participate in teleconferences and face-to-face meetings. At the time of scope development it is anticipated that bi-weekly teleconferences will continue throughout the period of this scope. In addition, at least one face-to-face meeting between team members is anticipated.

4.2 Specific assignments. It is anticipated issues and activities will arise during the period of this scope for which CEE-UMD will be tasked. If the level of effort involved requires significant additional time and resources, this scope may be modified to provide additional funds and time to CEE-UMD.

References

Wang, S. "Simulation and Optimization of Interdependent Waterway Improvement Projects", PhD Dissertation, University of Maryland, 2001.

Wang, S. and Schonfeld, P. "Development of Waterway Simulation Model", Annual TRB Meeting, Jan. 2002 (02-2194 on Conference CD-ROM).

Wang, S. and Schonfeld, P. "Scheduling Interdependent Waterway Projects through Simulation and Genetic Optimization," *Journal of Waterway, Port, Coastal and Ocean Engineering*, ASCE, Vol.131, No. 3, May/June 2005, pp. 89-97.

Wang, S. and Schonfeld, P. "SIMOPT", presented in July 2005 at Fort Belvoir, VA.

Wang, S. and Schonfeld, P. "Modeling Shipper Response to Scheduled Waterway Lock Closures", Annual TRB Meeting Jan. 2006 (06-1833 on CD-ROM).

Wang, S. and Schonfeld, P., "Genetic Algorithms for Selecting and Scheduling Waterway Projects", presented at NETS SYMPOSIUM, Salt Lake City, Jan. 2006.

Grant No. 03HQGR0126 Improvements of IWR Navigation Models

Basic Information

Title:	Grant No. 03HQGR0126 Improvements of IWR Navigation Models
Project Number:	2005MD142S
Start Date:	7/1/2003
End Date:	4/30/2005
Funding Source:	Supplemental
Congressional District:	05 MD
Research Category:	Engineering
Focus Category:	Models, None, None
Descriptors:	
Principal Investigators:	Paul Schonfeld

Publication

1. Wang, S.L. and Schonfeld, P., Scheduling Interdependent Waterway Projects through Simulation and Genetic Optimization, J. of Waterway, Port, Coastal and Ocean Eng., ASCE, Vol. 131, No. 3, May/June 2005, pp. 89-97.
2. Tao, X., and Schonfeld, P., A Simulation Method for Selecting and Scheduling Waterway Projects, Transp. Res. Record 1931, 2005, pp. 74-80.

Design of Simulation Kernel for NeoWAM

by Shiaaulir Wang, XianDing Tao, and Paul Schonfeld
Department of Civil and Environment Engineering
University of Maryland
College Park, MD 20742

Table of Contents

Table of Contents.....	1
Introduction	2
Object-Oriented Simulation.....	3
Design of Waterway Transportation Networks	4
Network Structure	5
Waterway Reaches	5
Waterway Nodes	6
Lock Components	7
Vessels	9
Tows	9
Recreational Craft	9
Lock Operation	10
Lockage Distributions	10
Locking Policies.....	10
Interference between Chambers.....	11
Discrete Event Waterway Simulation Model	11
Process-Based Modeling Approach	12
Event List.....	13
Node-Relevant Events	14
Reach-Relevant Events.....	14
Vessel-Relevant Events	14
Time-Relevant Events	15
Model Framework.....	15
Model Development.....	16
Port Processes	17
Vessel Generation	17
Demand Update.....	18
Lock Processes.....	19
Control Policies.....	19
Signal for Lock Interference	23
Lock Closures	24
Reach Processes	25
Reach Casualties	25
Reach Improvements.....	25
Time Processes.....	25

Time Slices.....	25
Vessel Processes	25
Route Determination	26
Vessel Arrivals	26
Vessel Movement on Links	27
Vessel Operation at Locks	28
References	31

Introduction

The U.S. Army Corps of Engineers has launched the Navigation Economic Technologies (NETS) program to support its mission by developing independently-verified economic models, tools and techniques. The NETS program encompasses a wide array of research and development activities such as coastal navigation, inland navigation and multimodal transportation. Regarding inland navigation, there are ongoing studies related to traffic analysis, demand forecasting, lock reliability and system modeling. For system modeling, a new inland navigation model is being developed as an important tool for assessing the costs and benefits of proposed changes to the nation's waterway systems, as well as for evaluating various operation and maintenance policies.

A well-developed inland navigation model should consist of a logical simulation kernel and desirable peripherals such as database I/O (input and output), GUI (graphical user interface) and animation. The simulation kernel controls the logic of tows' activities through different waterway facilities. It could mimic single lock operation in details or provides an overall evaluation of network performance from the planning point of view.

Several waterway simulation models have been developed in recent decades. NavSym (IWR, 2003) models barge traffic on inland waterways. While considering the navigation improvements, it allows users to assess the impact of system change on travel times and costs. Since proposed improvements are pre-specified for each individual reach, the selection, sequencing and scheduling of improvement projects would have to be considered outside the simulation process. Since it was originally developed for the GIWW, NavSym is particularly underdeveloped for analyzing operations at locks which constitute major bottlenecks in the waterway network.

WAM (U.S.A. Corps of Engineers, 1999) models details of single lock operation. It considers lock interference at existing multi-chamber locks and rescheduling of tow arrivals due to the unavailability of the scheduled chamber unavailability. Based on a lock's operational condition, it can generate capacity curves that relate required transit time to annual traffic throughput. With a pre-processed shipment list at each single lock, it does not model the randomness in waterway traffic or in frequency and duration of lock downtime. WAM's suitability for network-level analysis seems limited, according to the available documentation.

The major purpose of Wang's model (Wang, 2001) is to evaluate the performance of a network-level waterway system with various lock improvement projects and operating policies. Its inbuilt portability strengthens its applicability to different waterway segments. For multi-chamber locks, chamber preference is also modeled to account for the selection bias in lockage process. When multiple improvement projects are analyzed in a network, lock interdependence affects the evaluation of the combined

performance of project sets, sequences, and schedules. Therefore, an optimization model using a Genetic Algorithm (GA) is integrated into the simulation model to optimize the selection, sequencing and scheduling of the interdependent lock improvement projects under the budget constraints.

In order to better analyze the stochastic effects in the waterway systems and enable the simulation model to efficiently support optimization capabilities (e.g. for project selection and scheduling and for maintenance planning) and animation for a waterway network, a NeoWAM (New Generation of Waterway Analysis Model) based on WAM (Waterway Simulation Model) is proposed to model the probabilistic factors (e.g. traffic demand, lockage process, and lock closures) in the system, to analyze trip behavior, lock operations and demand variation, and to evaluate the system's performance. Two general capabilities are considered in the proposed model. "Portability" allows the model to be easily transferred to different parts of waterway networks. "Transparency" helps the model user follow the changes in system state variables during the simulation. The model's output will be very useful for estimating the costs and benefits of lock and channel improvement projects as well as for evaluating various operation and maintenance policies. Furthermore, project selection and scheduling can also be performed by combining the simulation and optimization models.

Object-Oriented Simulation

Recently, there has been growing interest in object-oriented programming, which evolved from procedural programming to object-based programming and then to object oriented programming. Developing a simulation model is time-consuming and requires considerable subsequent maintenance. In order to reduce the maintenance cost and produce a modifiable model, an Object-Oriented Programming (OOP) technique is introduced in the design and development of the system. With its significant commonalities in self-containing attributes and operations, OOP is advantageous in database and GUI applications.

To be able to utilize the constructs provided by an OOPL, objects and classes should be defined. An OO language, such as C++, will be used to code the simulation kernel and the advantages of modularity, extensibility, flexibility and reusability could be exploited. In this OO simulation, a simulated system is considered to consist of objects (such as vessels, ports, locks, and reaches) that interact with each other as the simulation evolves over time. Objects contain data and have functions (processes or operations). Data describe the state of an object at a particular point in time, while functions describe the actions that the object is capable of performing. With the features of *inheritance*, *polymorphism*, *encapsulation*, and *hierarchy*¹, the following benefits could be yielded from OOD (object-oriented design) simulation:

- Promote code reusability because existing objects can be reused or easily modified (*inheritance*)
- Enable programmers to write programs in a general fashion to handle a wide variety of existing and yet-to-be-specified related classes (*polymorphism*)

¹ Please refer to C++ book (Dietel & Dietel, 1998) for details.

- Help manage complexity by dividing the system into different objects (*encapsulation*)
- Make model changes easier when a parent object can be modified and its children objects follow the modifications (*hierarchy*)
- Facilitate large projects with several programmers

Design of Waterway Transportation Networks

A waterway transportation network is generally composed of reaches and node facilities, such as ports and locks. It can be simply sketched with a network diagram, as shown in Figure 1. A simple tree configuration is typical for waterway networks in which rivers and their tributaries are not interconnected by artificial canals. If such connectors exist, they allow “loops” and alternate paths between same origins and destinations, resulting in most complexity than in tree networks. The target network section for a study is designated with encircling dashed line.

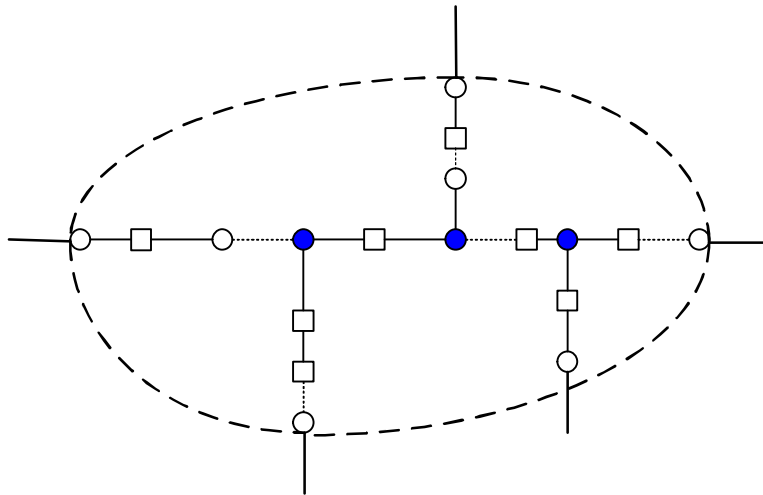
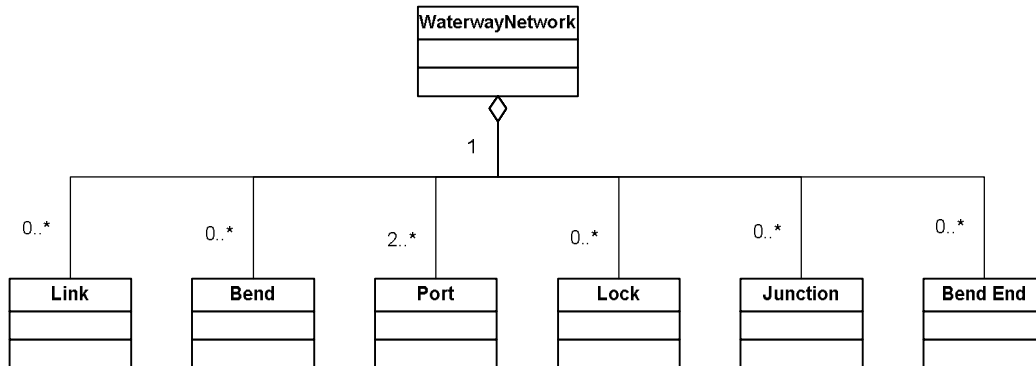


Figure 1 Representation of Sample Waterway Network

Based on their geometric and geographic features, reaches can be classified into restricted and unrestricted links (e.g. links and bends), which are connected by waterway junctions, bend ends, ports or locks. Accordingly, the restricted links refer to the reach segments constrained by physical conditions or operational rules. Some are limited to one-way traffic due to certain physical constraints, such as width or curvature. Those one-way links are alternately operated in the two directions. Other operational rules can also apply on the restricted links, such as speed limits, least separation distance, no passing, no meeting or no overtaking. The strictest one could be a “one-tow-at-a-time” segment. In contrast, there is no physical or operational limitation on the unrestricted links. Two-way traffic flows without any control restrictions are assumed on those links. As for locks and junctions, they are always located between ports and inside the network. The boundaries of a network area are always found at ports and dummy entry points.

Network Structure

In the proposed simulation model, a waterway network is represented as a collection of components including reaches and nodes. Reaches are classified into links and bends; nodes are classified as ports, locks, bend ends and natural waterway junctions. According to the “object-oriented” concept, each component is designed as a single class. A part-whole relation association among waterway network classes is shown in Figure 2. Each designed class is represented as a cell, in which the name of each class is defined and the attributes and operations of the created class will be specified in the second and third parts of each cell.



the common features from the “Reach” class. Such relations are presented in Figure 3. In addition to the common features, child classes also have their own specific features listed in their own class, respectively.

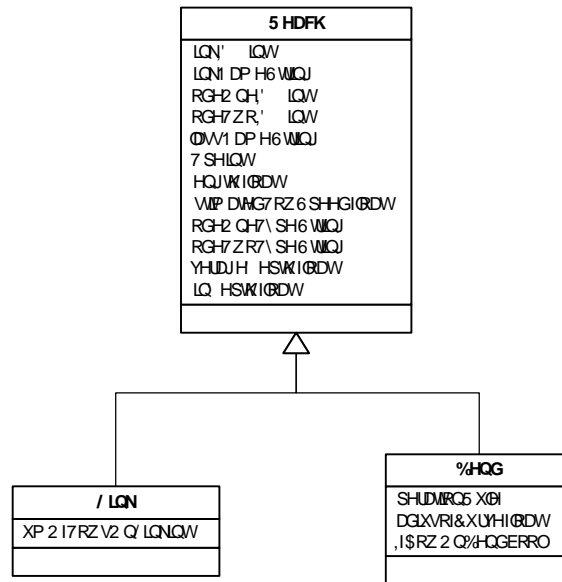


Figure 3 Inheritance Relations for the Waterway Link Class

Waterway Nodes

Similarly, the four node-related classes (port, lock, bend end and junction) share many common attributes such as longitude and latitude positions and can be generalized. First, a parent class called “Node” is created to carry these common attributes. The four classes, Port, Lock, Bend End and Junction, are then created as child classes and inherit all attributes of the “Node” class. Figure 4 illustrates the inheritance relationship for the waterway node classes. Common features are listed in the “Node” class and specific features are listed in the two inheriting classes.

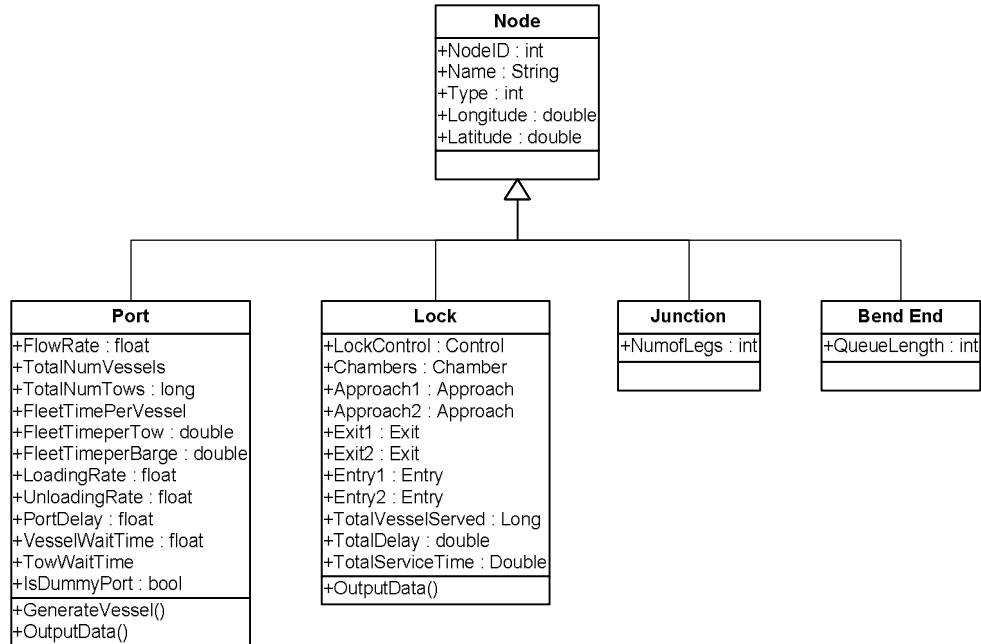


Figure 4 Inheritance Relations for the Waterway Node Classes

Lock Components

A typical waterway lockage is defined to include four components: approach, entry, chambering, and exit (as shown in Figure 5). In many cases, the approach area, defined from the approaching point (e.g. AP, arrival point) to the lock wall, can only contain one tow at a time. After approaching, vessels physically go through steps of entering, chambering, and exiting to end the lockage. Operationally, a lock is also equipped with a control scheme, which gives orders for dispatching vessels based on the locking policies and sends signals for start of lockage if lock interference occurs. If chamber are busy, waiting vessels are stored in the approach components from each direction. Whenever the dispatching order is determined, the selected vessel can start its approach for the lockage operation. Figure 6 describes the five components of a lock class. The detailed attributes of each component class are also displayed.

Similarly, figure shows the multiplicity of each association between classes. The symbols “1..*”, “1”, or “2” denote the least number or the exact number of any specified components required for constructing a lock. For example, a lock can have one or more chambers and symbol “1..*” is used to describe this feature. Also, one lock has one approach area for each direction, and the number “2” above the “Approach” class box is used to express that “a lock has 2 approach areas, upstream and downstream”. Attributes of each component are listed in the middle part of each cell with the specified data type. Corresponding operations will be presented in the third part of each cell. Generally, no further detailed operations are considered in these four components in the proposed model. Lockage times of each component will be simply specified with statistical distributions.

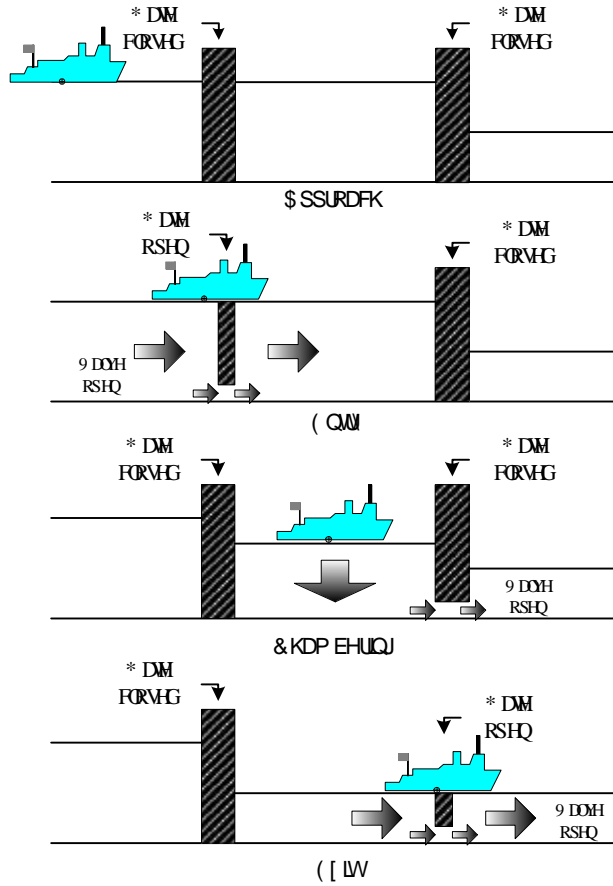
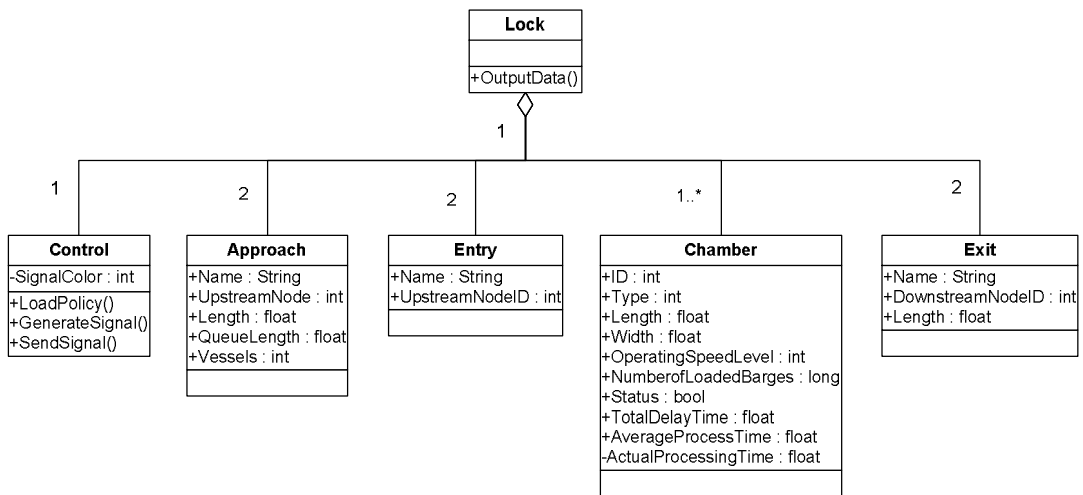


Figure 5 Four-Component Lockage Process



Vessels

Inland waterway traffic includes commercial vessels delivering cargo, and other vessels, mostly recreational, carrying passengers. There are several common features in these moving vessels such as longitude, latitude, origin and destination. As shown in Figure 7, a parent class is created as “Vessel” to carry the common attributes. Three children classes, namely tow, light boat and recreational craft, inherit all the attributes of the “Vessel” class.

Tows

Barge tows consist of a towboat pushing one or more barges, depending on the characteristics of the waterway facilities, type of cargo, and power of the towboat. Those moving tows constitute the major commercial traffic on U.S. inland waterways. Barges may be loaded or empty. They are moved between origins and destinations to serve the shipping demand. Light boats are those tows without barges. They travel through waterways to any origin ports as service equipment. Commercial passenger vessels and government vessels are grouped into this category.

Recreational Craft

Unlike commercial traffic, recreational craft carrying passengers usually share waterways as local or short-trip vessels. In general, those vessels are more sensitive to seasonal factors than commercial vessels. They also affect lock operations with dispatching priorities.

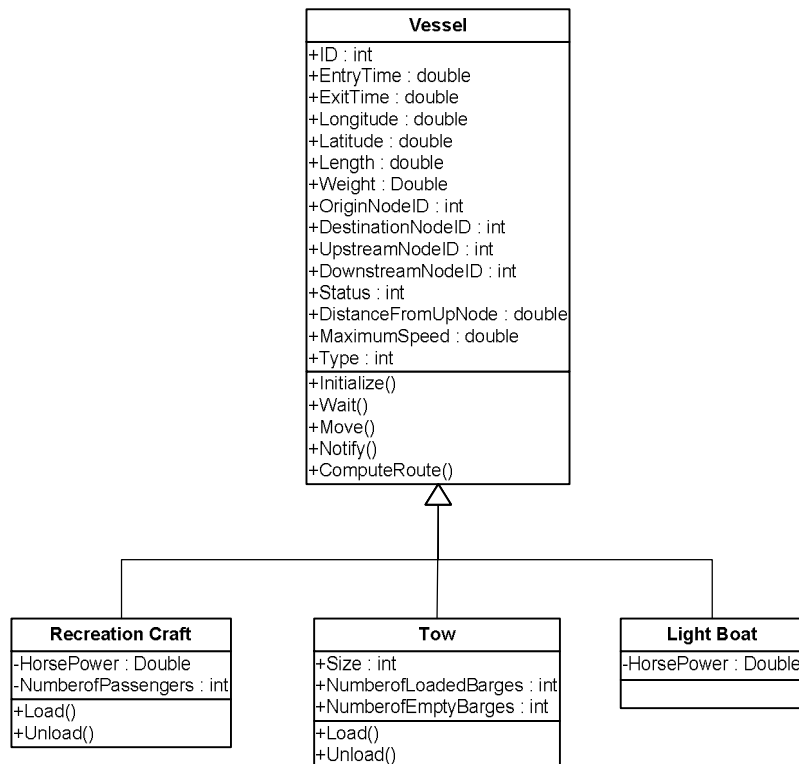


Figure 7 Inheritance Relations for the Waterway Vessel Classes

Lock Operation

As presented in previous section of lock's design structure, a lockage is completed with an operational control scheme and a physical 4-step process. The control scheme determines the sequence of waiting vessels and the timing of SOL (start of lockage). The lockage processing time varies with the size and configuration of traveling vessels and is randomly distributed in each lockage component. For single lock analysis, detailed operational maneuvers should be simulated in the model. However, for long-term planning purposes, a more macroscopic analysis, without details of individual maneuvers, would be preferable. That would emphasize the overall evaluation, for which approximate estimation of any single lock performance will be provided. The proposed model should be able to handle different levels of analytic details based on different levels or requirements of specific studies.

Lockage Distributions

In the LPMS data, the lockage process is classified into four components: approach, entry, chambering and exit. There are three types of entry and exit: fly, exchange, and turnback. Based on those categories, the lockage process time for each component or type can be estimated with statistical distributions at each lock. Besides, tow size, lockage cuts, and traveling directions might also affect the processing time. A well-developed service time estimation model is necessary, especially for new projects.

Locking Policies

Different locking policies have been applied in previously developed simulation models. NavSym employed three policies: longest queue, FIFO (First In First Out) and N-Up N-Down. WAM also modeled three policies: FIFO, 6-Up 6-Down and one-way (for locks with twin chambers). In addition to FIFO, Wang considered issues of priority and fairness with SPT (Shortest Processing Time) and FSPT (Fairer SPT) alternatives. The proposed model should incorporate the operational policies included in the previous models, especially in WAM. Other operational alternatives will be considered in future model development, including:

1. Assignment of tows to multiple chambers
2. Priorities and mixing rule for commercial and recreational traffic
3. Priorities based on relative service times, time values for tows and their contents, and relative lateness
4. Fairness objectives and constraints
5. Maximum saving control
6. Speed control
7. Integrated control of adjacent locks
8. Alternating platoons of variable size (M-up and N-down)
9. Appointment and reservation systems
10. Tow cutting and reassembly considerations
11. Chamber packing
12. Chamber packing with tow cutting
13. Auxiliary ("helper") towboats at congested locks

Interference between Chambers

Some physical interference between vessels is observed at multi-chamber locks. Such lock interference actually compels the waiting vessel to wait while another vessel finishes an action, even though its intended chamber is ready for service. Recreational craft and light boats cannot cause or are not affected by interference. Two kinds of interference are considered in WAM: approach area interference and gate area interference. Approach area interference considers lockage at the two-chamber locks as passing through a series of “single-server” approach area, “two-servers” chamber area, and another “single-server” approach area (as shown in Figure 8). When a vessel served at a lock completes its chambering, while it exits and occupies the approaching area in the conflicting direction, another approaching vessel cannot start its lockage even if the other chamber is idle. That is, if the existing vessel and the next travel in the same direction, the approach area for the next vessel is clear and no interference occurs.

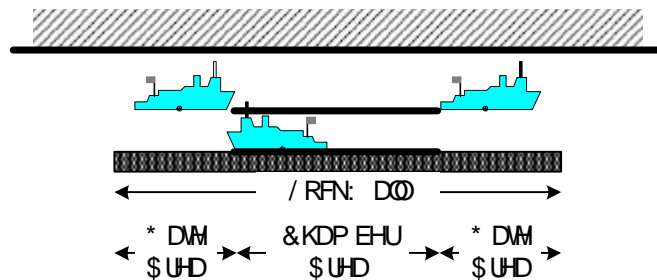
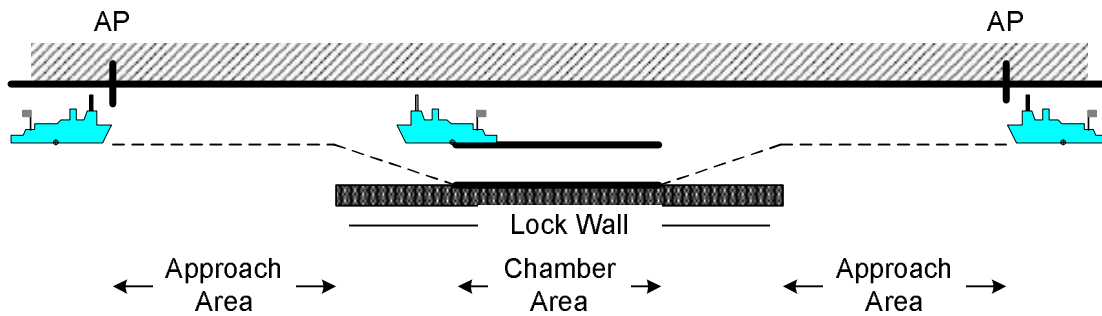


Figure 9 Gate Area Interference

Discrete Event Waterway Simulation Model

Unlike the time-driven simulation models, discrete event simulation models are driven by the atomic event elements. An “event” occurs as an instant in simulated time. Discrete-event simulation models a system as it evolves over time through event

occurrences in which the state variables change instantaneously at separate points in time. The proposed waterway simulation model is categorized as a discrete event simulation model. In an inland waterway system, a queuing network arises as tows travel through restricted reaches and locks. In addition to placing tows' arrival and departures at discrete time points, events could also be used to generate tows at ports, schedule the maintenance and improvement projects at locks, or apply navigation rules on reaches.

Process-Based Modeling Approach

In general, two approaches are considered in designing a discrete-event simulation model: event-based (e.g., event-scheduling) and process-based (e.g., process-interaction). With an event-based approach, the system is modeled by identifying its characteristic events and designing event routines to describe the change of states. The simulation runs over time by executing events in increasing order of their time of occurrence.

Unlike an event-based approach, a process-based approach is now used in most object-oriented simulation packages. A process is a time-ordered sequence of interrelated events, which describes the entire experience of an "entity" as it flows through a "system". That is, the process is expressed from an "entity" which visits several resources in the "system" and changes its states over time. Taking a single-server queue as an example, Figure 10 shows the possible events of arrival and departure. An event-based approach executes each scheduled-event along the time axis. Alternatively, Figure 11 shows a process describing the flow of an entity through the system. Each entity in single-server queue experiences the same process in the system. During a process, there may be break points for incoming events.

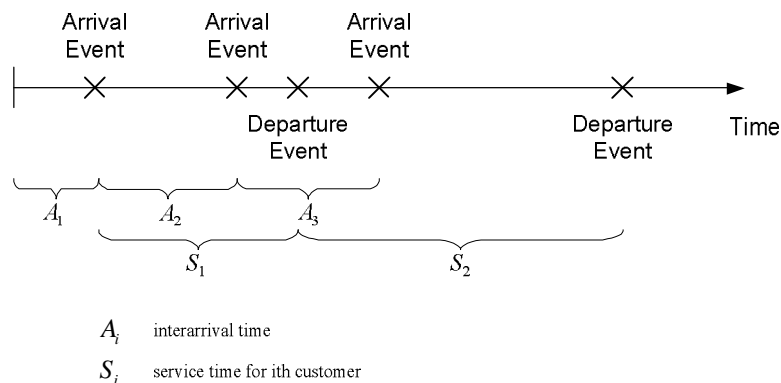


Figure 10 Event-Based Approach

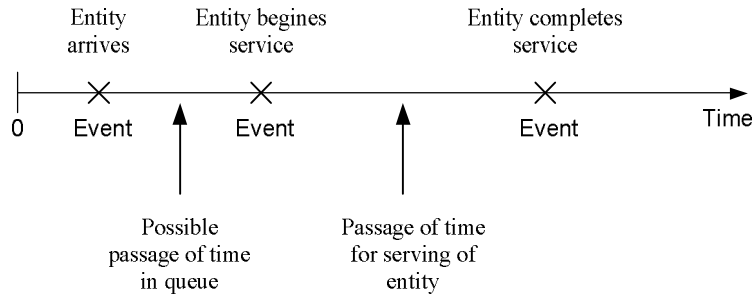


Figure 11 Process-Based Approach

In inland navigation, an “entity” may be defined as a “tow trip”. The “system” it goes through is actually the path / route between its origin and destination. For any single tow trip, “process” describes several “activities” while moving through the network, such as arrival / departure at locks, bends, links and ports. From an OOP viewpoint, those activities are the “behaviors” of the tow “object”. Accordingly, a “lock” can be viewed as an entity as simulation run. It experiences regular processes of chamber idle / busy, scheduled maintenance closures, unscheduled stall downtimes and planned expansion improvements. Those “lock activities” are then the “behaviors” of the lock “object”.

Event List

Several basic events occur in operating an inland waterway network: generation, arrival and exit events at ports, arrival and move events on reaches or bends, and arrival and departure events at locks. Other events, such as casualty events on the reaches, stall and maintenance events at locks, and improvement events at project locations, could also be specified based on the needs of particular studies. For the animation feature in the simulation model, a time-slice event should be specified in order to update the positions of tows in the network during the simulation time. Generation events at ports should be first initialized and scheduled in order to start the simulation. During the simulation run, event occurrences will then be scheduled either from themselves or other events and executed sequentially. Figure 12 shows the event graph for a simple waterway network with single lock. After executing a generation event, the arrival event at next node for that vessel and the next generation event are scheduled. After executing the arrival event, the departure event is scheduled and the next departure event is determined if there are vessels waiting in the queue.

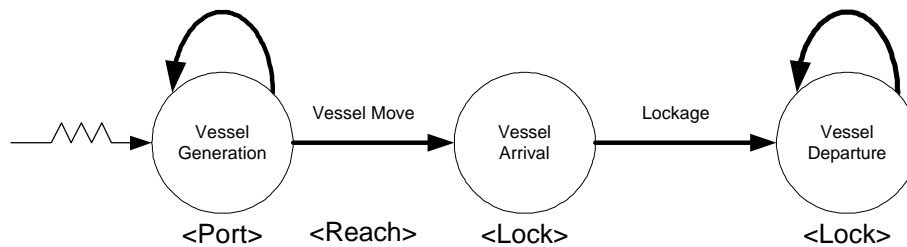


Figure 12 Event Graph for Waterway Network with Single Lock

Possible events are grouped below according to the components of network structure. Since each waterway component is designed as an object, the listed events are actually the operations or activities which are activated or preformed in the corresponding component and specified in the third part of each cell, as shown in previous defined object diagram.

Node-Relevant Events

1. Port
 - Generate Vessel
 - Update Demand
 - Output Data
2. Lock
 - Load Operation Policy
 - Generate Signal
 - Send Signal
 - Open
 - Close
 - Start / End Stall
 - Start / End Maintenance
 - Start / End Construction
 - Output Data
3. Bend End
 - Load Operation Policy
 - Generate Signal
 - Send Signal

Reach-Relevant Events

1. Link
 - Start / End Casualty
 - Start / End Improvement
 - Start / End Maintenance
2. Bend
 - Start / End Casualty
 - Start / End Improvement
 - Start / End Maintenance

Vessel-Relevant Events

- Initialize Attributes
- Compute Route
- Move
- Wait
- Load Freight
- Unload Freight
- Assemble / Disassemble

- Notify One's Arrival

Time-Relevant Events

- Time Slice

Model Framework

The overall structure of the defined problem is shown in Figure 13. Three blocks describe the required input, processes and produced output. The required inputs are grouped into three categories: network characteristics for building a waterway system, trip characteristics for vessel distributions, and operation characteristics for lockage information. Processes are actually the event-relevant activities, discussed in the previous section, occurring at different network components or entities. The measures of effectiveness (MOEs) are then shown in simulation outputs with throughputs, time-in-system, or bottleneck analysis.

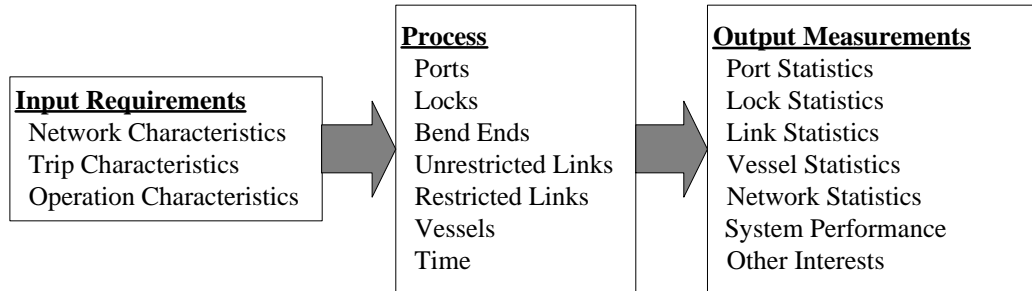


Figure 13 Development of Waterway Simulation Model

The logical organization among the event modules in this waterway simulation model is shown in Figure 14. After invoking the initialization process, the simulation model runs through the main event-updating routines, which are determined through the timing control module. Based on the simulation clock, different events occurring separately at either ports or locks change the state of the system. All events in this model occur at network nodes over the simulation time. After processing events, a statistical routine is used to update the relevant system variables, which are dependent on the study objectives. Different event modules might require different statistical data for updating. After all event-scanning procedures have been completed, a stopping rule is applied to terminate the simulation program and a performance report is generated.

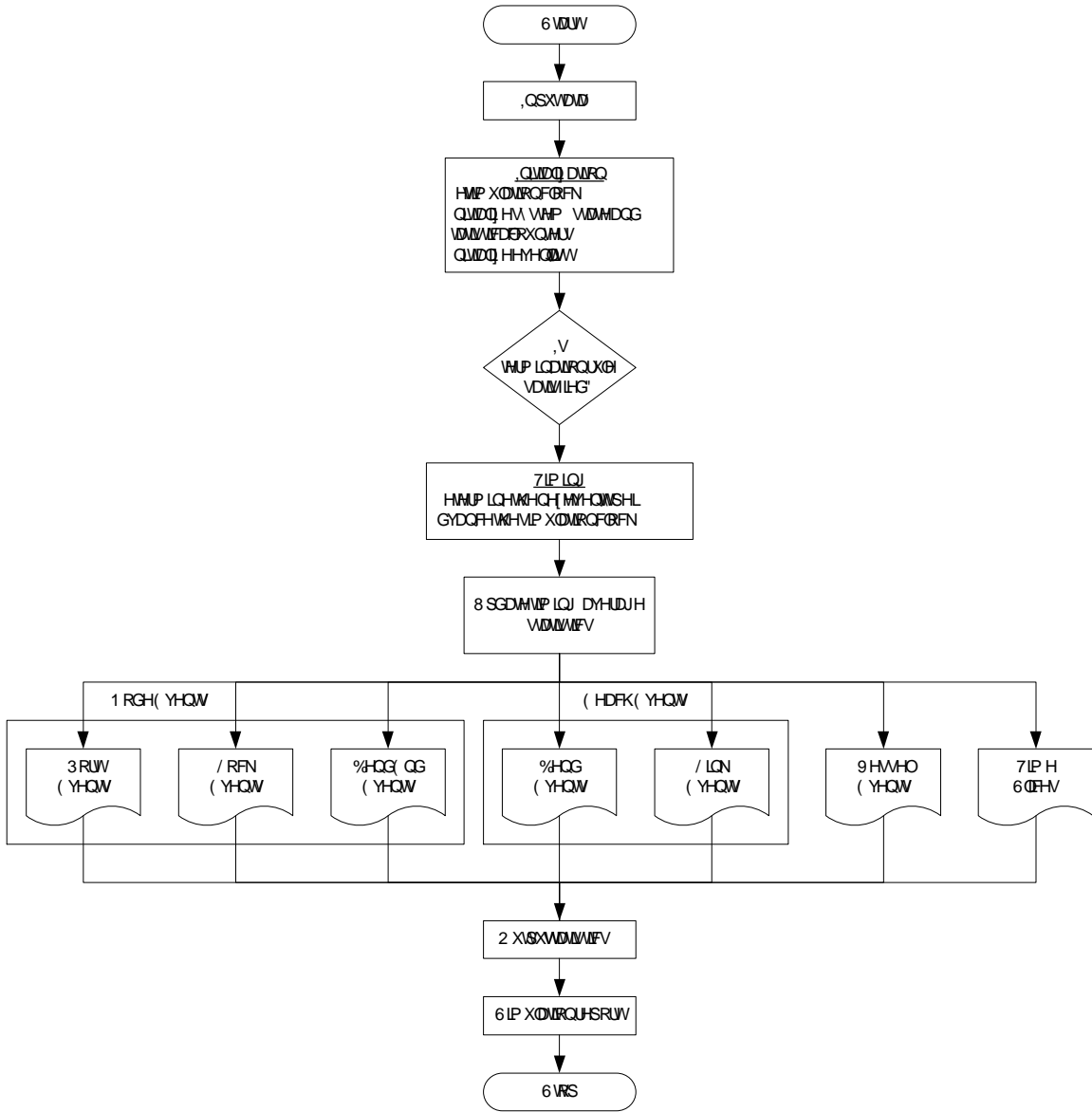


Figure 14 Overall Framework of Waterway Simulation Model

Model Development

In the proposed model, different types of processes occur in either network facilities or moving vessels. Basically, network processes start the simulation and perform the activities of updating the status of network components. They also record the network-relevant statistics time by time in order to evaluate the system performance. On the other hand, vessel processes are the major behaviors of the simulation model. They drive the vessels moving through the waterway network from their origins to destinations with logical operations. The following sections specify the relevant process with the help of an “activity flow” or “swim lanes” type of diagram. An “activity flow” diagram is a regular flowchart showing the steps of each process. In order to model the complex

interaction among objects, the “swim lanes” type of diagram is adopted in which each lane represents all activities associated with an individual interacting object.

Port Processes

In the simulation model, the port components are in charge of generating vessels, updating traffic demand, and fleeing barges. Based on the demand statistics, which may change over time, vessels with specified size, origin, destination and loading ratio are generated at ports and sent into network. In current model development, tow size is kept unchanged from the origin to its destination. In future development, barge fleeing could occur at the intermediate ports between the origin and destination.

Vessel Generation

A vessel is generated either at origin ports or boundary nodes which are a set of edges of the study area. Vessels generated from ports could be commercial or passenger vessels, based on the historical trip statistics. In the proposed model, there are three types of vessels traveling in the waterway network: tows, light boats and recreational craft. For regular tows, the number of pushed barges and the loaded fraction are generated statistically. A towboat whose horsepower corresponds to the generated tow size is assigned and the tow’s traveling speed is determined from pre-set distributions. In the long run, the total number of generated towboats and barges at ports should be conserved, if necessary by generating empty barges.

The vessel generation module is used to generate vessels (e.g., tows, recreation crafts and light boats) and push them into the waterway network. As shown in Figure 15, the vessels are generated by an operation of the port object. After this operation is executed, another operation of the port will determine the schedule of next vessel generation according to the OD flow rates that are stored in the port’s attributes. When a vessel is generated, some of its attributes will be automatically initialized, such as its vessel types, its longitude and latitude positions as well as its origin and destination nodes. At the same time, routes are determined to provide the path information. After that, the system will check the type of vessel and the type of the port where the vessel is generated. If the port is a boundary node or the vessel is a light boat, the vessel will move into a link immediately; otherwise, the vessel will execute the “loading” operation first and move into a link after the loading process is finished.

9 HVHO HQHDMRQ

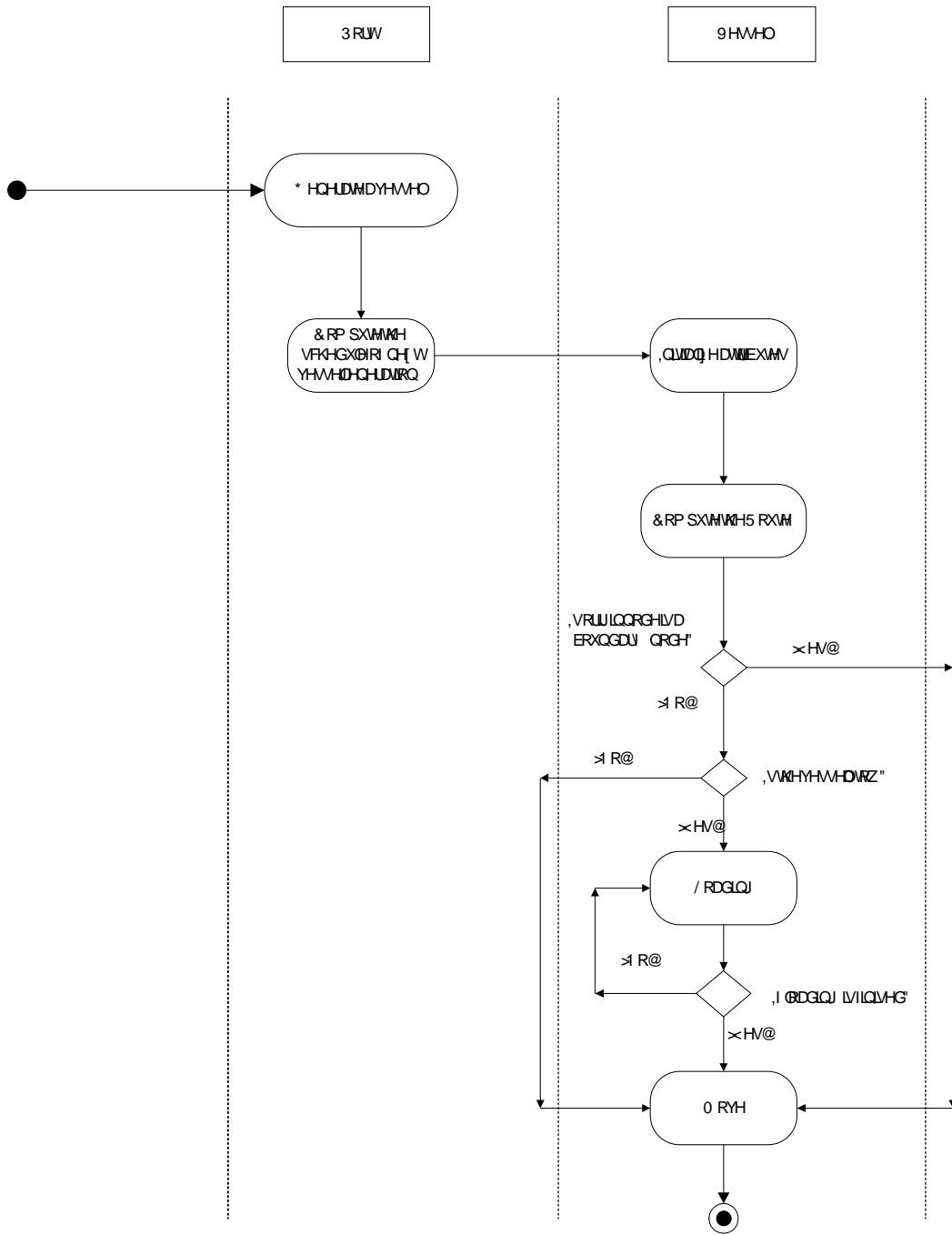


Figure 15 Activity Diagram for the Vessel Generation

Demand Update

In the proposed model, waterway traffic is modeled with seasonal changes, by seasons or by months, and economic growth is modeled with an annual growth rate. If

there are navigation projects, their improvements to the waterway network will also attract more traffic demand. In addition to the long-term demand change, the designed demand module also considers the short-term demand variation during the simulation, such as demand sensitivity to the level of service (e.g. total travel time), traffic alternation due to scheduled or unscheduled lock closures and demand diversion to other transportation modes if locks are closed for improvement work.

Lock Processes

Locks are almost always the bottlenecks in inland navigation. Operational procedures at locks affect their service times, capacities, and queuing delays. Maintenance and capacity improvements at locks can also significantly affect lock performance.

Control Policies

In the early stages of model development, locking policies are kept unchanged at each lock during the simulation. Dynamic locking policies based on traffic level and service variation may be considered in future model development.

WAM models three locking policies. The most common policy used in waterway operation is FIFO, which is fair and not to be inefficient for uncongested locks. A policy of N-up and N-down is usually adopted at congested locks with a long approach area. If this policy is in effect, alternate cycles of N upbound vessels followed by N downbound vessels are used. A one-way policy may occasionally be effective for two-chamber locks. Generally, it dedicates one chamber to upbound vessels and the other to downbound vessels.

Policies other than FIFO are usually used in combination with FIFO. That is, with an N-up and N-down policy, FIFO is in effect until queue lengths reach N. Similarly, with a one-way policy, if queue is formed in only one direction and the other chamber is idle, FIFO is in effect until a queue arises in the other direction. Figure 16 shows the simple modeling logic of WAM's three existing policies. The criteria of 6-Up 6-Down and one-way policies are always checked after completing one alternate cycle or one lockage.

The locking policies applied in WAM are mainly designed for process the commercial tows. Among all vessels in WAM, commercial tows always have priority over recreational craft. Even if a recreational craft is passed, a maximum number of commercial lockages ahead of its own lockage is specified. However, recreational craft have first priority in sharing chambers if space permits. Sometimes, when an empty chamber turnback is required, recreational craft traveling in the proper direction are permitted to make their lockage with the turnback. Besides, at two-chamber locks, the first available chamber is selected. If both chambers are available, tows are always assume to use the chamber which can complete the lockage sooner. Usually, tows without cuts use the smaller chamber in order to minimize the water use.

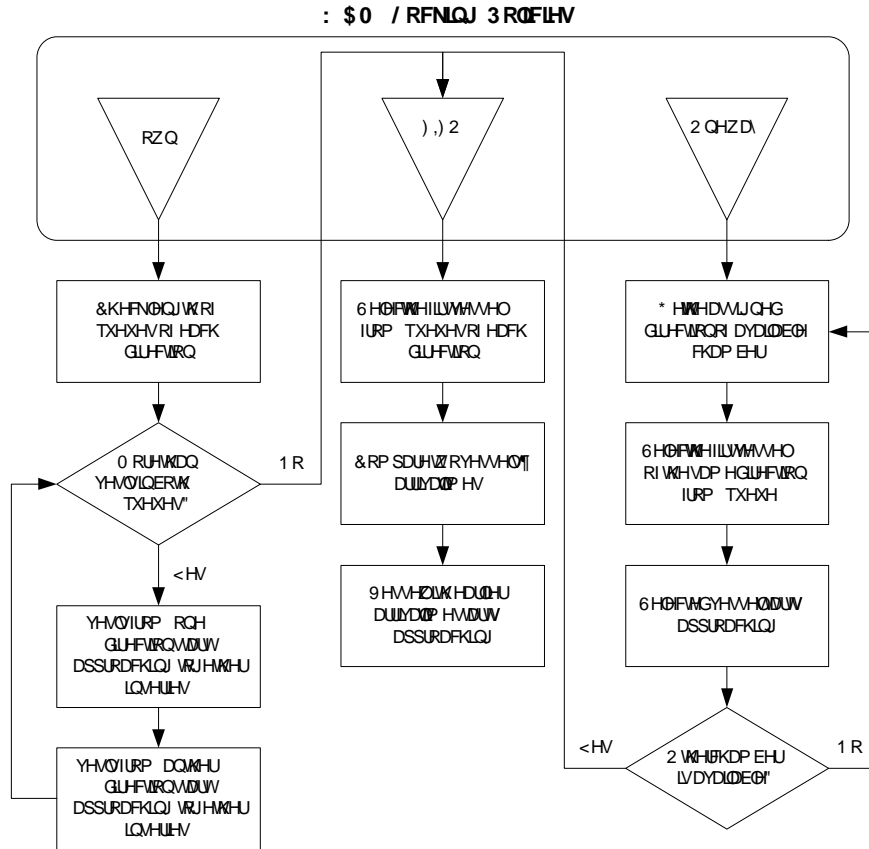


Figure 16 Locking Policies in WAM

Other control policies will be considered in future model development, including the ones used in Wang’s model (Wang 2005) and in Schonfeld’s previous studies (Ting and Schonfeld, 1996, 1998, 2001). Most proposed control policies were designed and tested for individual locks (Ting and Schonfeld, 1996, 2001). Only a few of them (Ting and Schonfeld, 1998) have been tried on small lock series (e.g. 2 adjacent locks or 4 locks in series). In Wang’s model policies such as FIFO, SPF, and FSPF, are analyzed at the network level. The control logic is discussed below.

As shown in Figure 17, SPF gives priority according to the criterion of shortest processing time *per unit value* (e.g. per barge or per loaded barge). Since it is possible that the small tows may be repeatedly passed by larger ones, the fairness issue is considered with FSPF by specifying a *fairness constraint*. This can be defined as a maximum waiting time after arriving or a maximum number of tows who arrive later but pass ahead.

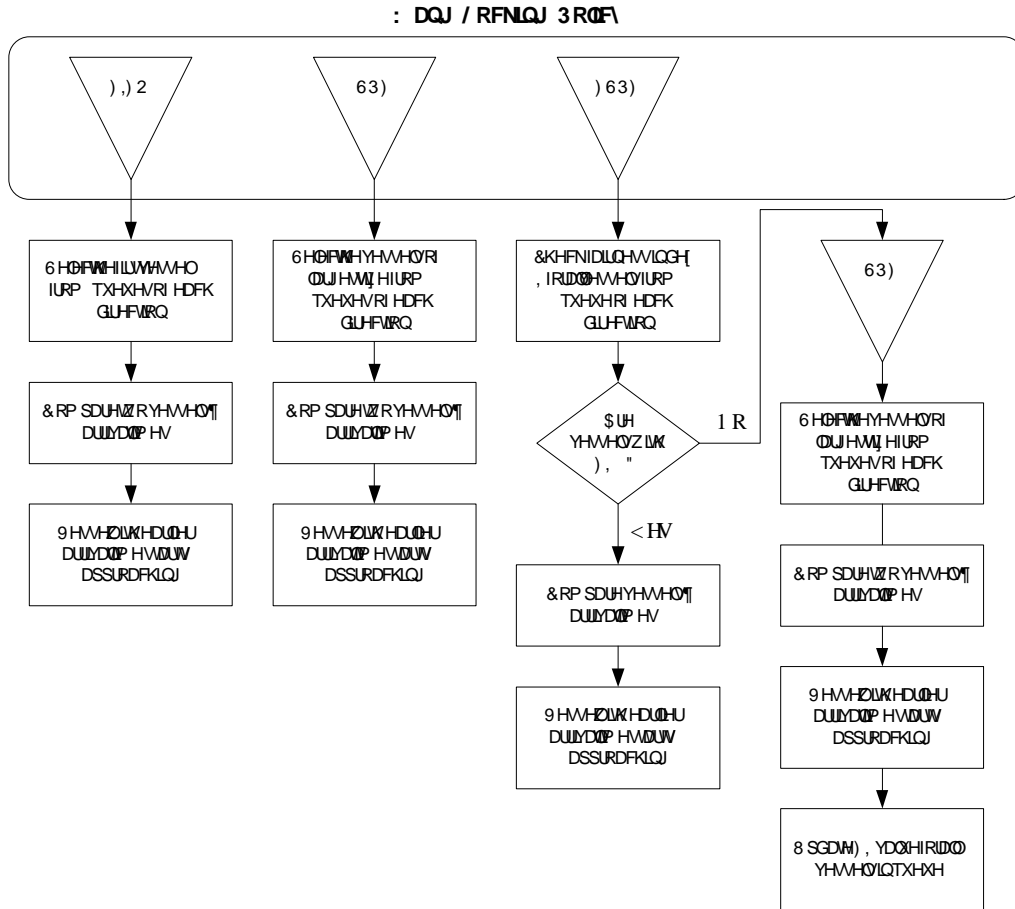
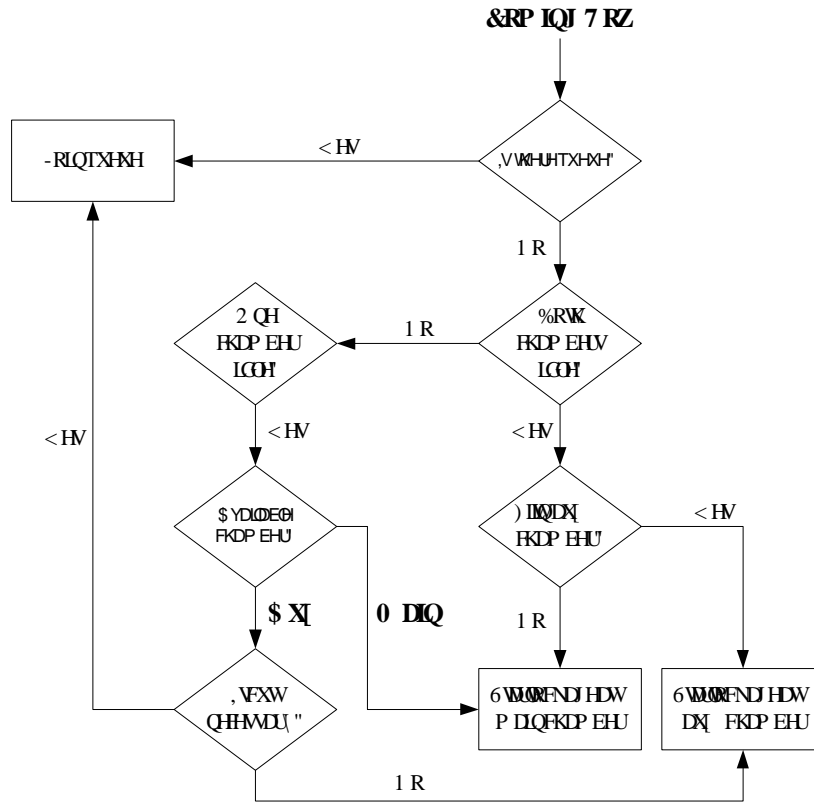
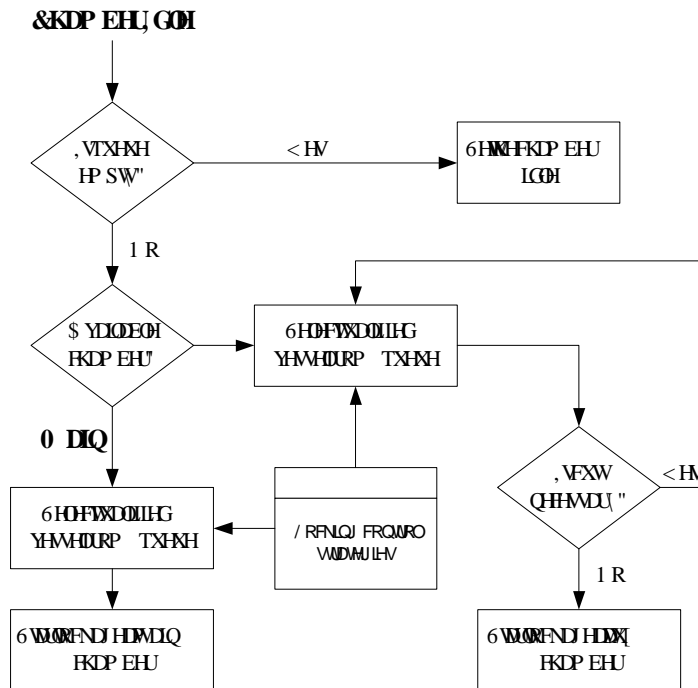


Figure 17 Control Policies in Wang's Model

Chamber assignment as well as chamber preference will also be considered in multi-chamber locks in order to reduce the processing time by avoiding the lockage cuts (as shown in Figure 18 (a) and (b)). Chamber selection is needed when a vessel arrives at or departs from a multi-chamber lock. As can be seen, the auxiliary chamber is preferred for tows without lockage cuts (e.g. 1-cut tows), if both chamber are available. The main chamber is preferred for tows with lockage cuts (e.g. 2-cut tows), even though the auxiliary chamber is available. The proposed logic should be consistent with the one modeled in WAM. However, recreational craft are given first priority in Wang's model based on observations in LPMS data. The numbers of non-recreational vessels passed over is unlimited.



(a)



(b)

Figure 18 Chamber Assignment / Chamber Preference for Multi-Chamber Locks

Signal for Lock Interference

Figure 19 illustrates how a lock control system generates a signal for the vessels waiting before the approach. First, the control runs the lock operation policy and selects a vessel in queue as the next one to enter the approach. Then the lock control checks the availability of the approach, gate and chambers. If either the approach or the gate is already occupied, or if all chambers are serving vessels, then the control will generate a red signal to the selected vessel, and require the vessel to keep waiting before the approach. If both the approach and gate are empty, and all chambers are available for serving the next vessel, the control system generates a green light for the selected vessel, and permits the vessel to enter the approach. If both the approach and gate are empty, and one chamber is serving a vessel and another is idle, then the control will check the direction of the chambering vessel. If the waiting vessel and the vessel in chambering are opposite directed, then the control system compares the end time of chambering and the arrival time of the waiting vessel. The control will generate a green signal to the selected vessel if its arrival time is earlier than the end time of the chambering, or a red signal if its arrival time is later than the end time of the chambering. If the selected vessel and the chambering vessel move in the same direction, the control system generates a green signal to the selected vessel.

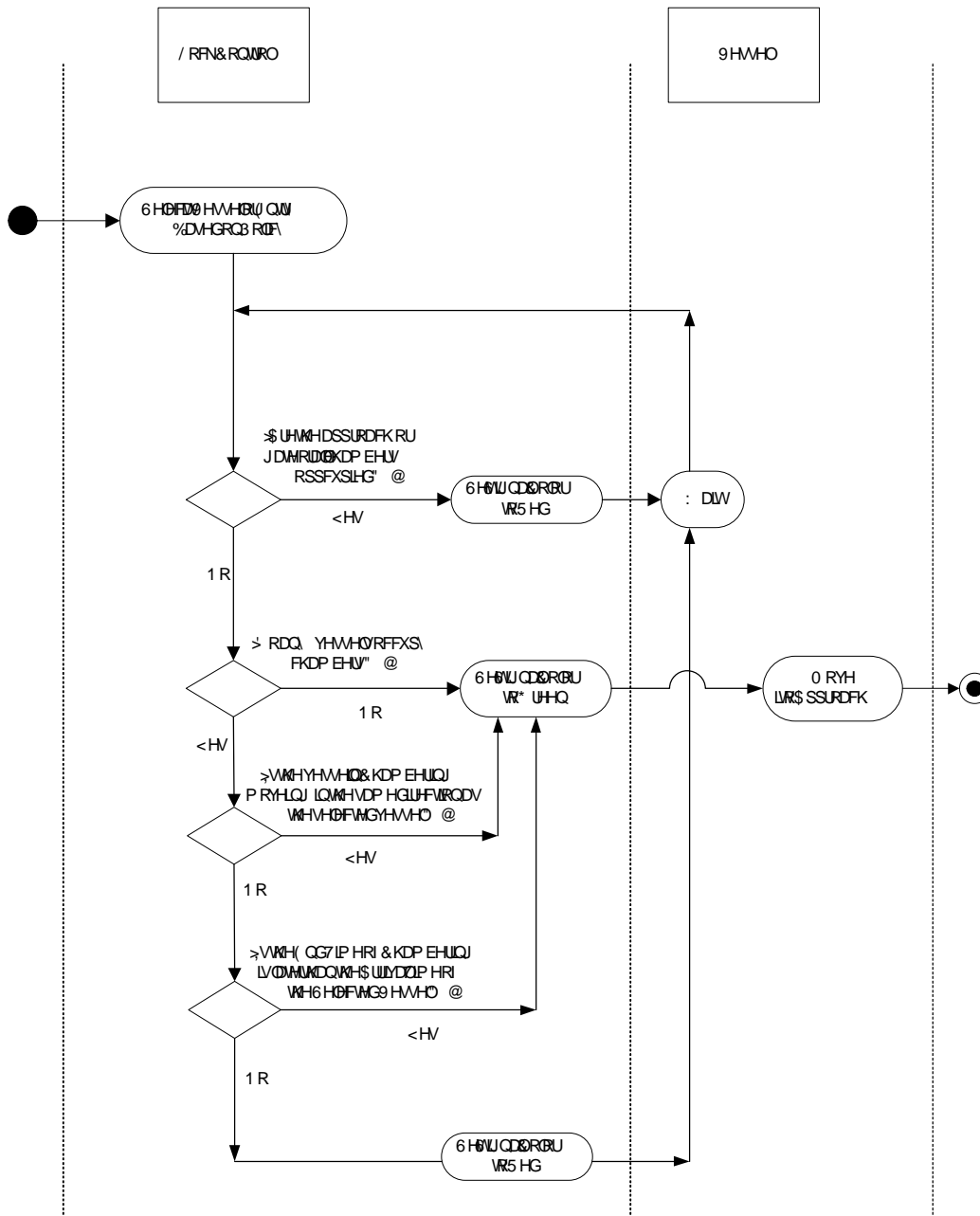


Figure 19 Signal Generation for Approach

Lock Closures

There could be several periods at which the lock capacity is changed and affects the waterway traffic. Three possible situations are considered in the proposed model: lock stalls, lock maintenance, and lock improvements. The most frequent ones are the short-duration lock stalls which are treated as random downtimes during normal lock operation. At two-chamber locks, those unscheduled closures might only affect part of the traffic since both chambers would rarely be unavailable at the same time. Regularly scheduled lock maintenance affects waterway traffic during the closure periods but should increase the reliability of lock facilities. With higher reliability, the probability of facility failures

decreases. In addition, to deal with serious delays contributed by aging locks and increasing traffic, lock improvement projects are considered by expanding the existing chambers or adding new parallel chambers. Before the project completion time, chamber capacity may decrease, possibly to zero, and the waterway traffic might be diverted to other transportation mode. After construction, lock capacity is increased and the improved lock operation may shorten the lockage time and thus attract more waterway traffic.

Reach Processes

Reach Casualties

Vessel casualties are regarded as accidents or other incidents that affect pre-planned trip by causing delays or damages. There may be different types of casualties, collisions between vessels, allisions between vessel and fixed structure or facilities, or groundings (when vessels hit the bottom of channels). If casualties occur on unrestricted links, costs are only incurred by the vessels involved. If casualties occur on restricted links, extra travel time waiting for the clearance might be caused for the following vessels based on the specified restricted rules.

Reach Improvements

Reach improvements include dredging, widening or straightening the channel. During the project period, the specified reach rules may be changed to stricter ones. With navigation improvements, the number of casualties may be reduced, thus reducing transportation costs and times.

Time Processes

Time Slices

A specified time interval is defined to create time slices which are evenly distributed during the simulation time. Whenever the simulation clock reaches one of the time slices, the vessels' position in the network is updated and recorded for animation purposes.

Vessel Processes

The most important vessel-related modules in Neo-WAM include vessel generation, vessel movement on link and vessel operation at lock. Figure 15, Figure 21 and Figure 22 describe the activities for these three modules. In order to model the complex interaction among objects, the “swim lanes” type of diagram is adopted in which each lane represents all activities associated with an individual interacting object.

Route Determination

Whenever a vessel is generated, its travel route should be determined. A route consists of nodes and reaches, and is defined as a path along which a vessel moves through the waterway network from its origin port to destination port. In most cases, a route is unique for each O/D pair due to tree network. If there are loops in the network, multiple routes between the same O/D pairs would be considered. At the same time, route choice is determined based on river flow, transit time or travel condition (e.g. restricted rules).

Vessel Arrivals

While traveling on the waterway network, vessels pass through a series of nodes and reaches. As vessels reaches nodes, their arrival notice activates different processes for different types of nodes. As shown in Figure 20, there are three cases in which vessels just continue moving on the connecting reaches and the next arrival timing is calculated: a port which is not destination node, a junction, and a bend end which sends out a “green” signal for passing through it. When reaching a lock, the arriving vessel will join the queue if there already is one. If a “green” signal is sent out, the vessel starts the lockage and its departure time is updated. In some cases at two-chamber locks, if approach area interference exists, the arriving vessel receives a “red” signal even though the chamber is available. In general, departure time is recorded as the start of lockage time plus the required service time, which is composed by the four lockage components. If gate area interference occurs at a two-chamber lock, the required service time might be longer as tows waiting to exit after completing their chambering. Similarly, if a bend is occupied by opposite direction vessels or if there are other vessels waiting at the bend end, then the “signal” to this vessel is “red”, which means the vessel must wait at the bend end; otherwise, the “signal” to this vessel is “green” which means the vessel can enter the bend.

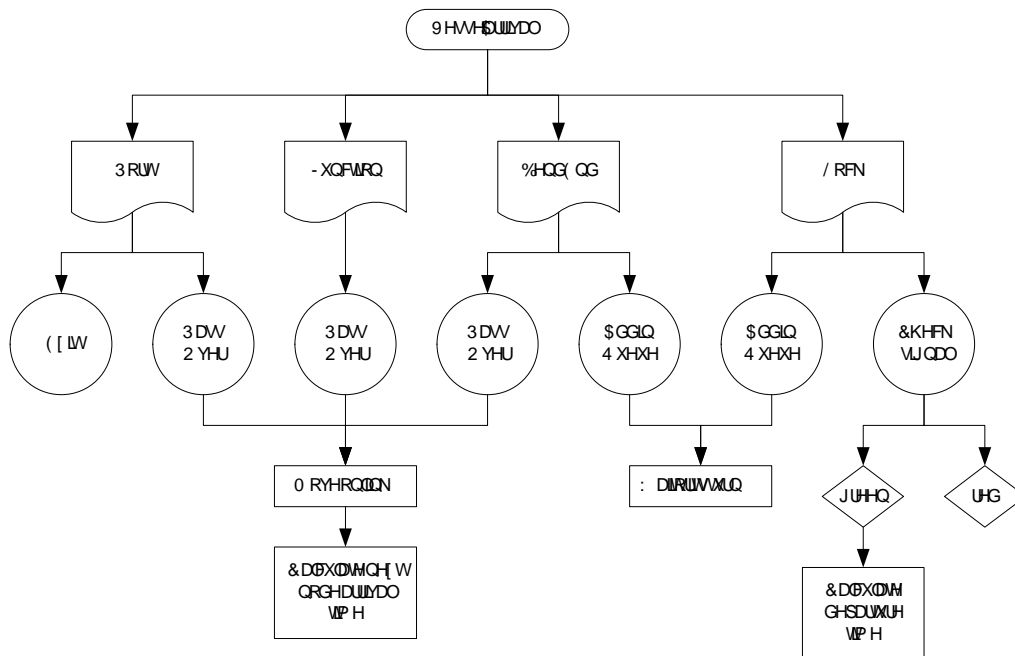


Figure 20 Vessel Arrivals at Waterway Components

Vessel Movement on Links

This module is used to push vessels through reaches either unrestricted links and restricted bends. When a vessel enters a link, its arrival time at the next node is computed. Before the vessel reaches its next node, it performs its “move” operation that updates its longitude and latitude. When its next node is reached, the vessel checks the type of the node reached. If the next node is a waterway junction or a port that is not its destination, the vessel enters it immediately. If the next node is a lock, the vessel sends a message to the lock’s control object to announce its arrival. The control object will generate a signal to indicate if the lock is occupied and the vessel should wait just before it approaches. If the next node is a bend end, the vessel must check if the bend is occupied by opposite direction vessels and determine if it should wait for the clearance. We model such an operation with virtual “signal” concept.

generates a signal to the vessel according to the lock' occupancy status and its operation policies, which are input initially when the waterway network is constructed. If the signal to this vessel is green, then the vessel starts its approach; otherwise it must wait before the approach for the lock clearance. When the vessel starts the approach, the start of entering time will be computed. The vessel continuously moves until it reaches the entry gate. When it enters the gate, the start of chambering time is determined. The status of the chamber is updated when the vessel enters chamber. After the chambering is completed, the vessel starts exiting immediately.

9 HVHO RYHP HQDZ RFN

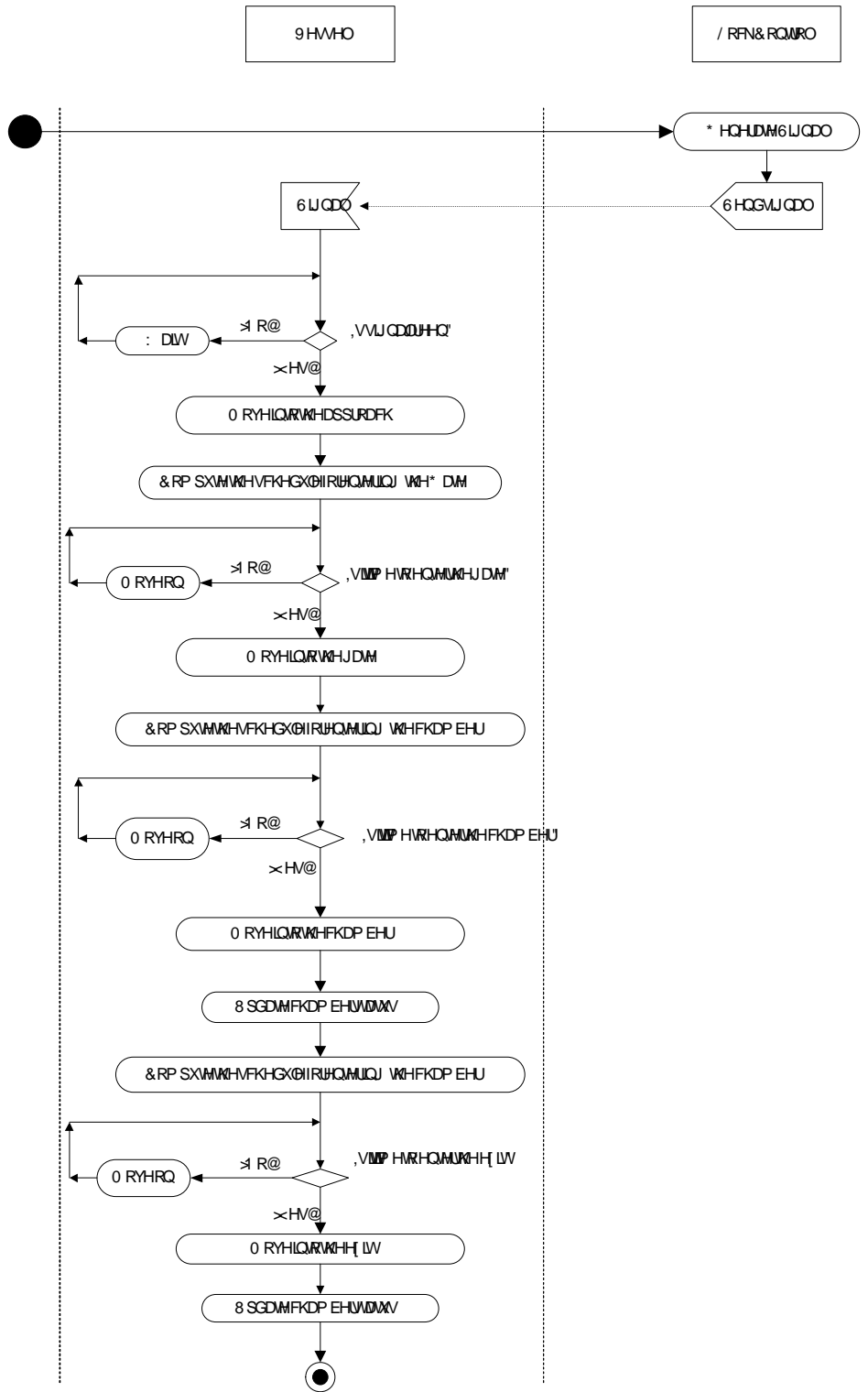


Figure 22 Activity Diagram for the Vessel Operation on Locks

References

- IWR (2003), NavSym Application User's Manual
- IWR (1999), WAM Shallow-Draft Version User's Manual
- Wang (2001), Development of Waterway Simulation Model for Interdependent Project Scheduling, Ph. D. Dissertation, University of Maryland, College Park
- Wang and Schonfeld (2005), Scheduling Waterway Projects Through Simulation and Genetic Optimization, forthcoming in the ASCE Journal of Waterway, Port, Coastal, and Ocean Engineering
- Ting and Schonfeld (1996), *Effects of Tow Sequencing on Capacity and Delay at a Waterway Lock*, ASCE Journal of Waterway, Port, Coastal, and Ocean Engineering
- Ting and Schonfeld (1998), Integrated Control for Series of Waterway Locks, ASCE Journal of Waterway, Port, Coastal, and Ocean Engineering, July/Aug., pp. 199-206
- Ting and Schonfeld (1999), *Effects of Speed Control on Tow travel Costs*, ASCE Journal of Waterway, Port, Coastal, and Ocean Engineering, July/Aug., pp. 203-206
- Ting and Schonfeld (2001), *Control Alternatives at a Waterway Lock*, ASCE Journal of Waterway, Port, Coastal, and Ocean Engineering, Mar./April, pp. 89-96
- Ting and Schonfeld (2001), *Efficiency and Fairness in Priority Control*, ASCE Journal of Waterway, Port, Coastal, and Ocean Engineering, Mar./April, pp. 82-88
- Law and Kelton (2000), Simulation Modeling and Analysis, Third Edition
- Deitel and Deitel (1998), How to Program C++, Second Edition

Information Transfer Program

On November 18, 2005, the Center held a symposium on Urbanization: Stresses on Maryland's Water Resources. Over 100 participants attended the symposium. This was our largest symposium to date, primarily due to the widespread interest in the subject by a large number of members of our water community. Maryland is experiencing a tremendous period of urbanization. As Maryland's population continues to grow, water supply and natural water ecosystems are increasingly stressed. Our keynote speaker was Dr. Robert Hirsh, Associate Director of Water, U. S. Geological Survey, Reston, VA. Six additional speakers, representing University and State scientists covered a host of related issues. One theme of a number of speakers dealt with the growing problems associated with stormwater runoff from impervious surfaces. Several studies are underway to design systems that will reduce the amount of contaminants from storm water runoff. In many ways, Maryland is at the forefront in dealing with water issues related to urbanization. The symposium was cosponsored by the Maryland Sea Grant College. Presentations from the symposium can be found at the Center webpage.

Student Support

Student Support					
Category	Section 104 Base Grant	Section 104 NCGP Award	NIWR-USGS Internship	Supplemental Awards	Total
Undergraduate	5	0	0	0	5
Masters	3	0	0	0	3
Ph.D.	1	0	0	2	3
Post-Doc.	0	0	0	1	1
Total	9	0	0	3	12

Notable Awards and Achievements

Publications from Prior Projects

1. 2002MD4B ("Sustainable Oil and Grease Removal from Stormwater Runoff Hotspots using Bioretention ") - Articles in Refereed Scientific Journals - Hong, E., Seagren, E.A., and Davis, A.P. 2006. Sustainable Oil and Grease Removal from Synthetic Storm Water Runoff Using Bench-Scale Bioretention Studies, Water Environ. Res., 78(2), 141-155.
2. 2002MD10B ("Summer Research Assistantship") - Articles in Refereed Scientific Journals - Rose. C.,G, Paynter, K.,T., and Hare, M.P. 2006 Isolation by Distance in the Eastern Oyster, *Crassostrea virginica* in Chesapeake Bay Journal of Heredity 97(2) 158-170.